



Erasmus+



REB-BUILT Project

*Rehabilitation of the Built Environment in the Context of Smart City and Sustainable Development
Concepts for Knowledge Transfer and Lifelong Learning*

Erasmus+ Programme – Strategic Partnership

Project Nr: 2018-1-RO01-KA203-049214

This project has been funded with support from the European Commission under the Erasmus+ Programme



- Meetings with practitioners and experts in the RE-BUILT Project took place twice during the RE-BUILT Project implementation:

- 1. during the C4 Programme for teaching in Sofia, Bulgaria (February 2020) - "Days for the REBUILT Construction Sector" – A RE-BUILT Project Workshop supporting the built environmental rehabilitation in Europe, <http://www.rebuilt.ce.tuiasi.ro/resources/meetings/C4.pdf> and
 2. during the C6+C10 Programmes for teaching and learning in Orleans, France (Nov-Dec 2021) - The 3-day Autumn Doctoral School. http://www.rebuilt.ce.tuiasi.ro/resources/meetings/C6_C10.pdf

In addition to the presentation given by each academic delegate from partner universities, a series of case study papers and technical documents for these meetings have been prepared in the form of presentations <http://www.rebuilt.ce.tuiasi.ro/outputs/>. Only parts of these files are shown below. Nine materials for each meeting are given as an example.

RE-BUILT - SOFIA, BULGARIA - 02.2020 Days for the REBUILT Construction Sector

RE - BUILT

REHABILITATION OF THE BUILT ENVIRONMENT IN THE CONTEXT OF SMART CITY AND SUSTAINABLE DEVELOPMENT CONCEPTS FOR SMART CITY AND SUSTAINABLE DEVELOPMENT CONCEPTS FOR KNOWLEDGE TRANSFER AND LIFELONG LEARNING

Days for the REBUILT Construction Sector
A RE-BUILT Project Workshop Supporting the Built Environmental Rehabilitation in Europe
Sofia, 17 - 27 February 2020

**Todor Kableshkov Higher School of Transport,
Sofia, Bulgaria**



**'Gheorghe Asachi'
Technical University of Iasi,
ROMANIA**



**Universita Degli Studi Di Cassino
E Del Lazio Meridionale,
ITALY**



**Universitaet Fuer
Bodenkultur Wien,
AUSTRIA**



**Univerza v Mariboru,
SLOVENIA**



**Universite D'orleans,
FRANCE**



**Todor Kableshkov
Higher School of Transport,
BULGARIA**

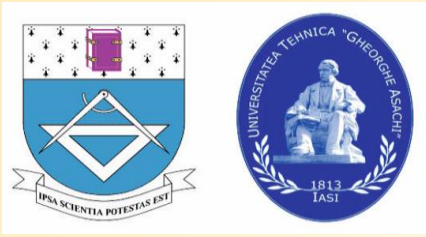


**Universidad De Sevilla,
SPAIN**



**Brno University of Technology,
CZECH REPUBLIC**





Technical University Gheorghe Asachi from Iasi, Romania
Faculty of Civil Engineering and Building Services
Structural Mechanics Department

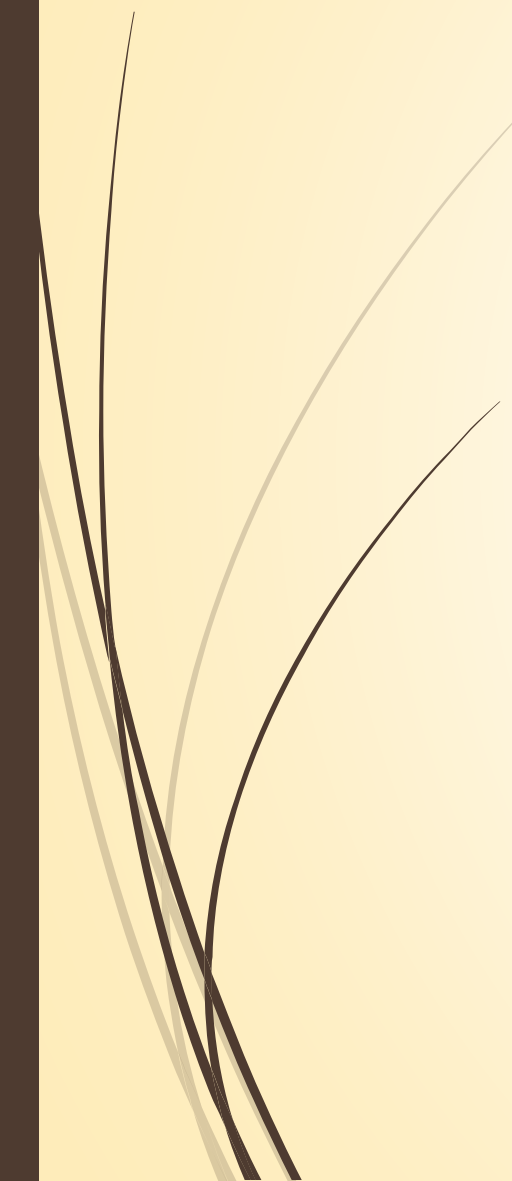
Teaching and learning in a prestigious university from Iasi, Romania

Senior Lecturer **Ioana Olteanu-Dontov, PhD**

ioana.olteanu@tuiasi.ro



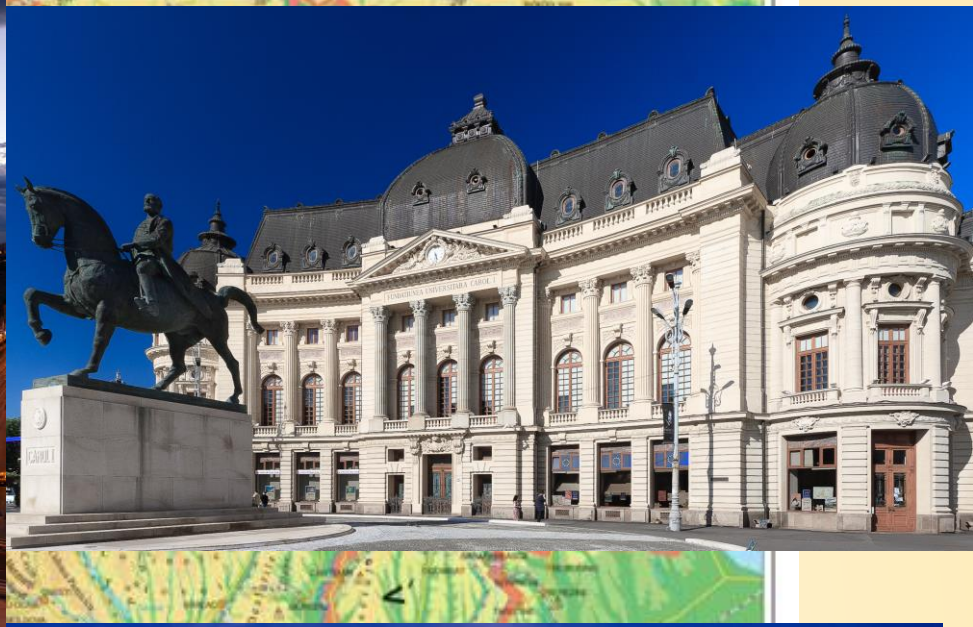
Presentation layout

- ▶ Some information about Romania
 - ▶ Some information about Iasi
 - ▶ Some information about the Technical University Gheorghe Asachi and the Civil Engineering and Building Services Faculty
 - ▶ Area of interest
 - ▶ Building Rehabilitation case study
- 

Romania



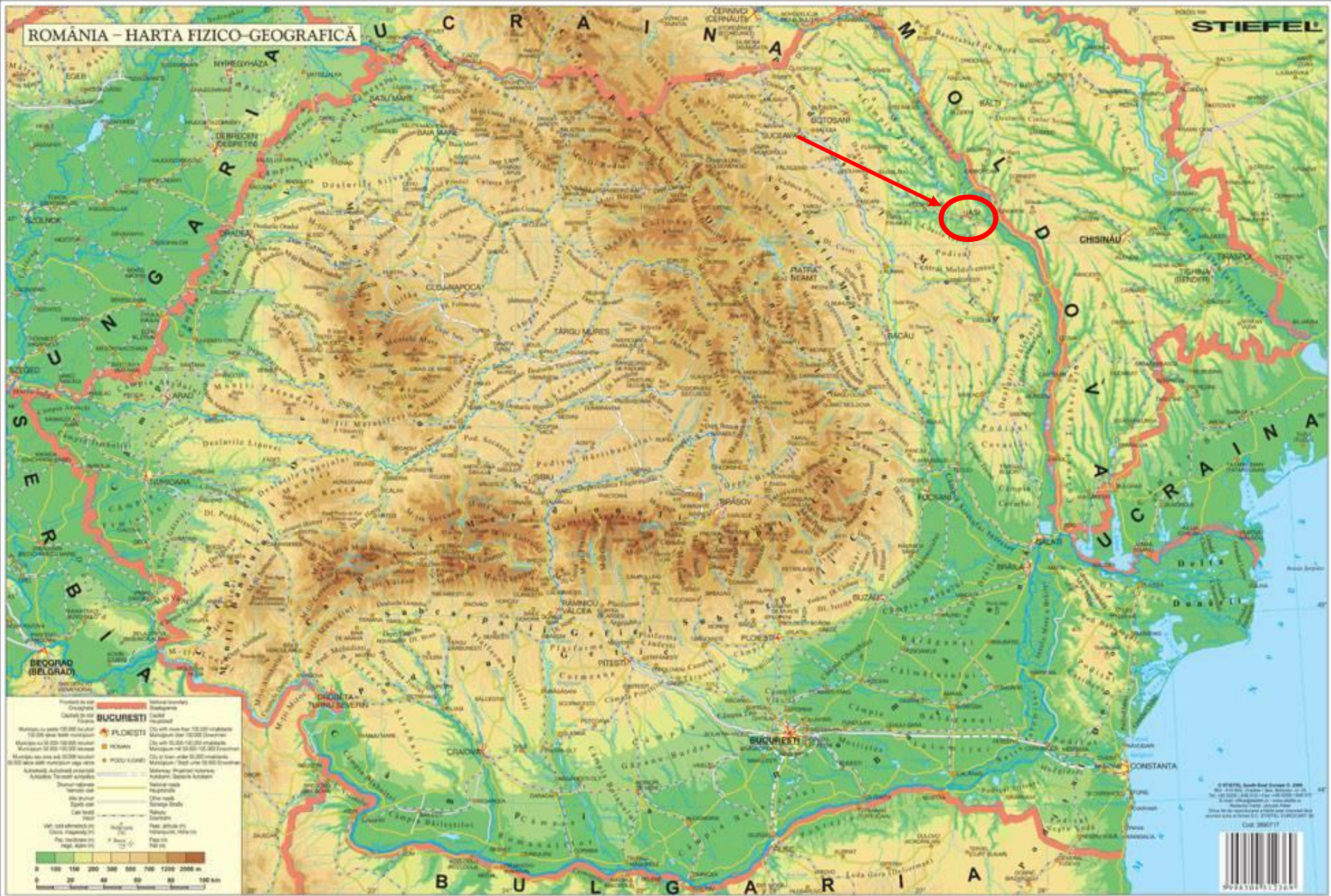








ROMÂNIA - HARTA FIZICO-GEOGRAFICĂ



BUCUREȘTI
Municipiu cu peste 100.000 locuitori
100.000 - 200.000 locuitori
Municipiu cu 50.000 - 100.000 locuitori
Municipiu cu între 10.000 și 50.000 locuitori
Localitate cu mai puțin de 10.000 locuitori

ALTE CATEGORII DE LOCALITĂȚI
Orășel
Localitate turistică
Localitate de interes local
Localitate de interes regional
Localitate de interes național
Localitate de interes internațional

ALTE CATEGORII DE LOCALITĂȚI
Localitate de interes local
Localitate de interes regional
Localitate de interes național
Localitate de interes internațional

ALTE CATEGORII DE LOCALITĂȚI
Localitate de interes local
Localitate de interes regional
Localitate de interes național
Localitate de interes internațional

© 2007, South-West Europe S. 2007
The copyright in this map is owned by the publisher.
All rights reserved. No part of this map may be reproduced or transmitted in any form or by any means electronic or mechanical, including photocopying, recording, or by any information storage and retrieval system, without the prior written permission of the publisher.

Code: 200711



lasi



Iasi



Iasi

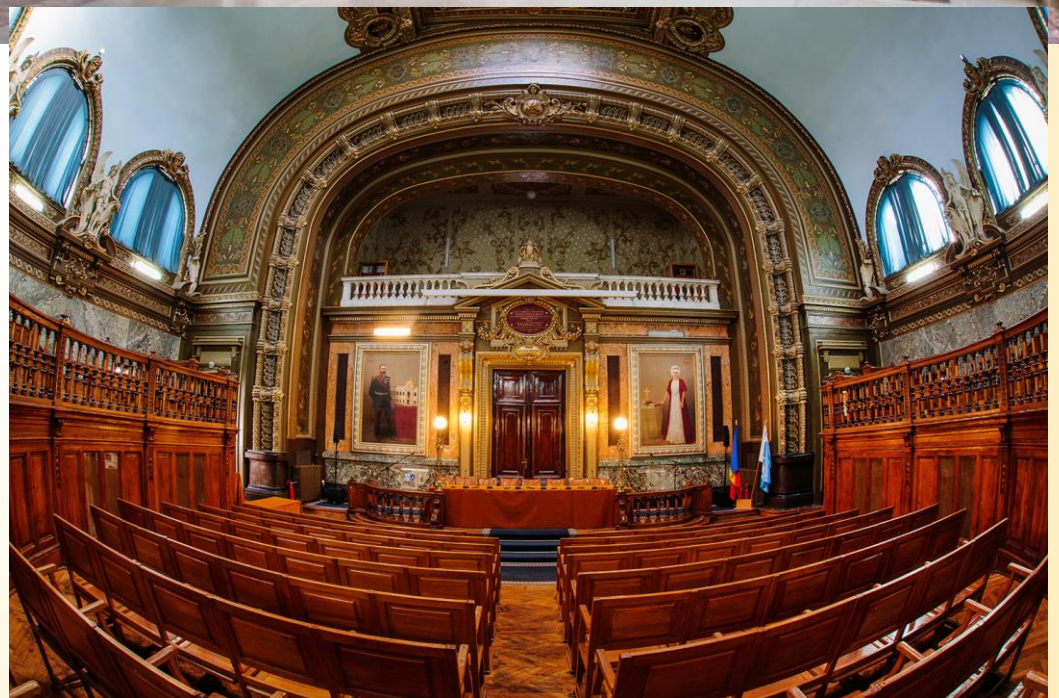


M. Eminescu Library





Université Technique "Gh. Asachi" and Université "A.I. Cuza"
(Mathématique, Physique, Lettres, Histoire, Chimie, Géographie etc.)



Iasi




Technical University Gheorghe Asachi



1813 Gheorghe Asachi founded the first school of land surveyors and civil engineers with instruction in Romanian.

Présidence de l'Université

- 
- Faculty of Automatic Control and Computer Engineering
 - Faculty of Civil Engineering and Building Services
 - “G.M. Cantacuzino” Faculty of Architecture
 - Faculty of Chemical Engineering and Environmental Protection
 - Faculty of Machine Manufacturing and Industrial Management
 - Faculty of Electronics, Telecommunications and Information Technology
 - Faculty of Electrical Engineering
 - Faculty of Hydrotechnical Engineering, Geodesy and Environmental Engineering
 - Faculty of Material Science and Engineering
 - Faculty of Mechanical Engineering
 - Faculty of Textiles, Leather and Industrial Management.

13184 students

685 university teachers

4000 scholarships

7600 beds in ‘Tudor Vladimirescu’ Student Campus



Faculty of Civil Engineering and Building Services



Faculty of Civil Engineering and Building Services

Offers 4 specialties at Bachelor level:

- Civil, Industrial and Agricultural Engineering
- Civil Engineer in English
- Railways, Roads and Bridges
- Building Services Engineering

Offers 11 Master Programs, among which are:

- Building Services Engineering
- Structural Engineering (Romanian and English)
- Building Engineering
- Geotechnical Engineering
- Structural Rehabilitation and Safety Increase of Buildings
- Modern Materials in Civil Engineering









Faculty of Civil
Engineering and
Building Services
Iași, Romania



CIMNE
International Center
for Numerical
Methods in
Engineering
Barcelona, Spain



"Matei-Teiu Botez"
Academic Society
Iași, Romania



"Prof. Anton
Sesan" Academic
Society for
Constructions



the 15th Computational Civil Engineering Conference

May 30th - 31th , Iași, Romania



**Computational
Civil
Engineering**
International Conference

May 30th-31st
Iași Romania
2019

Organized by:

Faculty of Civil Engineering and
Building Services Iași, Romania

The International Centre for
Numerical Methods in
Engineering, Barcelona, Spain

"Matei Teiu Botez" Academic
Society Iași, Romania

"Anton Sesan" Civil Engineering
Academic Society Iași, Romania

<http://www.cce.ci.tuiasi.ro/>

Senior Lecturer Ioana Olteanu-Donțov

- ▶ 2008 – 2011 – **PhD in Civil Engineering**, Doctoral School of Civil Engineering and Building Services Faculty, “Gheorghe Asachi” Technical University Iasi, Romania and Polytechnic University from Catalunya, Barcelona, Spain.
- ▶ 2008 – 2009 – **Master Degree in Rehabilitation and Safety Increase in Construction**
- ▶ 2004 – 2009 – **Bachelor of Psychology**, Psychology and Education Sciences Faculty, “Alexandru Ioan Cuza” University Iasi, Romania.
- ▶ 2006 – 2008 – **Sailing coach**, National School of Coaches, Bucharest, Romania
- ▶ 2003 – 2008 - **Bachelor of Science**, Civil Engineering and Building Services Faculty, “Gheorghe Asachi” Technical University Iasi, Romania

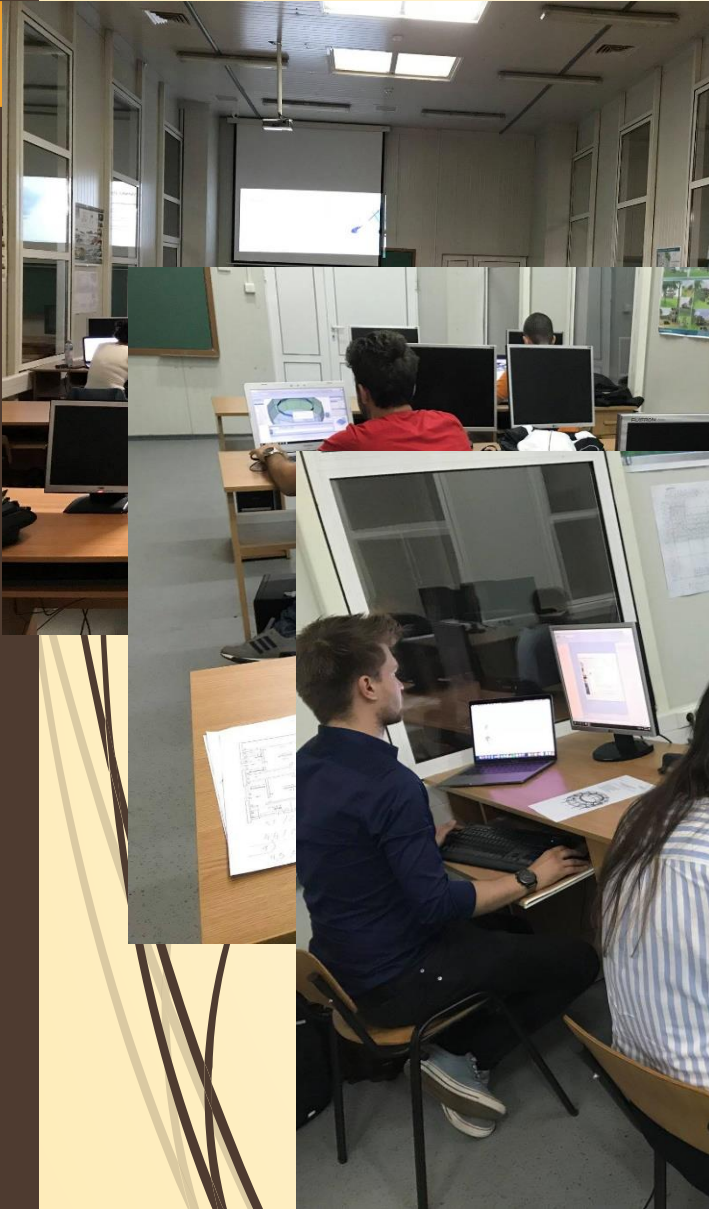
OTHER INFORMATION

- Member in the implementation team for 4 national projects and 2 international one.
- Scientific publications: 4 books 40 articles in BDI journals, ISI proceeding conferences and other international conferences.
- Member in scientific committee for several international conferences and international journals.
- 14 prizes won in national and international student contest

- 1-14 July 2018, 1st BIM – International Summer School, organized by Civil Engineering and Building Services Faculty, Architecture Faculty from “Gheorghe Asachi” Technical University Iasi and ALLBIM.net and SACS (<http://www.iss.ci.tuiasi.ro>) – organizer and team member

November 2017 – Participant at Allplan basic and advanced courses, held by Allbim Romania at Civil Engineering and Building Services Faculty, “Gheorghe Asachi” Technical University Iasi, Romania.

- November 2017 – Participant at SCIA basic and advanced courses, held by Allbim Romania at Civil Engineering and Building Services Faculty, “Gheorghe Asachi” Technical University Iasi, Romania.
- February – April 2017 – Participant at EMIT English as Medium of Instruction for Technical Higher Education, “Gheorghe Asachi” Technical University Iasi, Romania.
- 16 – 19 November 2016 - International Conference - Towards a Sustainable Urban Environment (EBUILT-2016), Civil Engineering and Building Services Faculty, “Gheorghe Asachi” Technical University Iasi, Romania.
- 24-28, July 2016 Participation at 5th International Conference on Integrity–Reliability-Failure, Porto, Portugal.
- 21st June – 1st July 2016 – main organizer of practical courses of Allplan and SCIA held by Nemetschek Romania at, Civil Engineering and Building Services Faculty, “Gheorghe Asachi” Technical University Iasi, Romania.
- 16-29 August 2015 – Participant Școală de vară în cadrul programului „Adoptă o Casă la Roșia Montana – Campania 2015”, organizat de Asociația „Arhitectură. Restaurare. Arheologie” (Summer School “Adopt a house in Rosia Montana” - 2015 campaign, organized by “Architecture. Restoration. Archeology” Association), Rosia Montana, Romania.
- 10-11 June 2015 - Participation at “Building Smart for smarter Cities”, organized by Austrian Federal Economic Chamber and the Enterprise Europe Network Austria, Vienna, Austria.
- 12-14 September 2012 – Participant at Advanced course for Atena software organized by Cervenka Consulting Prague, Czech Republic.
- 16-30 September 2012 – Participant at Summer School on Advances in Heat Transfer Enhancement: from basic to nano, 2-nd edition, “Gheorghe Asachi” Technical University Iasi, Romania.



2ND

BIM-iss

BIM - International Summer School

24.06

5.07

2019

LEARN HOW TO BUILD THE FUTURE

in a comprehensive training that prepares you to successfully face any architectural/engineering challenge, conducted by ALLBIM NET trainers and by professors from the Faculty of Civil Engineering and Building Services, TUIASI.

Training fees:

- > 125 Euro - Bachelor, Master and PhD students; professors
- > 250 Euro - architects; engineers

BIM-iss Contact: Ioana Olteanu-Dontov

ioana.olteanu@tuiasi.ro +40 742 459 730
"Gheorghe Asachi" Technical University of Iasi, Romania

www.iss.ci.tuiasi.ro

Event organizers:



Event partners:



LEARN HOW TO BUILD THE FUTURE

1ST BIM-iss

1-13.07.2018

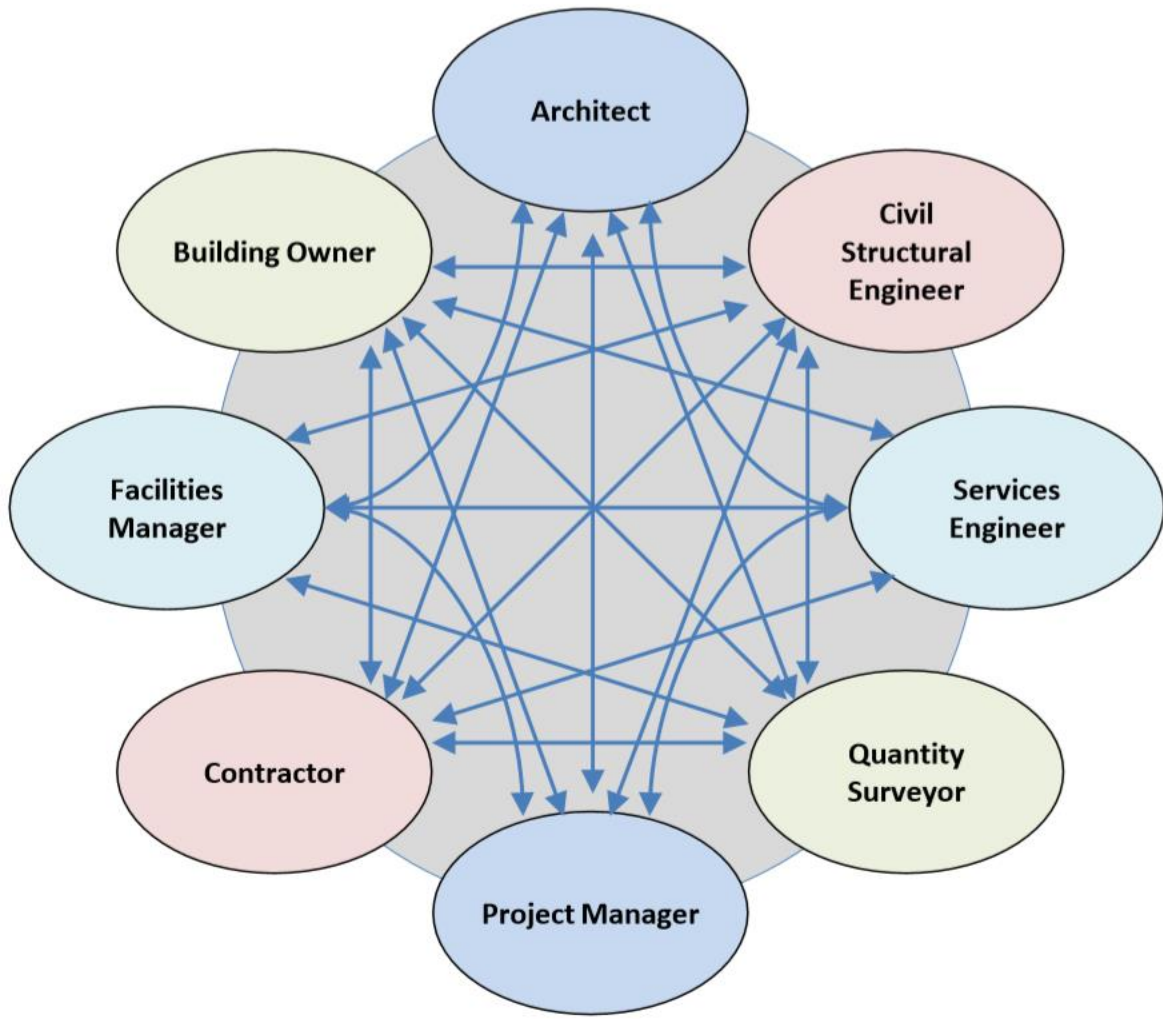


Event partners:

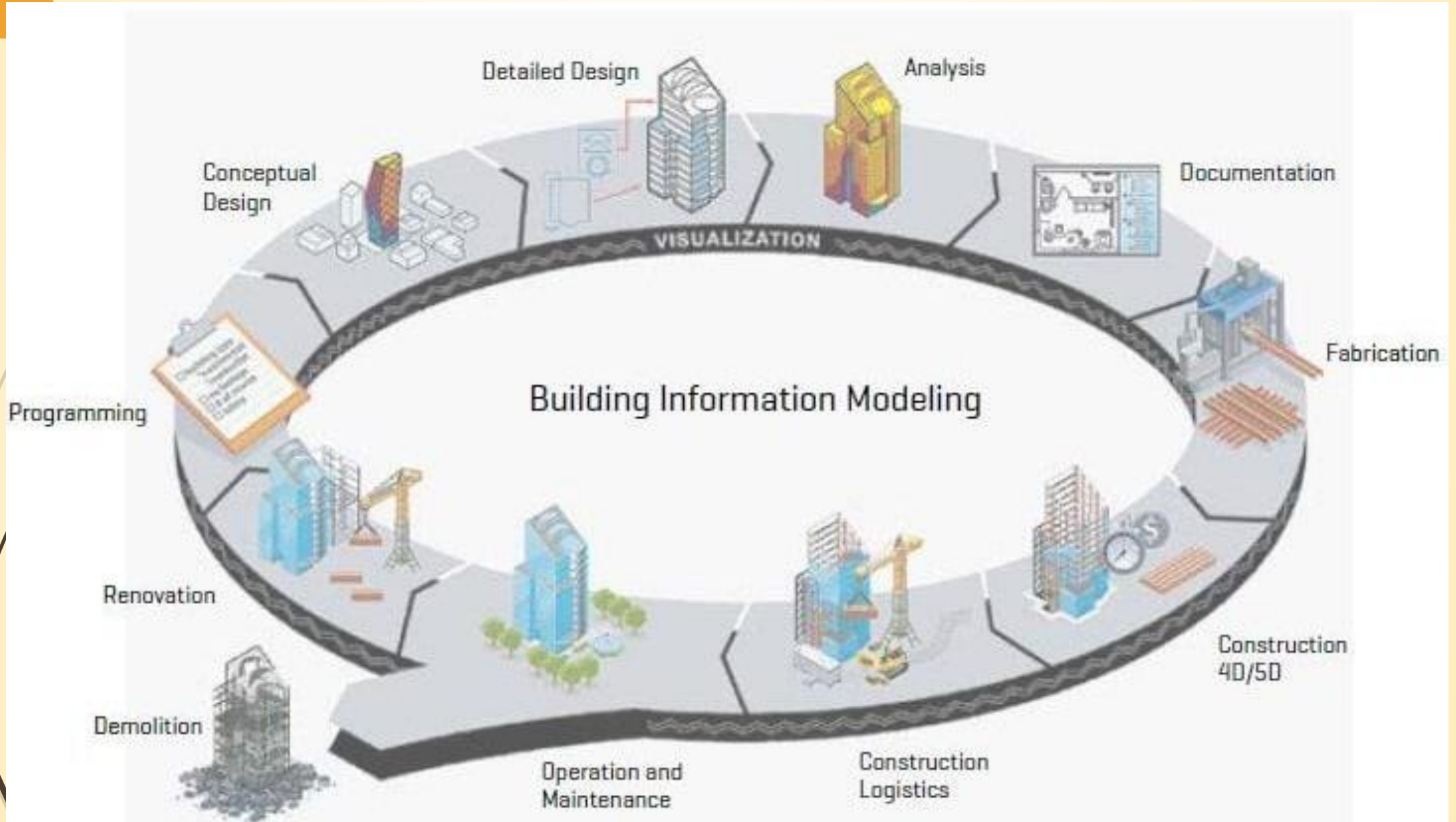


My research





Building SMART for a sustainable building industry



Enhanced visualizations

Time and costs savings

Refined end product

Improved project monitoring

Improved end-user/customer satisfaction

Ease of information exchange across the entire value chain

Benefits of BIM

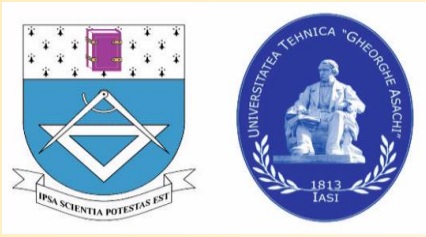
Improved quality

Increased sustainability

Expedites pace of the Construction Cycle

Clarity and accountability in decision making

Helps improve coordination



Technical University Gheorghe Asachi from Iasi, Romania
Faculty of Civil Engineering and Building Services
Structural Mechanics Department

Teaching and learning in a prestigious university from Iasi, Romania

Senior Lecturer **Ioana Olteanu-Dontov, PhD**

ioana.olteanu@tuiasi.ro

Criteria for a Primary Assessment of Buildings for Soft Story Existence: The Case of Sofia Center



Scale of the problem under consideration

- more than 850,000 victims since the beginning of the 21st century, worldwide, as a result of earthquakes;
- collapse of buildings or structures cause more than 75% of the human casualties;
- significantly more human casualty levels in bottom-up collapsed buildings.



Potential financial losses

- $\approx 11,562\text{m}^2$ threatened by the presence of a weak floor;
- approximately EUR 270 million Euro;
- potential damage and destruction in adjacent buildings, sidewalks, cars and so on;
- potential losses from missed benefits.

Seismic risk and geological characteristics of the Sofia Valley

- Sofia city population of more than 1,5 mil.;
- peak ground acceleration (PGA) of 0,26g.

Geological features of the studied area

- soil below the section consists of Alluvial clays and gravel;
- relatively high groundwater level;
- predisposition to liquefaction during the earthquake.



I. First Stage of the Study

Collecting information from a foreign experience related to the soft story presence. It includes the results of **experimental investigations, computer modeling** and **analyzes** of previous earthquakes with significant financial and human losses.

Main causes for appearance of soft floor

- misunderstanding of the role of masonry infills;
- location of destruction- in the masonry or in the surrounding reinforced concrete frame;
- location of masonry infills in plan and height;
- energy dissipation;
- horizontal drift;
- infills with hollow bricks;
- new door or window openings in masonry;
- undesirable formation of short columns and joints.



Accompanying structural factors that have a strong effect on the seismic capacity and for the formation of the soft floor

Report highlights the structural defects that led to 780,000 building collapses or damage beyond repair - "Observed Seismic Behavior of Buildings in Northern Pakistan during the 2005 Kashmir Earthquake" :

- lack of proper confinement in columns;
- improper compaction of concrete;
- notching of concrete column for door and window lintel beam;
- inadequate steel anchoring;
- incorrect joint implementation;
- short column;
- strong beam-weak column;
- soft story.

II. Second stage of the study - Comparison of the foreign earthquake experience with the Bulgarian building practices. Analysis of the endangered load-bearing elements in the buildings constructed before 1987.



For the buildings surveyed in the field study, three basic structural systems were applied:

- **wall bearing system** of masonry with clay or natural stones, wooden floor and roof structures - up to 1920;
- **wall bearing system of solid**, reinforced masonry with reinforced concrete slabs and girders. The last floor level and the roof are of wooden structures – 1920 - 1957;
- **reinforced concrete skeleton** systems with columns, beams and slabs, masonry fillings of solid or hollow bricks. Wooden roof structures - after 1957



1



3



2

Buildings are often calculated as frames without taking into account the effect of masonry infills. Most likely this is the reason why they are not considered as load-bearing elements during the mass renovations aiming for new openings.

Design related problems

- **irregularity** in plan and height;
- many **illegal spatial transformations** affecting the load-bearing structure;
- absence of a mandatory **safety distance between the buildings**;
- **lack of shear walls** according to EC2[], EC6[], EC8[];
- **small number and size of transverse reinforcement** in the columns, girders and shear walls;
- **open hooks in the anchoring** zone of the reinforcement;
- use of **mild steel plain reinforcement** bars, including in longitudinal direction;
- **low density of slab reinforcement**. $6\text{mm}/22\div 30\text{cm}$, which is far below the minimum required;
- **bad detailing** of the column-beam connections;
- floor slabs **saging**;
- **insufficient anchorage length**;
- **absence of reinforced concrete slab in basement** - the floor is visible soil.



Construction quality

- below the minimum **concrete cover** of the reinforcement;
- **weak concrete mixture**;
- **incorrect mixture vibration**;
- improperly arranged **masonry bond**;
- **insufficient slab thickness** in the middle of the sections - often around 6÷7 cm;
- **steel double T profiles** or mild steel plain reinforcement of the slabs;
- **lack of adequate connections** in the wooden roof elements/.

Reinforcement with profiles or sparsely located reinforcement, minimal thickness and large sagging of the slabs are a precondition for incorrect distribution of horizontal forces during the earthquake. Loads transfers from the horizontal elements to the vertical ones will be distributed according to the masses, not according to the stiffness. As a result, early loss of load-bearing capacity is expected in the **weaker vertical elements of the soft floor.**

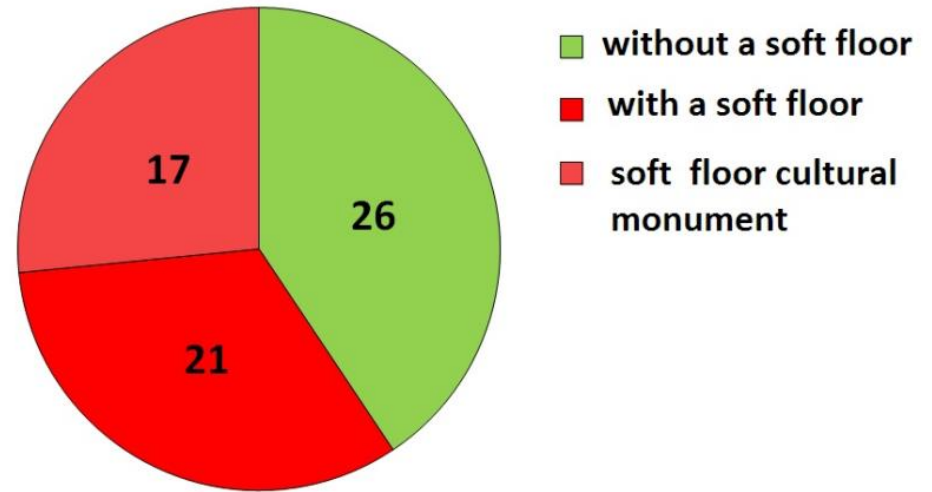
Building reconstructions, age and maintenance related load-bearing deficiencies

- ground floor reconstructions;
- lack of strengthening measures;
- destruction fatigue in materials

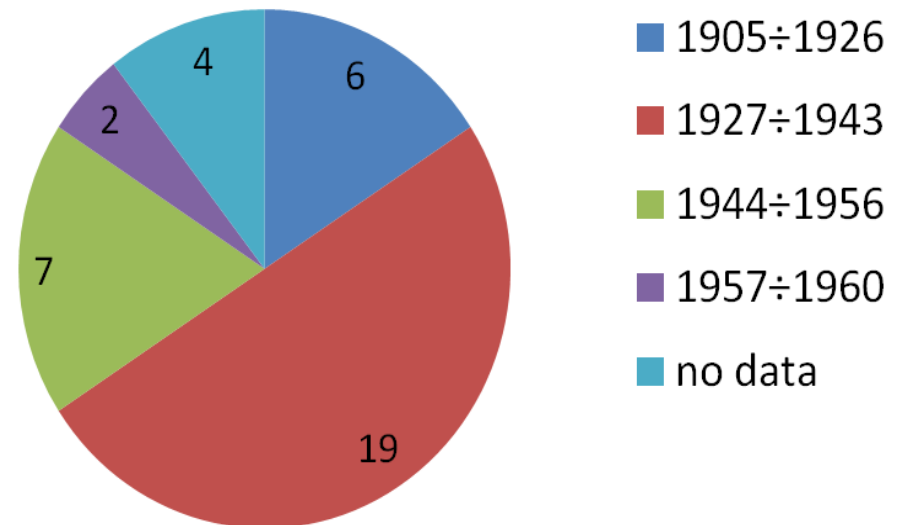
III. Third stage of the study - application of the foreign experience related to the formation of a soft floor for a section of the central boulevard in Sofia.

Analysis of the data collected

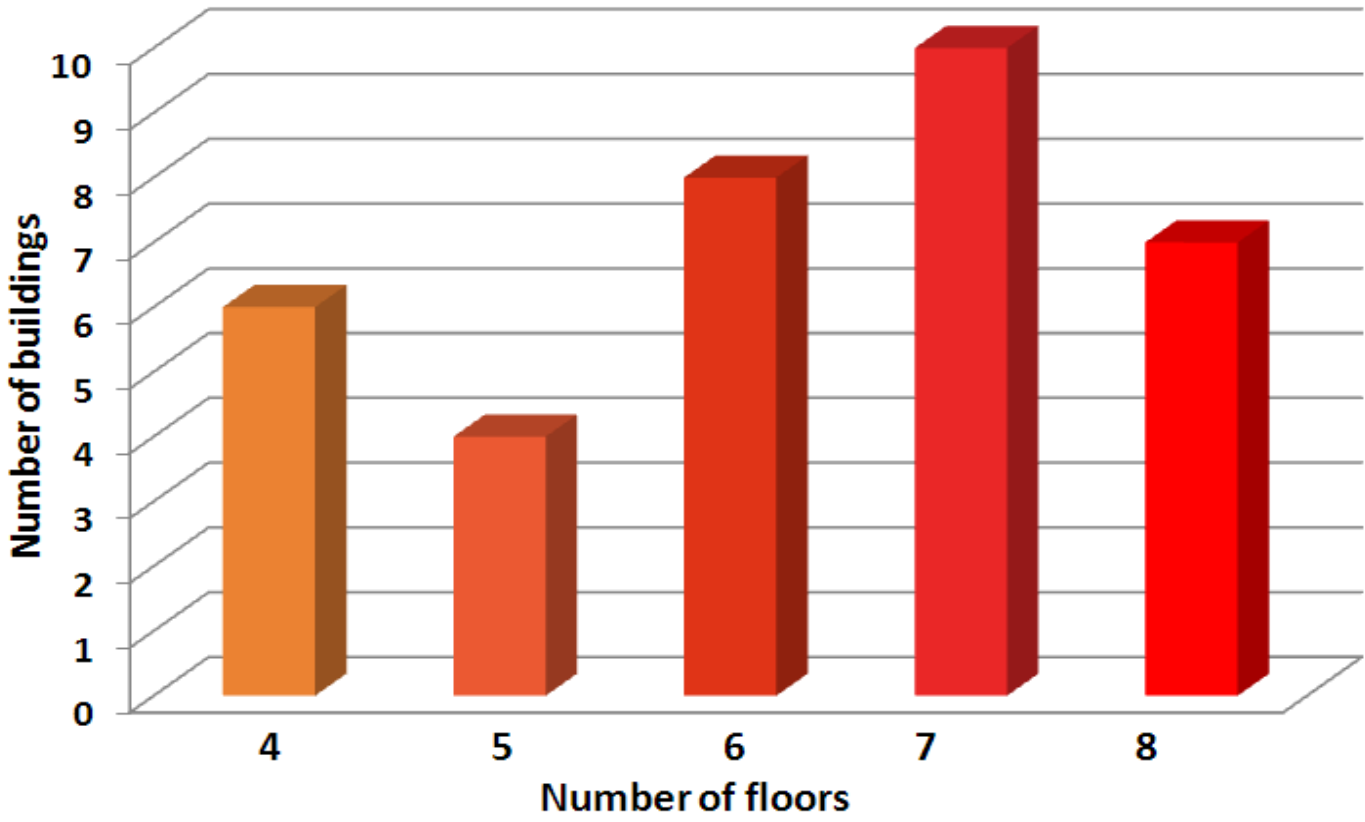
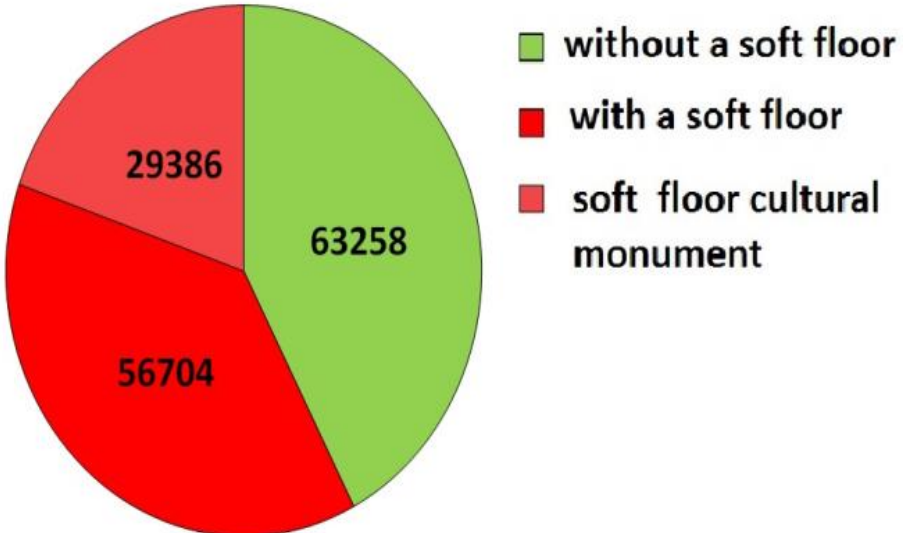
Classified as “soft” storey according to set up criteria



“Soft” storey buildings, according to the year of construction



Built-up area in the examined buildings





Conclusions

- The structural deficiencies summarized in the article clearly outline the vulnerability of earthquake impacts to the buildings in question;
- The scale of destruction predicted in the article, even in a future low-devastating earthquake (EMS), covers more than half of the buildings along the considered section;
- The most expected mechanism of destruction for these buildings is "bottom-up" collapse due to the presence of a ground "soft" floor;
- The financial balance of potential material losses, as well as human losses, requires measures to be taken at a national level;
- Urgent need of identification and more detailed constructive survey of the most vulnerable to seismic impact buildings;

- Conducting analysis and feasibility study;
- Scope of prevention measures.
- The financial balance of potential material losses, as well as human losses, requires measures to be taken at a national level;
- Identification and more detailed constructive survey of the most vulnerable to seismic impact buildings;
- Scope of prevention measures;
- Establishment of a national program for the implementation of building reinforcement systems.

Thank you!





Masonry Structures FE Simulations for Technical Assessment According to Romanian Design Codes

Authors:

V.M. Venghiac - *Technical University "Gheorghe Asachi" Iasi*

C.P. Neagu - *Technical University "Gheorghe Asachi" Iasi*

Contents:

1. Introduction

2. Theoretical requirements according to P100/3-2019

3. Finite element modelling

3.1. Structural description

3.2. Finite element modelling

3.3. FE analyses results

4. Conclusions

5. References

1. Introduction

Brick structural masonry simulations are challenging from the point of view of modeling their real behavior. On the other hand, there are several design codes requirements for technical assessment of brick masonry rehabilitation that should be considered which increase the difficulty of numerical simulations.

In Romania, a lot of brick masonry structures have withstood important earthquakes during their life cycle and require rehabilitation.

2. Theoretical requirements according to P100-3/2019

Bearing capacity of structural walls under in plane loading

Capable Shear force for eccentric compression failure

$$V_{f1} = \frac{N_d}{c_p \lambda_p} (1 - 1.15 v_d)$$

Capable Shear force for horizontal joint failure

$$V_{f21} = \frac{1.33}{CF \gamma_M} \left(f_{vko} \frac{l_{ad}}{l_c} + 0.4 \sigma_d \right) t l_c$$

Capable Shear force

$$V_{f2} = \min(V_{f21}, V_{f22})$$

Capable Shear force for diagonal failure

$$V_{f22} = \frac{t l_w f_{td}}{b} \sqrt{1 + \frac{\sigma_0}{f_{td}}}$$

Design bearing capacity

$$V_{Rd} = \min(V_{f1}, V_{f2})$$

3. Finite element modeling

A residential building with groundfloor and 2 levels made of unreinforced solid brick masonry with RC slabs is discussed.

Input data:

Peak ground acceleration $a_g=0,2g$;

Year of construction: 1925;

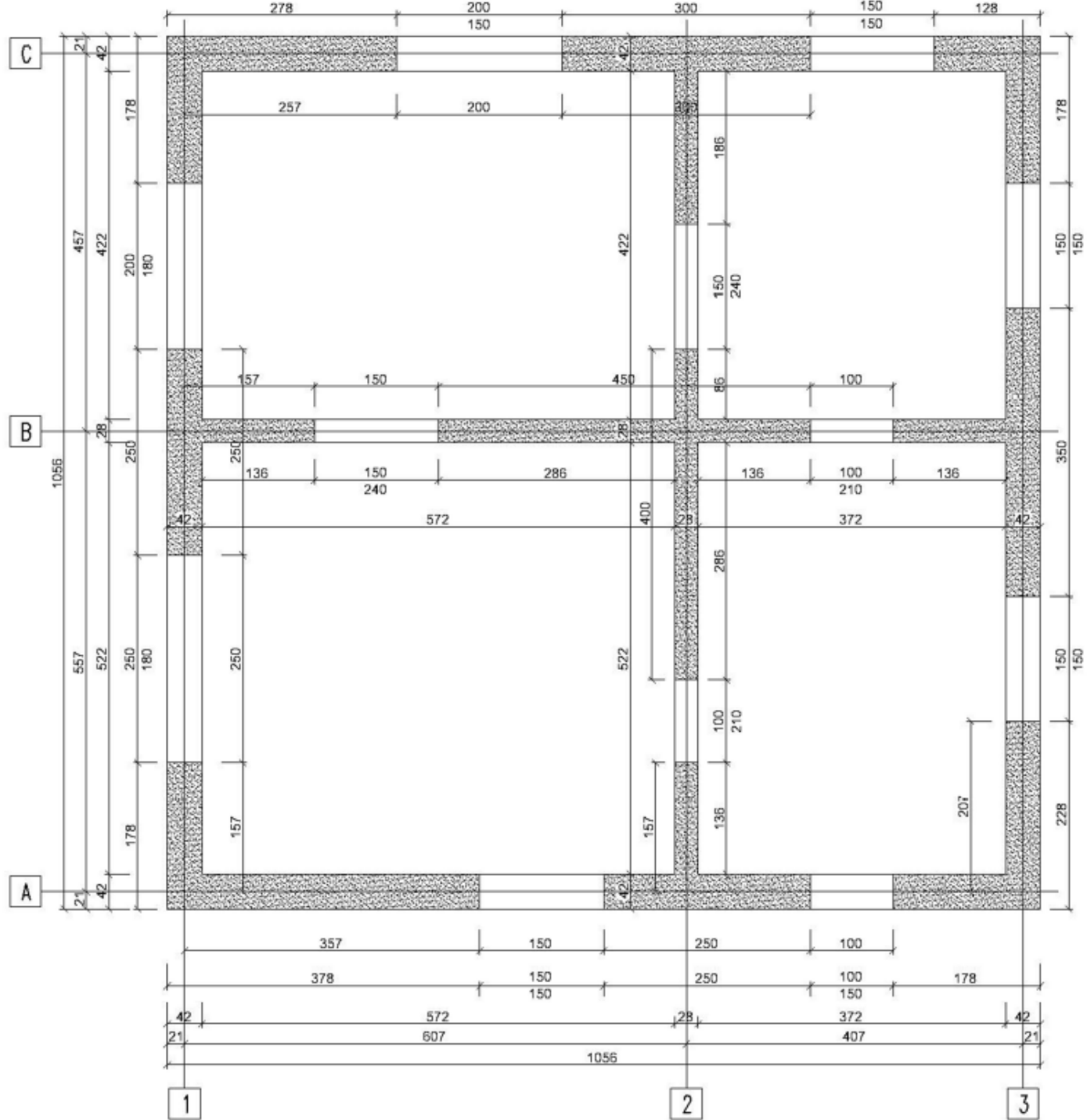
Wall thickness: exterior 42 cm and interior 28 cm;

Same structural layout on all levels;

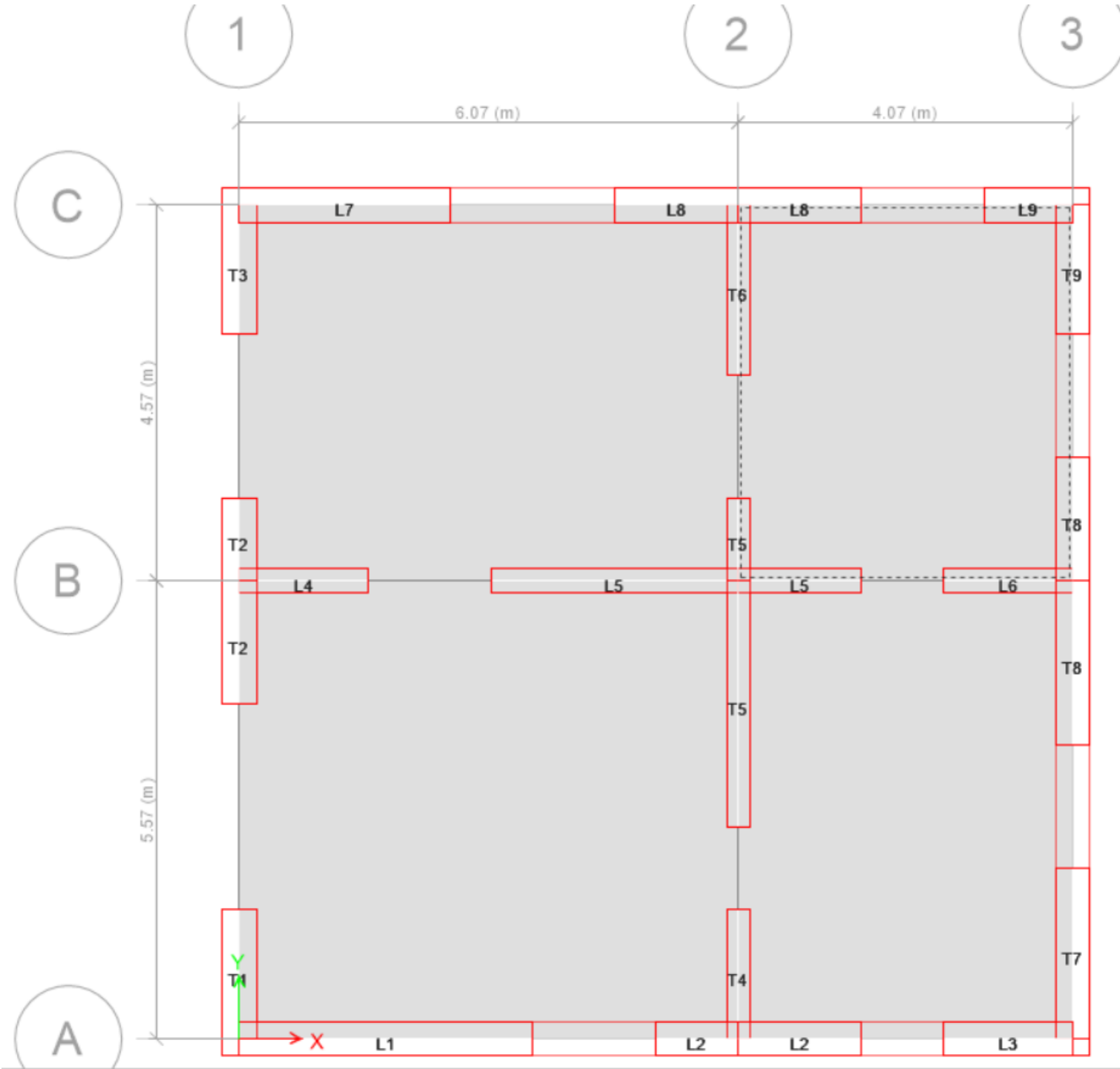
There are no visible degradations from previous earthquakes;

There are no original plans or other technical documents from the time the building was constructed;

The floor plan from the building survey is presented in the following figure.



PIER LABELS

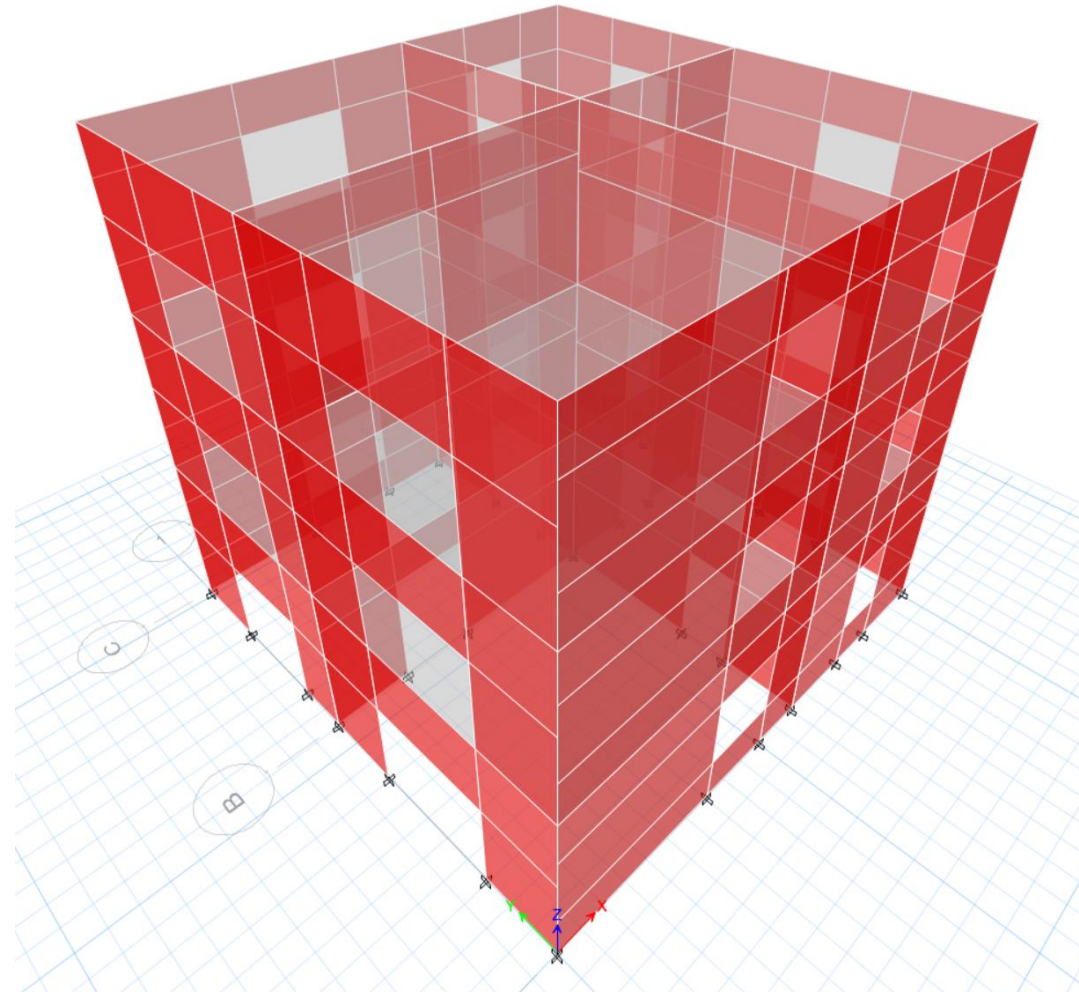


3. Finite element modeling

Model 1 Brick masonry walls with brick spandrels and different lintel types

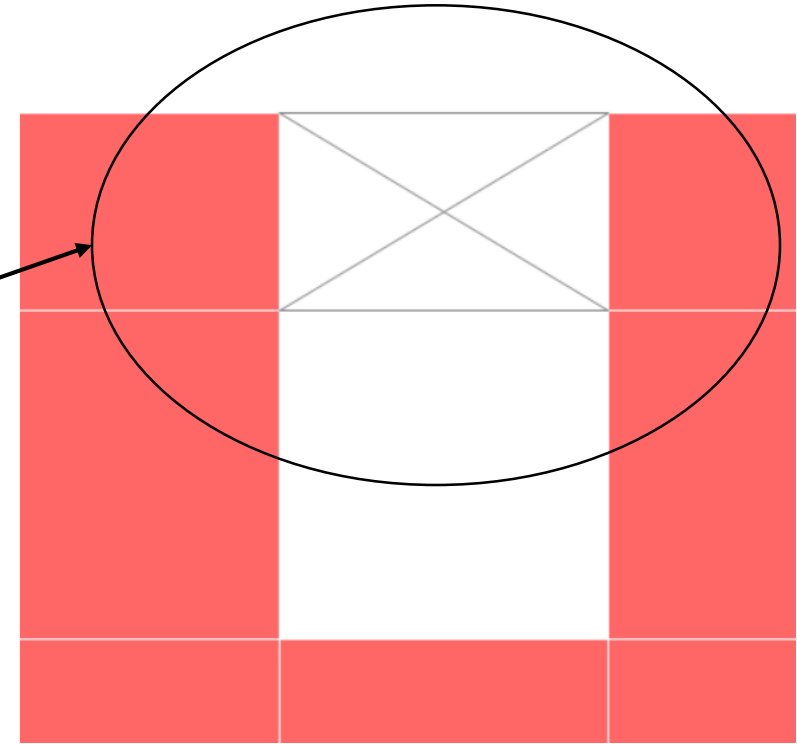
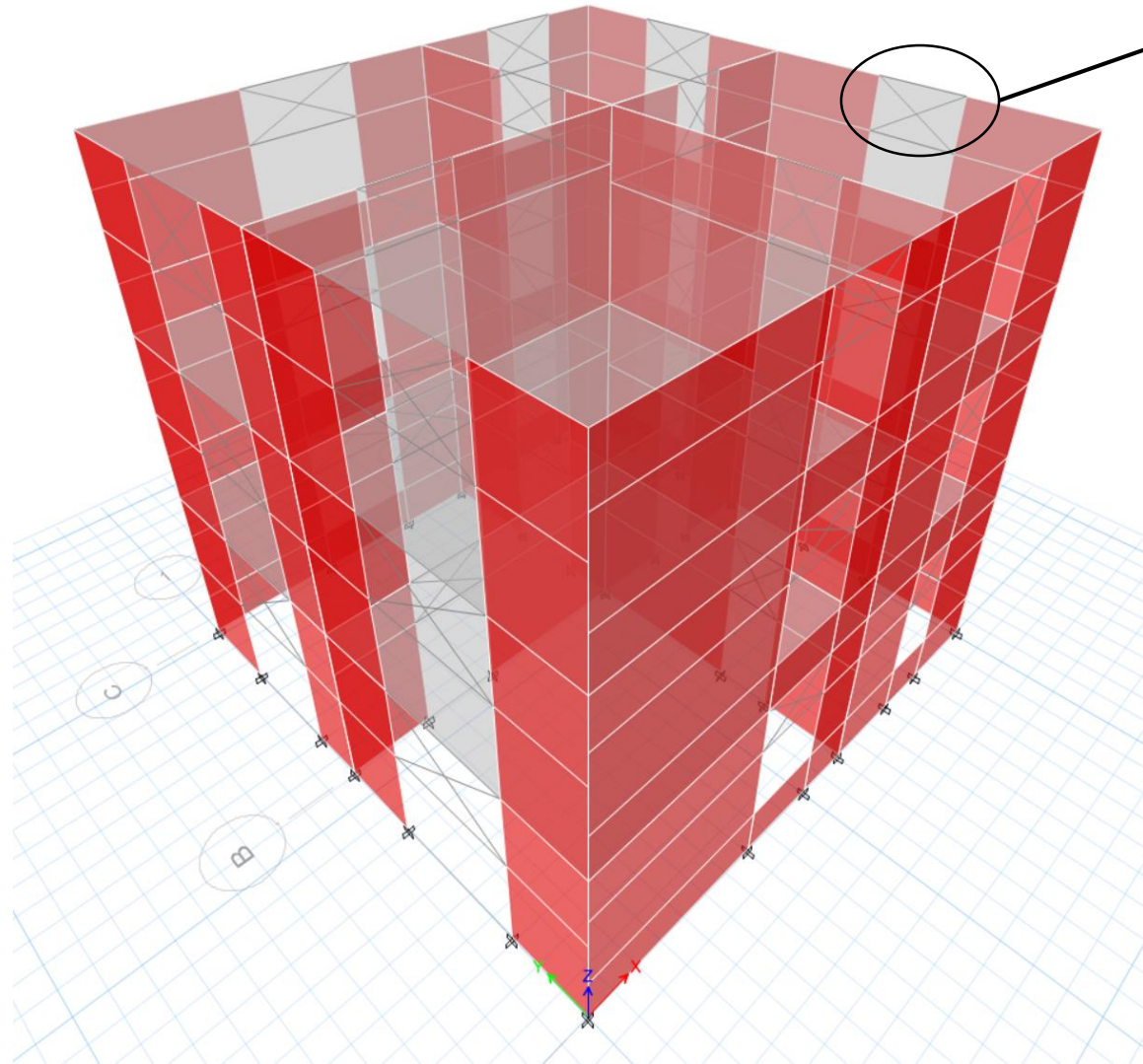
Model 1.1. with timber lintel

Model 1.2 with concrete lintel



3. Finite element modeling

Model 2 Brick masonry walls with line spandrels



Material properties used in the models

Description of material properties		
Model	Material type	Young modulus [N/mm ²]
Model 1	Red brick	2310
Model 1.1	Timber	21000
Model 1.2	Concrete C 16/20	29000
Model 2	Red brick	2310

Response spectrum function (P100-1/2013)

$$S_d(T) = \eta \frac{a_g \beta(T)}{q}$$

where:

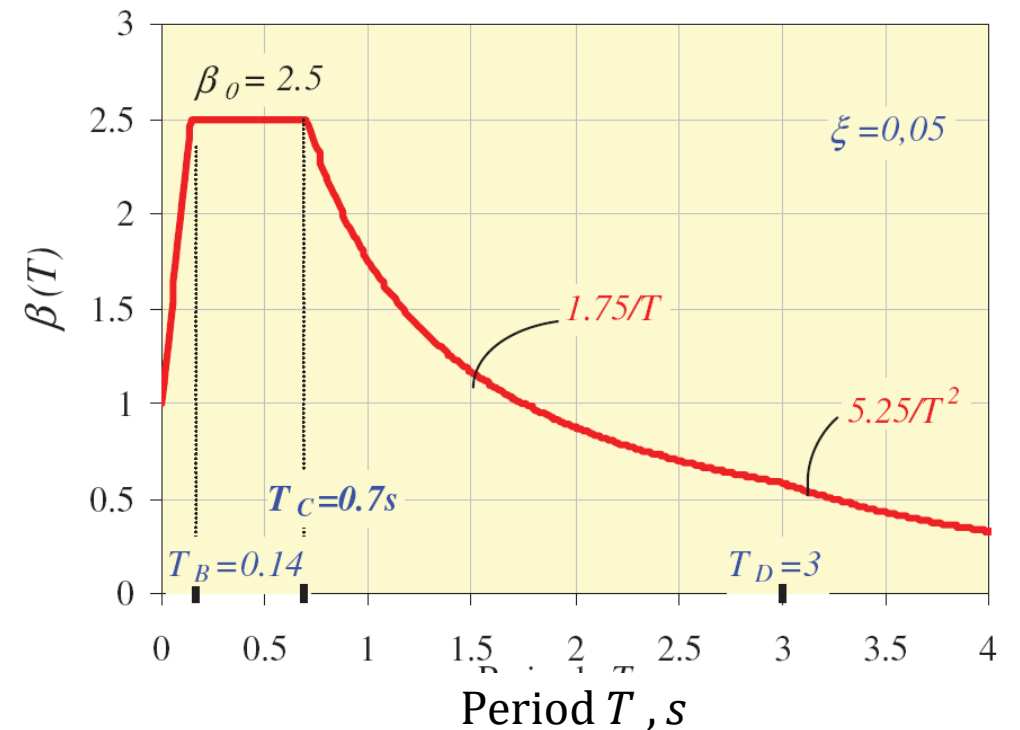
$S_d(T)$ is the design spectral value;

η – correction coefficient taking into account the masonry damping ($\eta = 0.88$);

a_g – peak ground acceleration ($a_g = 0.2g$);

$\beta(T)$ – normalised elastic spectral value (see figure below);

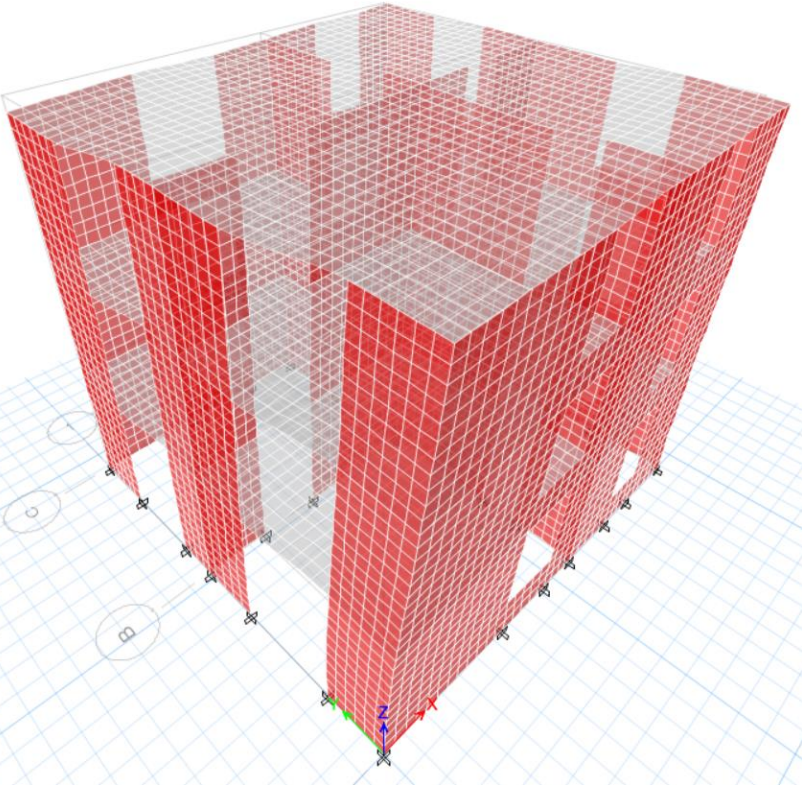
q – behaviour factor (for unreinforced brick masonry $q = 1.5$).



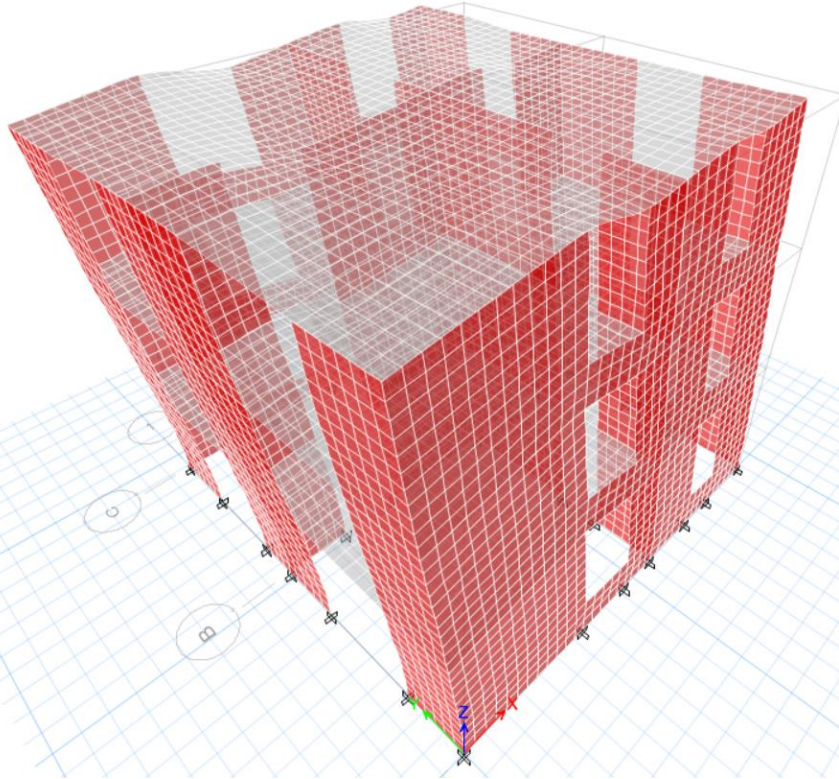
MODAL ANALYSES RESULTS

Periods of vibration [sec]					
	Model 1	Model 1.1	Model 1.2	Model 2	Model 3 Hand computation
1 st mode	0.168 s	0.165 s	0.166 s	0.251 s	0.251 s
2 nd mode	0.160 s	0.158 s	0.158 s	0.192 s	-
3 rd mode	0.111 s	0.109 s	0.110 s	0.139 s	-
4 th mode	0.056 s	0.056 s	0.056 s	0.073 s	-

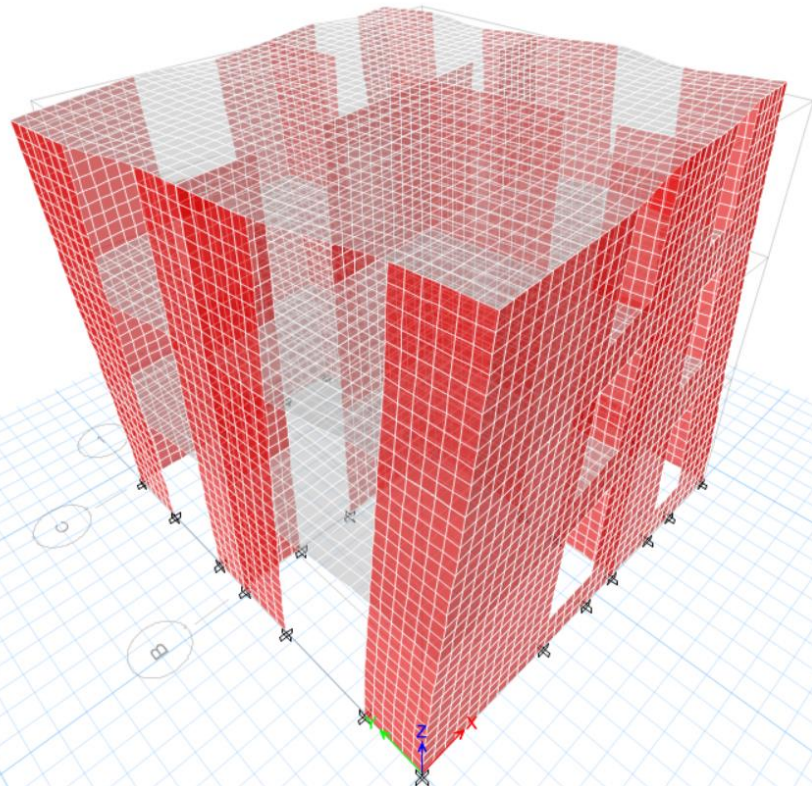
MODAL ANALYSES RESULTS



Mode 1



Mode 2



Mode 3

TABLE RESULTS – SEISMIC RISK CLASS ACCORDING TO P100-3/2019

MODEL 1

Pier	Load Case/ Combo	P	V2	M3	Vf1	Vf21	Vf22	Vf2min	Vcap	R3i	Ved	Failure type (Ductile/ Fragile)				
		kN	kN	kNm	kN	kN	kN	kN	kN		kN					
T1	GSY+ Max	-216.9	97.57	104	99.161	54.009	50.599	50.599	50.599	0.5186	97.572	F	R3T	R3L	R3	Risk class
T2	GSY+ Max	-408.4	228	341.6	246.19	66.801	92.319	66.801	66.801	0.2929	228.04	F	0.56519	0.78006	0.56519	RsII
T3	GSY+ Max	-208	116.7	114.5	95.803	30.674	49.658	30.674	30.674	0.2629	116.68	F				
T4	GSY+ Max	-145.8	44.82	49.16	66.545	66.434	33.856	33.856	33.856	0.7554	44.817	F				
T5	GSY+ Max	-482.6	200.1	387.5	449.67	161.2	135.94	135.94	135.94	0.6795	200.07	F				
T6	GSY+ Max	-182.4	70.29	86.69	107.12	75.296	44.476	44.476	44.476	0.6327	70.295	F				
T7	GSY+ Max	-161.5	63.36	73.96	101.71	101.93	53.018	53.018	53.018	0.8368	63.361	F				
T8	GSY+ Max	-424.3	155.9	274.3	381.8	200.43	148.9	148.9	148.9	0.955	155.92	F				
T9	GSY+ Max	-81.4	45.18	73.75	41.398	13.316	33.465	13.316	13.316	0.2947	45.182	F				
L1	GSX+ Max	-405.6	167.7	254.1	402.28	230.63	152.27	152.27	152.27	0.908	167.7	F				
L2	GSX+ Max	-292.2	105.6	126.2	189	150.89	79.26	79.26	79.26	0.7503	105.64	F				
L3	GSX+ Max	-90.47	56.92	70.44	45.697	14.799	34.875	14.799	14.799	0.26	56.922	F				
L4	GSX+ Max	-164.2	38.81	46.1	73.251	81.577	35.736	35.736	35.736	0.9208	38.812	F				
L5	GSX+ Max	-498	223.3	462.7	538.18	170.47	147.33	147.33	147.33	0.6597	223.33	F				
L6	GSX+ Max	-138	51.22	49.06	63.632	61.45	33.039	33.039	33.039	0.645	51.224	F				
L7	GSX+ Max	-270.5	97.78	137	200.15	151.02	90.351	90.351	90.351	0.924	97.78	F				
L8	GSX+ Max	-408.7	135.3	215.5	308.24	187.53	122.32	122.32	122.32	0.904	135.31	F				
L9	GSX+ Max	-92.62	25.9	30.95	32.674	34.816	28.977	28.977	28.977	1.1188	25.9	F				

TABLE RESULTS – SEISMIC RISK CLASS ACCORDING TO P100-3/2019

MODEL 1.1

Pier	Load Case/ Combo	P	V2	M3	Vf1	Vf21	Vf22	Vf2min	Vcap	R3i	Ved	Failure type (Ductile/ Fragile)				
		kN	kN	kNm	kN	kN	kN	kN	kN	kN	kN		kN			
T1	GSY+ Max	-224.2	101.5	104.5	101.87	59.205	51.359	51.359	51.359	0.506	101.51	F	R3T	R3L	R3	Risk class
T2	GSY+ Max	-415.4	229.2	329.4	249.32	47.809	93.05	47.809	47.809	0.2086	229.23	F	0.55714	0.77237	0.55714	RsII
T3	GSY+ Max	-219.5	117.5	111.8	100.13	44.764	50.871	44.764	44.764	0.381	117.49	F				
T4	GSY+ Max	-148.4	44.59	48.24	67.544	69.481	34.135	34.135	34.135	0.7655	44.591	F				
T5	GSY+ Max	-482.4	198.1	373.1	449.52	167.98	135.91	135.91	135.91	0.6862	198.06	F				
T6	GSY+ Max	-189.6	70.83	84.73	110.56	82.368	45.256	45.256	45.256	0.639	70.827	F				
T7	GSY+ Max	-162	65.47	73.3	101.99	103.61	53.086	53.086	53.086	0.8108	65.471	F				
T8	GSY+ Max	-427.4	159.1	268.3	384.07	206.87	149.38	149.38	149.38	0.9392	159.06	F				
T9	GSY+ Max	-82.65	46.24	72.69	41.995	13.521	33.663	13.521	13.521	0.2924	46.237	F				
L1	GSX+ Max	-402.4	169.8	249.5	399.61	232.11	151.74	151.74	151.74	0.8937	169.79	F				
L2	GSX+ Max	-293.1	107.4	124.4	189.52	153.4	79.377	79.377	79.377	0.739	107.42	F				
L3	GSX+ Max	-91.39	57.89	69.71	46.131	14.95	35.015	14.95	14.95	0.2583	57.888	F				
L4	GSX+ Max	-168	39.82	46.14	74.564	83.531	36.105	36.105	36.105	0.9068	39.819	F				
L5	GSX+ Max	-504.7	222	446.8	543.43	181.35	148.23	148.23	148.23	0.6676	222.02	F				
L6	GSX+ Max	-141.3	51.36	48.08	64.879	65.141	33.389	33.389	33.389	0.6501	51.359	F				
L7	GSX+ Max	-264.2	100	135.4	196.11	148.12	89.418	89.418	89.418	0.8942	100	F				
L8	GSX+ Max	-412.1	138.2	210	310.32	193.9	122.79	122.79	122.79	0.8882	138.25	F				
L9	GSX+ Max	-91.04	25.94	30.5	32.173	34.378	28.768	28.768	28.768	1.1092	25.937	F				

TABLE RESULTS – SEISMIC RISK CLASS ACCORDING TO P100-3/2019

MODEL 1.2

Pier	Load Case/ Combo	P	V2	M3	Vf1	Vf21	Vf22	Vf2min	Vcap	R3i	Ved	Failure type (Ductile/ Fragile)				
		kN	kN	kNm	kN	kN	kN	kN	kN	kN	kN		kN			
T1	GSY+ Max	-227.2	102.7	105.9	102.98	59.578	51.67	51.67	51.67	0.5031	102.71	F	R3T	R3L	R3	Risk class
T2	GSY+ Max	-422.2	232	332.8	252.3	50.016	93.75	50.016	50.016	0.2156	231.99	F	0.5561	0.76729	0.5561	RsII
T3	GSY+ Max	-222.9	119.2	113.1	101.41	45.814	51.228	45.814	45.814	0.3843	119.22	F				
T4	GSY+ Max	-150.2	45.11	48.78	68.178	69.765	34.313	34.313	34.313	0.7606	45.112	F				
T5	GSY+ Max	-486.3	200.2	377.2	452.12	168.11	136.43	136.43	136.43	0.6814	200.21	F				
T6	GSY+ Max	-192.3	71.62	85.66	111.84	83.081	45.546	45.546	45.546	0.6359	71.621	F				
T7	GSY+ Max	-164	66.2	74.08	103.09	104.07	53.353	53.353	53.353	0.8059	66.203	F				
T8	GSY+ Max	-431.8	160.9	271.2	387.35	207.47	150.09	150.09	150.09	0.9329	160.88	F				
T9	GSY+ Max	-84	46.78	73.58	42.635	13.74	33.874	13.74	13.74	0.2937	46.78	F				
L1	GSX+ Max	-407	171.7	251.9	403.44	233.22	152.51	152.51	152.51	0.8884	171.67	F				
L2	GSX+ Max	-295.8	108.6	125.7	190.93	153.7	79.697	79.697	79.697	0.7339	108.59	F				
L3	GSX+ Max	-91.82	58.55	70.52	46.333	15.02	35.081	15.02	15.02	0.2565	58.549	F				
L4	GSX+ Max	-170.7	40.41	46.71	75.523	84.247	36.376	36.376	36.376	0.9003	40.405	F				
L5	GSX+ Max	-508.9	224.5	451.6	546.81	181.54	148.82	148.82	148.82	0.6629	224.48	F				
L6	GSX+ Max	-143	51.95	48.59	65.523	65.504	33.569	33.569	33.569	0.6462	51.947	F				
L7	GSX+ Max	-267.7	101.2	137.1	198.37	148.85	89.94	89.94	89.94	0.8883	101.25	F				
L8	GSX+ Max	-417.5	140.1	212.3	313.53	195.07	123.52	123.52	123.52	0.8817	140.09	F				
L9	GSX+ Max	-92.76	26.32	30.87	32.72	35.244	28.996	28.996	28.996	1.1018	26.318	F				

TABLE RESULTS – SEISMIC RISK CLASS ACCORDING TO P100-3/2019

MODEL 2

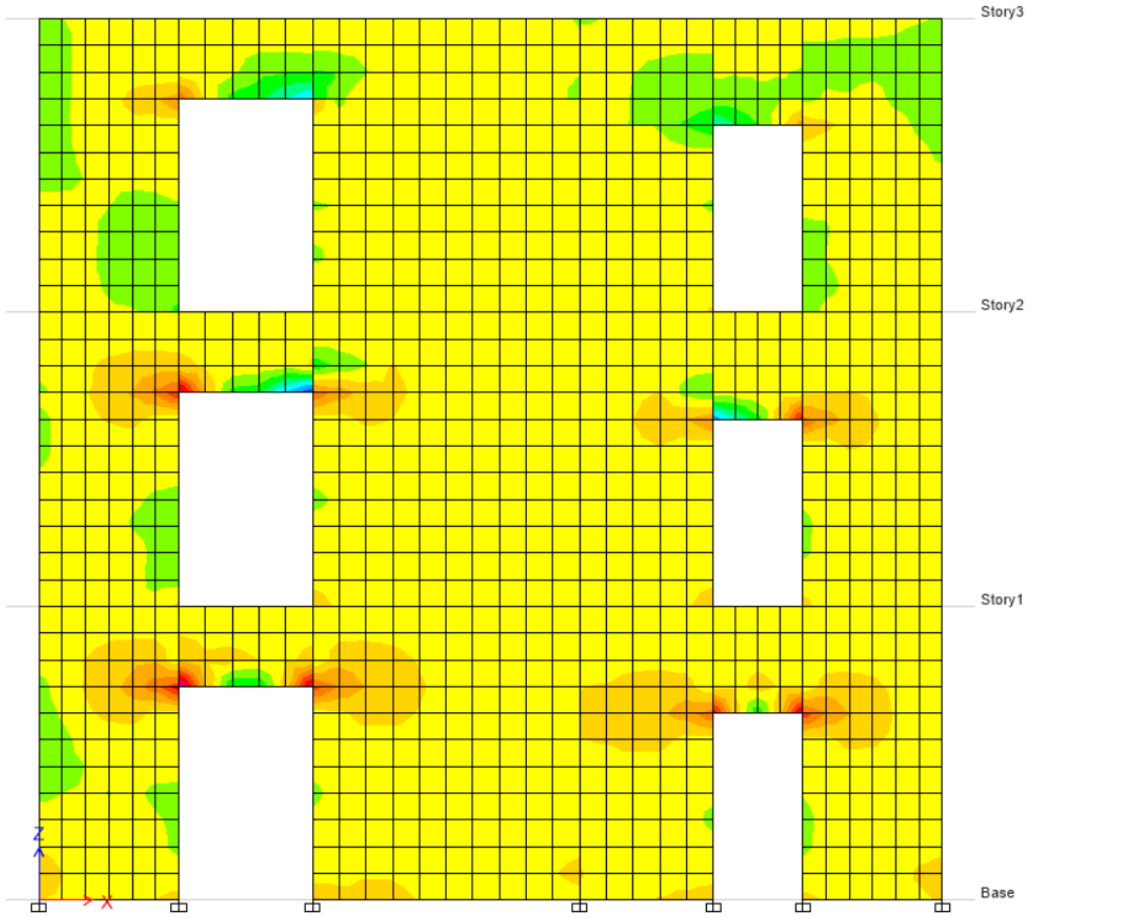
Pier	Load Case/ Combo	P	V2	M3	Vf1	Vf21	Vf22	Vf2min	Vcap	R3i	Ved	Failure type (Ductile/ Fragile)				
		kN	kN	kNm	kN	kN	kN	kN	kN	kN	kN		kN			
T1	GSY+ Max	113.5	79.52	136	56.328	18.562	38.221	18.562	18.562	0.2334	79.517	F	R3T	R3L	R3	Risk class
T2	GSY+ Max	-312.6	134.3	505.5	199.77	51.127	81.701	51.127	51.127	0.3808	134.27	F	0.36364	0.72683	0.36364	RsII
T3	GSY+ Max	122.2	76.88	140.6	60.255	19.989	39.416	19.989	19.989	0.26	76.879	F				
T4	GSY+ Max	-57.24	40.93	66.68	29.014	9.3639	22.777	9.3639	9.3639	0.2288	40.931	F				
T5	GSY+ Max	-396.8	198.4	673.1	389.11	64.914	124.19	64.914	64.914	0.3271	198.45	F				
T6	GSY+ Max	-67.31	68.11	125	43.932	11.011	29.251	11.011	11.011	0.1617	68.109	F				
T7	GSY+ Max	-103.5	47.34	101	67.464	16.934	44.301	16.934	16.934	0.3577	47.336	F				
T8	GSY+ Max	-389.8	125.3	378.3	355.86	93.48	143.35	93.48	93.48	0.7463	125.26	F				
T9	GSY+ Max	-28.24	26.75	77.25	14.931	4.6196	23.551	4.6196	4.6196	0.1727	26.747	F				
L1	GSX+ Max	-418.3	157.7	360.1	412.84	159.34	154.37	154.37	154.37	0.9789	157.7	F				
L2	GSX+ Max	-267.6	77.75	150.3	175.62	106.64	76.217	76.217	76.217	0.9803	77.752	F				
L3	GSX+ Max	-104	40.59	70.5	52	17.013	36.881	17.013	17.013	0.4192	40.585	F				
L4	GSX+ Max	-91.02	33.25	53.3	44.389	9.012	27.537	9.012	9.012	0.271	33.255	F				
L5	GSX+ Max	-474.3	201.8	669.5	518.89	58.727	144.04	58.727	58.727	0.291	201.8	F				
L6	GSX+ Max	-69.15	34.56	52.08	34.582	11.312	24.561	11.312	11.312	0.3273	34.564	F				
L7	GSX+ Max	-286.2	88.14	183.4	210.07	111.87	92.627	92.627	92.627	1.051	88.136	F				
L8	GSX+ Max	-362.8	105.3	282.6	279.95	100.14	115.9	100.14	100.14	0.9507	105.33	F				
L9	GSX+ Max	-101.6	16.98	27.53	35.509	54.717	30.143	30.143	30.143	1.7752	16.98	F				

TABLE RESULTS – SEISMIC RISK CLASS ACCORDING TO P100-3/2019

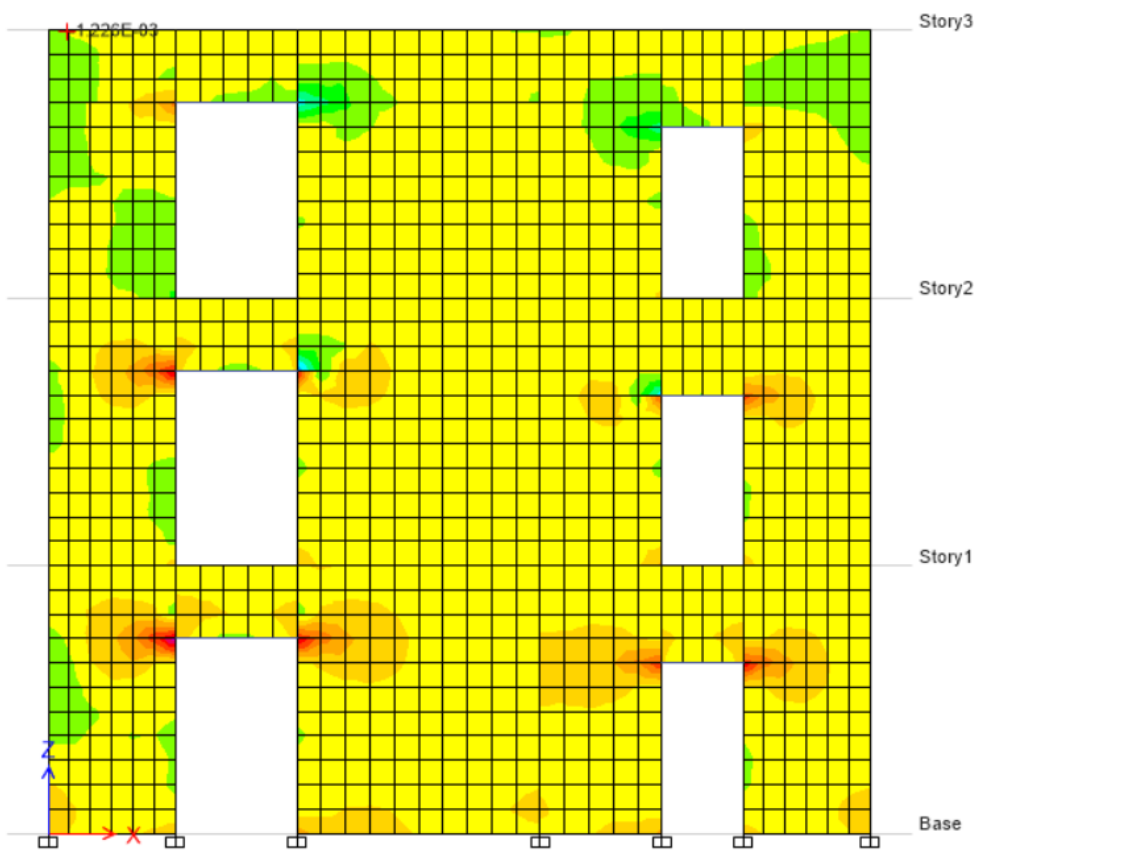
MODEL 3 PRESENTED IN P100-3/2019

Pier	Vf1	Vf21	Vf22	Vcap	R3i	Ved	Failure type (Ductile/ Fragile)				
	kN	kN	kN	kN		kN					
T1	26.69	46.7	57.63	26.69	0.445	60.01	D	R3T	R3L	R3	Risk class
T2	57.5	74.1	85.68	57.5	0.426	135.05	D	0.258	0.257	0.257	Rsl
T3	26.69	46.7	57.63	26.69	0.445	60.01	D				
T4	17.42	30.3	37.93	17.42	0.326	53.43	D				
T5	99.98	81.9	92.71	81.9	0.252	325.44	F				
T6	28.78	39.1	48.79	28.78	0.301	95.49	D				
T7	36.2	46.9	66.03	36.2	0.218	166.1	D				
T8	94.36	81.6	107.41	81.6	0.224	420.54	F				
T9	23.67	39.9	53.64	23.67	0.254	93.25	D				
L1	108.23	86.3	114.85	86.3	0.206	418.5	F				
L2	55.87	72.0	83.25	55.87	0.324	172.34	D				
L3	23.67	39.9	53.64	23.67	0.305	77.58	D				
L4	17.42	30.3	37.93	17.42	0.419	41.55	D				
L5	127.91	92.7	104.88	92.7	0.286	324.03	F				
L6	17.56	30.6	38.11	17.56	0.423	41.55	D				
L7	53.85	57.2	80.53	53.85	0.373	144.51	D				
L8	69.38	70.0	92.1	69.38	0.407	170.58	D				
L9	12.22	28.7	38.53	12.22	0.564	21.67	D				

Interior wall S11 stresses

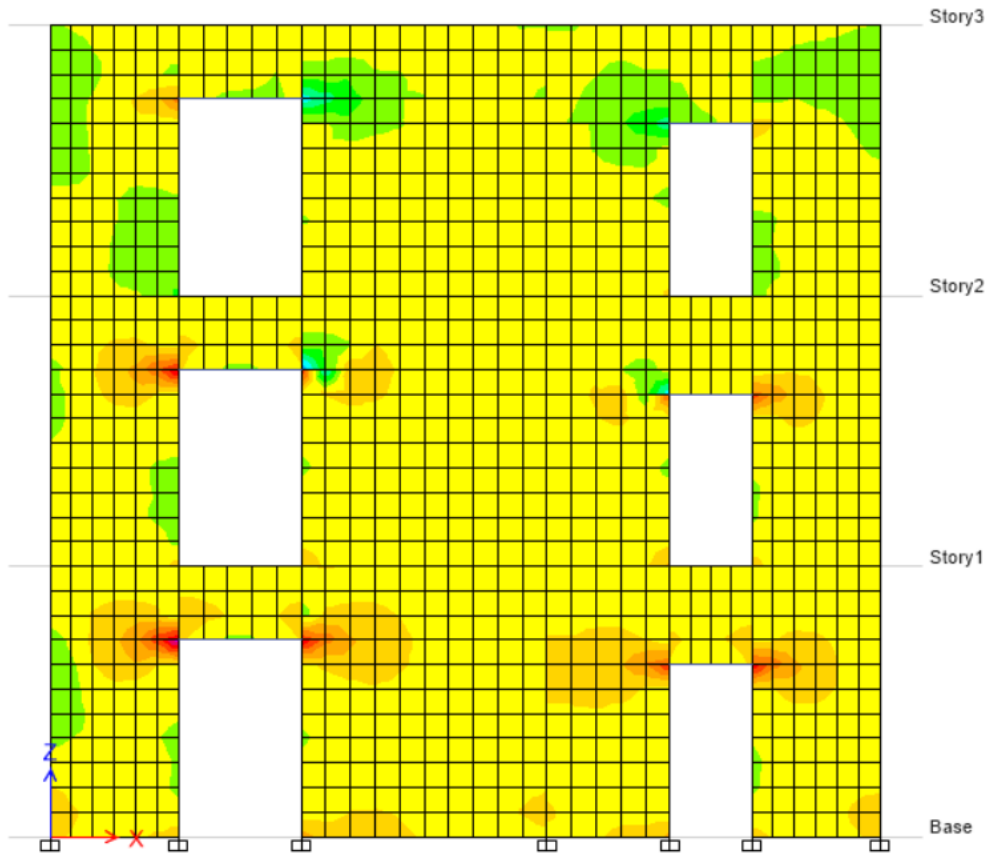


Model 1

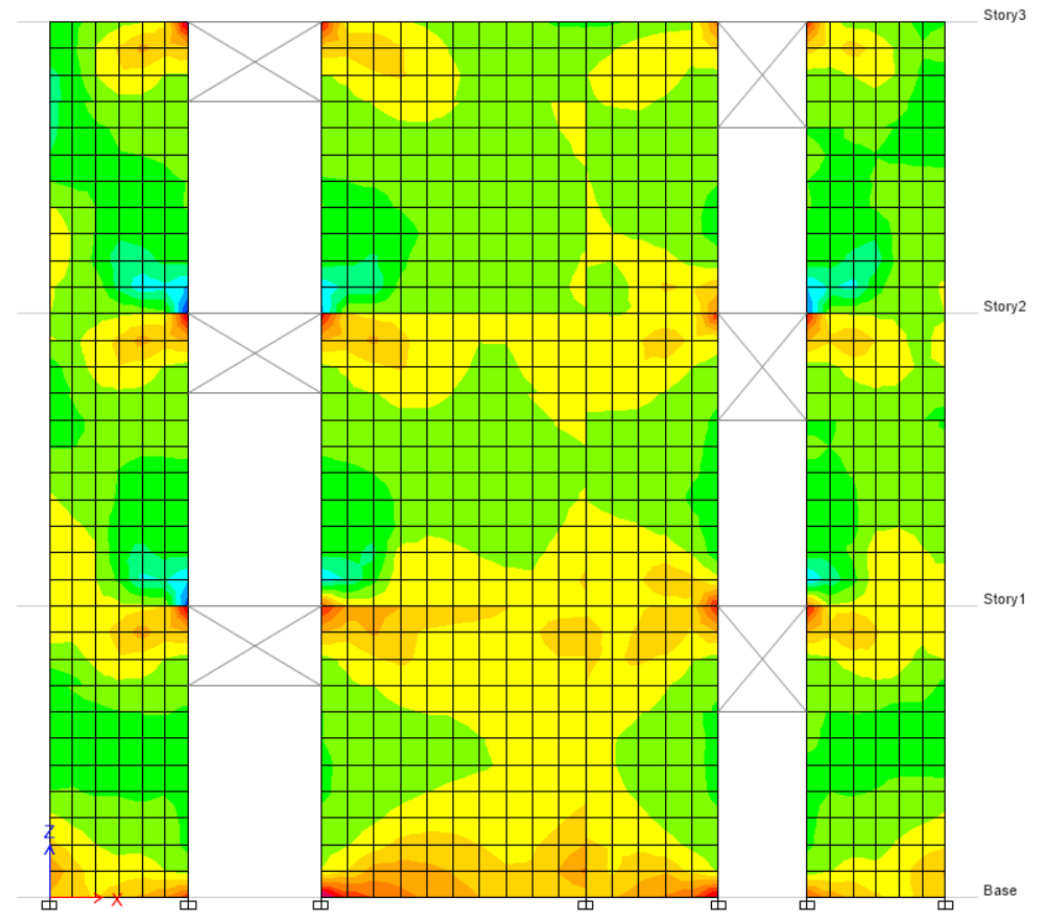


Model 1.1

Interior wall S11 stresses

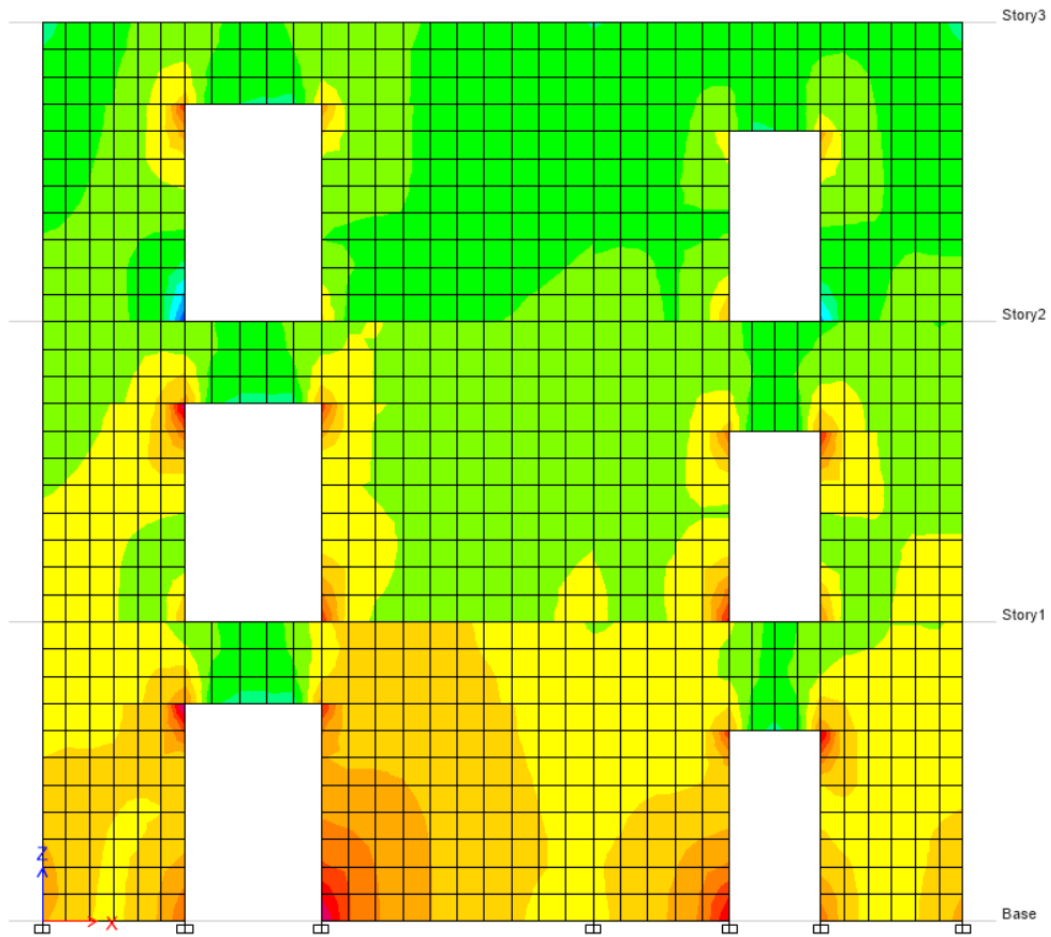


Model 1.2

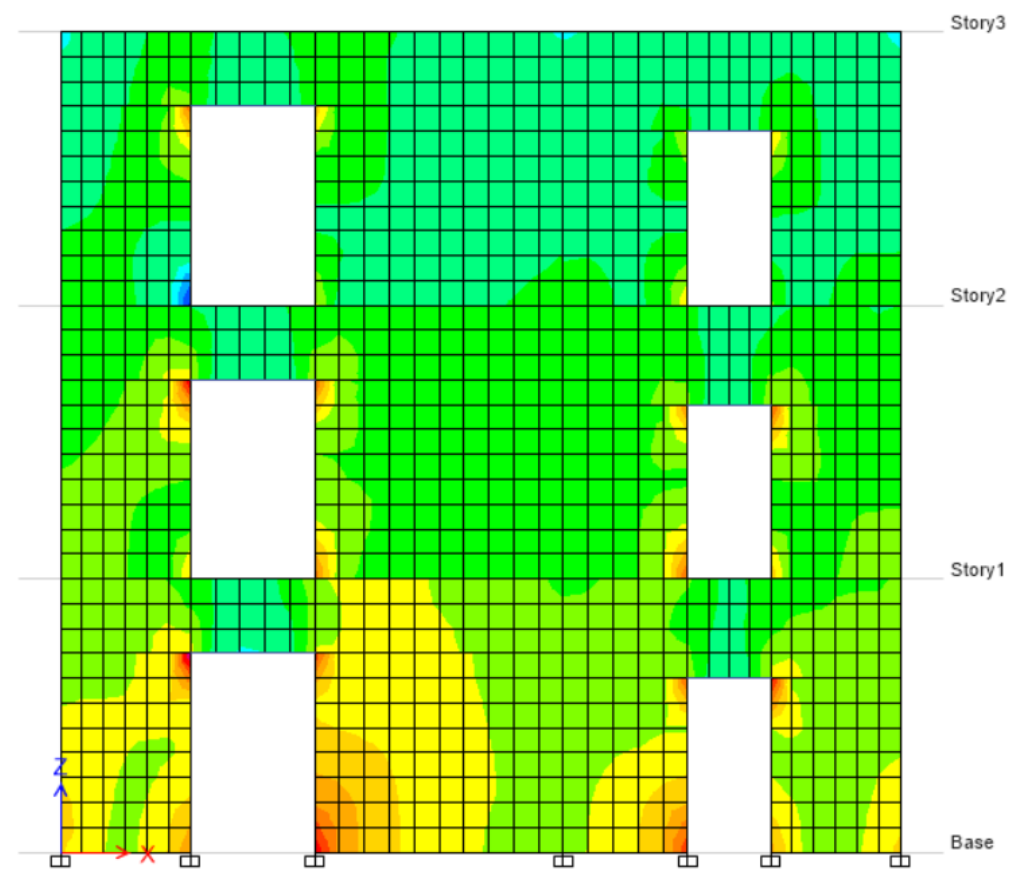


Model 2

Interior wall S22 stresses

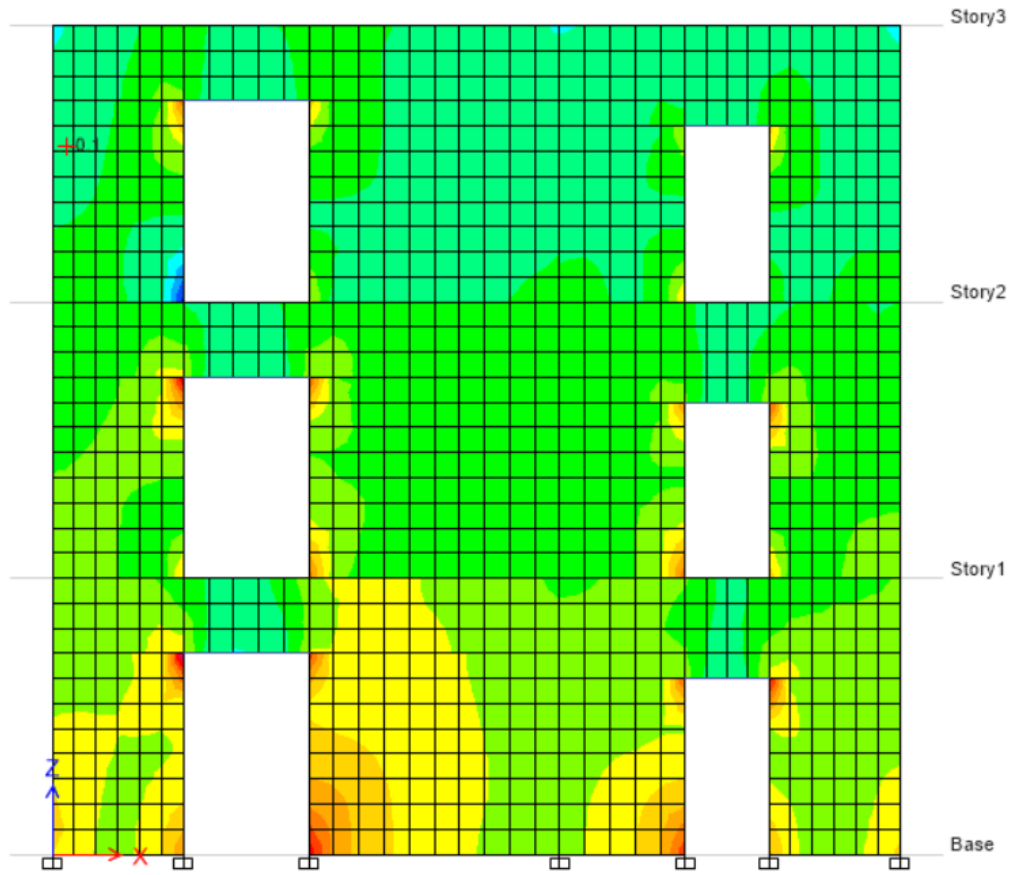


Model 1

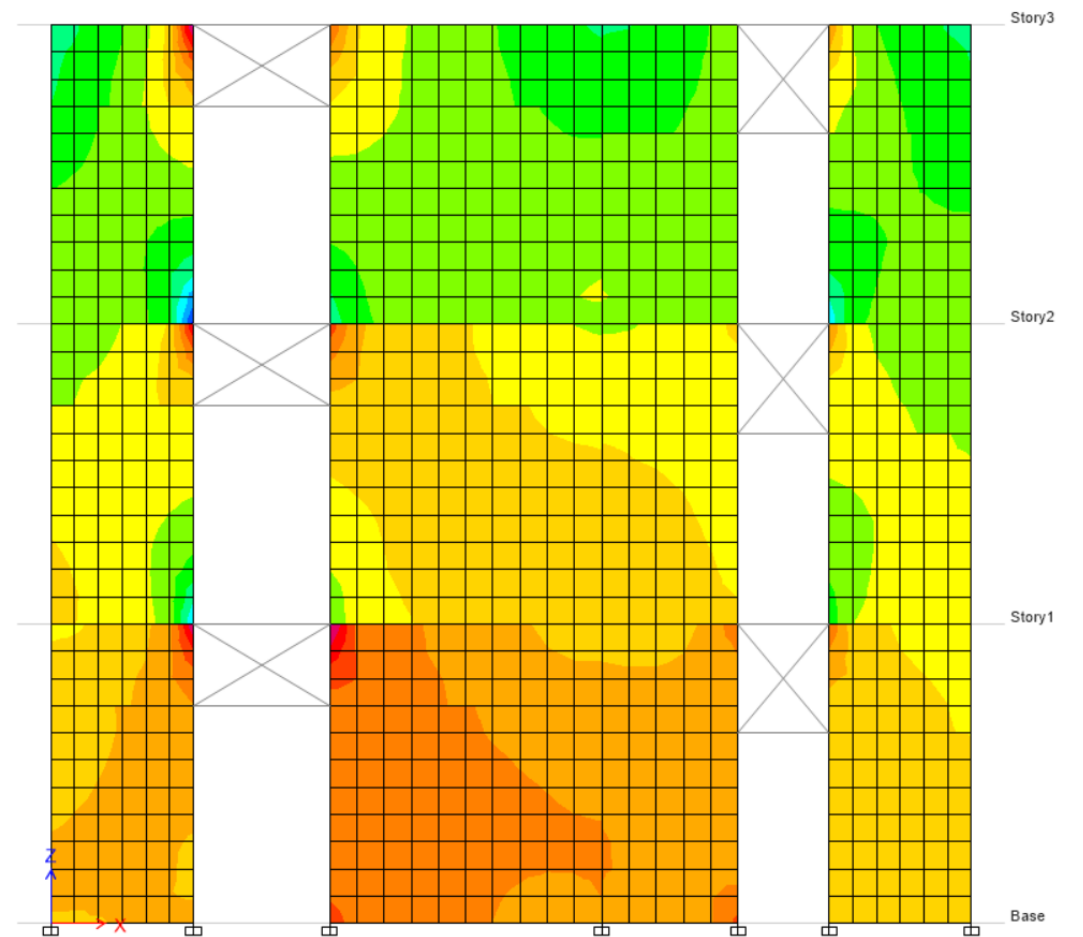


Model 1.1

Interior wall S22 stresses

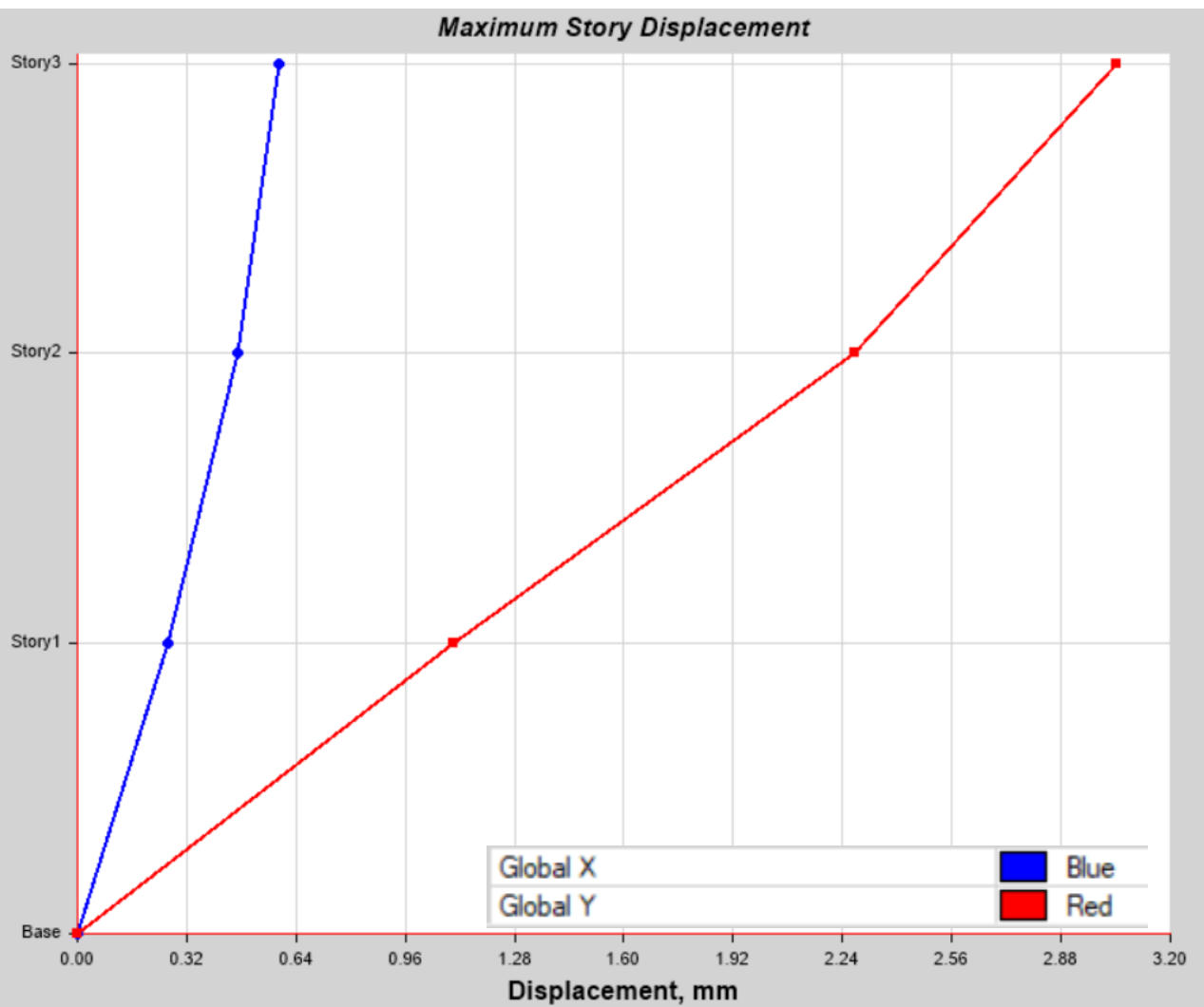


Model 1.2

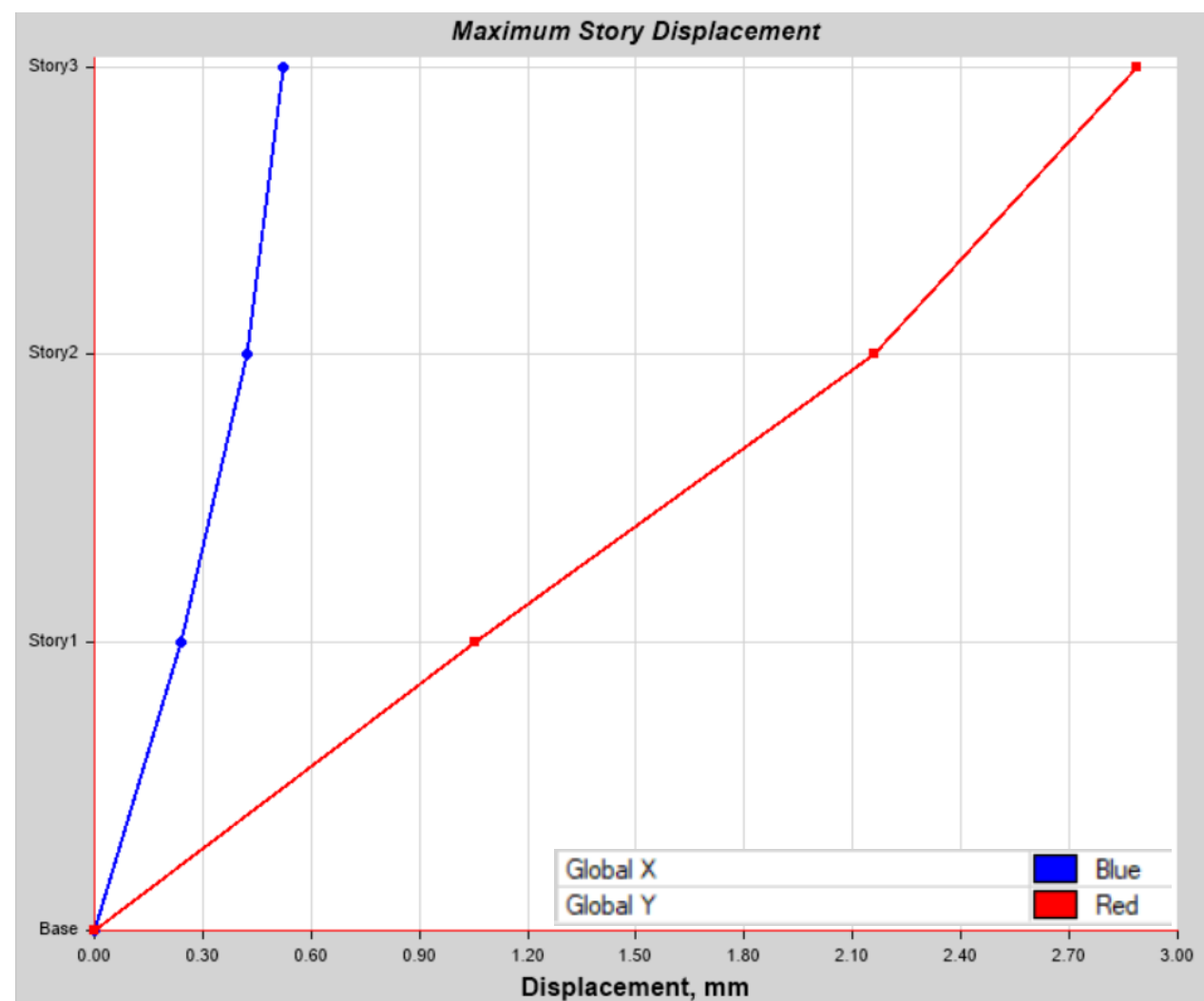


Model 2

Maximum story displacements (earthquake on Y)

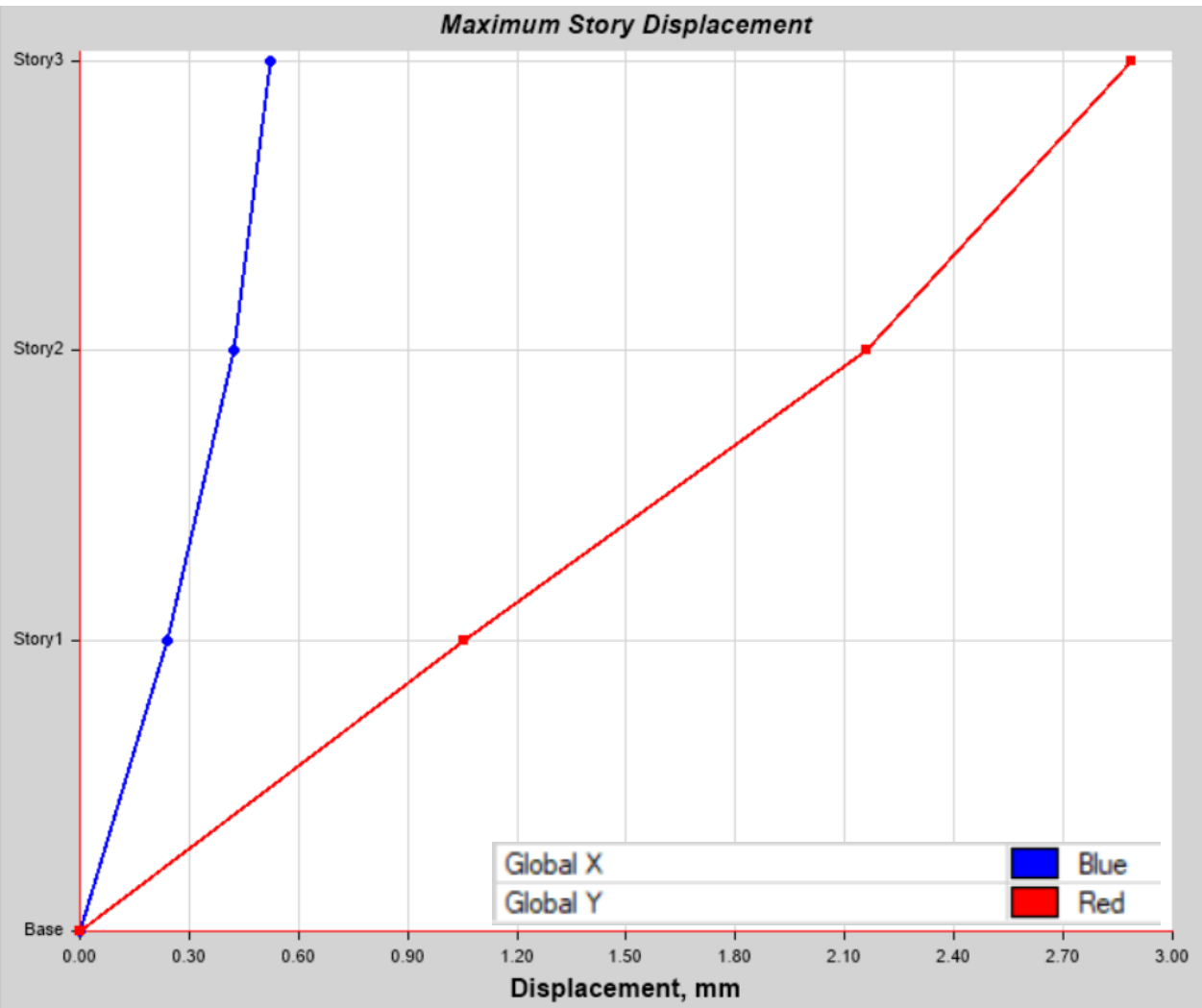


Model 1

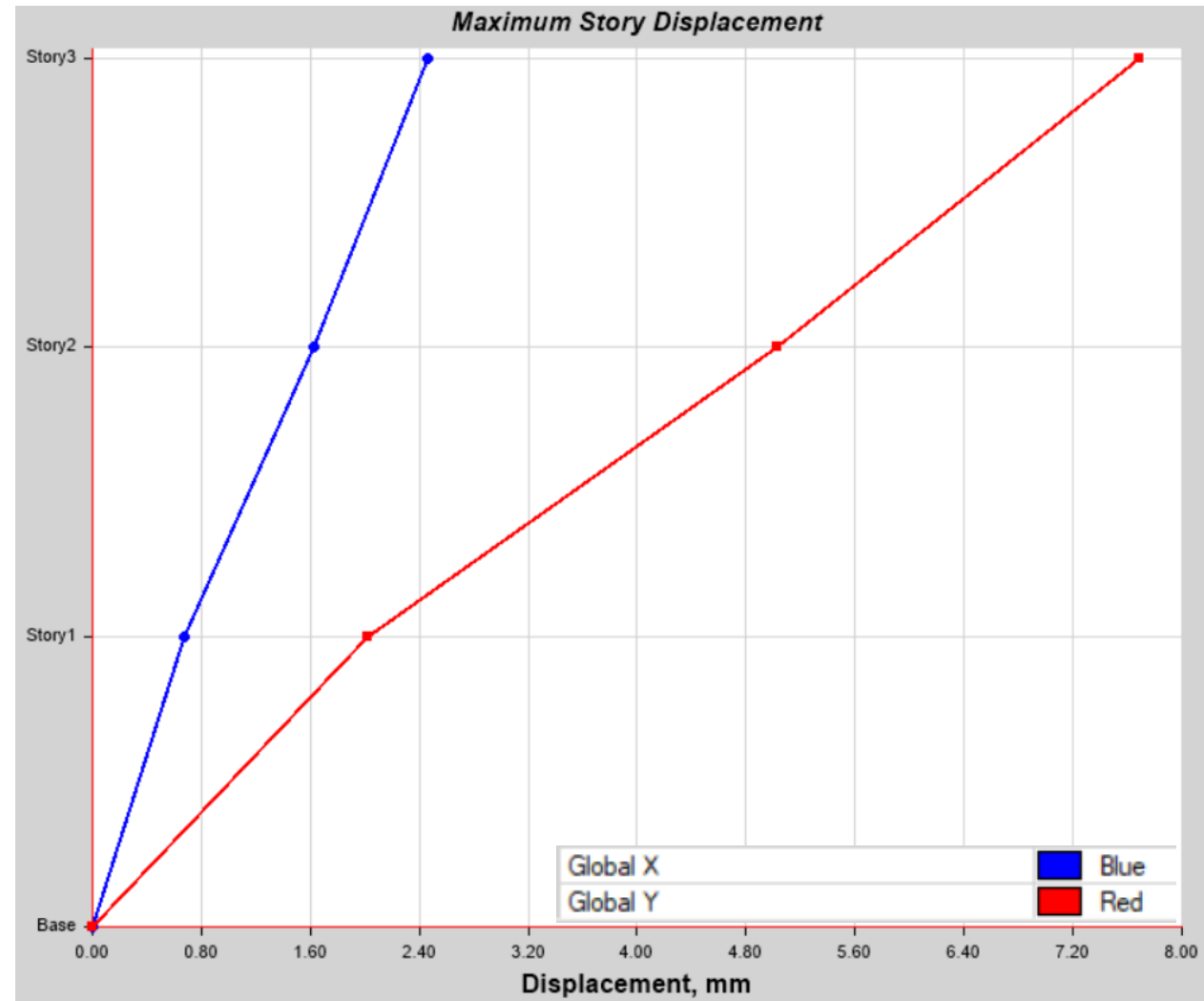


Model 1.1

Maximum story displacements (earthquake on Y)



Model 1.2



Model 2

Conclusions

- The paper presents the differences between structural analysis performed according to P100-3/2019 (manual computation) and by using a computer software (ETABS).
- Design according to P100-3/2019 (evaluation of forces on piers) is a very time demanding process and the results are not as accurate as the ones provided by the computer software environment. At the same time the accuracy of the structural modelling is important (in this case the behavior and boundary conditions of the spandrels).
- In case of Model 1, Model 1.1 and Model 1.2, they have a high stiffness according to the modal results and story displacements.
- The results of the manual computation presented in P100-3/2019 are the most restrictive ones, however they do not reflect the real behavior of the building.
- Model 2 is more flexible due to the spandrel's boundary conditions and it simulates the real behavior of the structure more accurately.

5. References

- Code for seismic evaluation of existing buildings – P100-3:2019 (in Romanian).
- Masonry structures design code – CR 6-2013 (in Romanian).
- A.K. Chopra, Dynamics of structures, 3rd edition, Prentice Hall, NJ, USA, 2006.
- FEMA 450, NEHRP recommended provisions for seismic regulations for new buildings and other structures, Part 1-15, Washington D.C., 2003.
- Katrin Beyer, Peak and residual strengths of brick masonry spandrels, Engineering Structures 41, 533-547, 2012

Influence of the Reconstruction of the Sofia Ring Road on the Travel Time of Fire and Rescue Service Vehicles

Researcher

PhD. Teodor Berov

Associate Professor , Faculty of Transport Management, Todor Kableshev University of Transport, Sofia, Bulgaria



This material discusses the reconstruction of a section of the Sofia Ring Road (SRR).

INTRODUCTION

Research Objectives

- The aim of this study is to identify and analyze the impact of the reconstruction of a section of the Sofia Ring Road on the traffic of cars with a special traffic regime.

The research approach is:

- - determining the main indicators of repair activity, affecting the traffic of the cars;
- - main factor for comparison - travel time of the vehicle pre- and post-repair, respectively;
- - determination of routes for comparison;
- - calculation of the travel time on routes pre- and post-repair, respectively;
- - analysis of the obtained results.

Based on:

- Use existing traffic data
- A real urban street network

MAIN INDICATORS OF REPAIR ACTIVITY

The existing road II-18 before the reconstruction is two-lane with gauge 12.00 m and is in poor condition, which leads to the formation of kilometers of columns of cars.

The parameters set in the construction are:

Project elements of the road infrastructure in reconstruction.	
Design parameters of the road	Measurement
Design speed of the direct route	80 km/h
Road width	46 m
Maximum longitudinal slope	5 %
Minimum Radius of Crest Curves	4 400 m
Minimum Radius of Sag Curves	1 300 m
Minimum Horizontal Curve Radius	250 m
Minimum length of a circular curve	45 m
Cross slope	2.5%
Category of traffic	very heavy

Main exploitation differences between the pre- and post-repair road sections

Main exploitation differences between the pre- and post-repair road sections.		
Parameter	Pre-repair	Post-repair
Road	2Lane	6Lane (0.50m+3.25m+3.25m+3.00m+0.50m)×2
Road width	12,00 m	46.00 m
Central dividing strip	–	3 m
Dividing strips between the local roads and the direct route	–	2×3.00 m
Local lanes	–	2×6.00 m
Sidewalk	–	2×2.00 m
Intersections on one level	Yes	–
Road junctions	–	Yes

INFLUENCE OF REPAIR ON THE TRAVEL TIME OF THE FRSV

The Emergency rescue vehicles are designed to eliminate the consequences of disasters, accidents and catastrophes, as well as to rescue endangered and injured people from the affected areas.

The vehicles used [9] are extremely diverse:

- Firefighting vehicles – for urban environments (light, medium and heavy capacities), for forest fires (light, medium).
- Specialized cars – rescue vehicles (light, medium and heavy class; chemical, for climbers and for divers).
- Lifting equipment, tanks/water carriers and auto-filling stations.
- Engineering equipment, safety equipment, etc.

Emergency vehicles travel in different road conditions [10]. The characterizing features of hazards are:

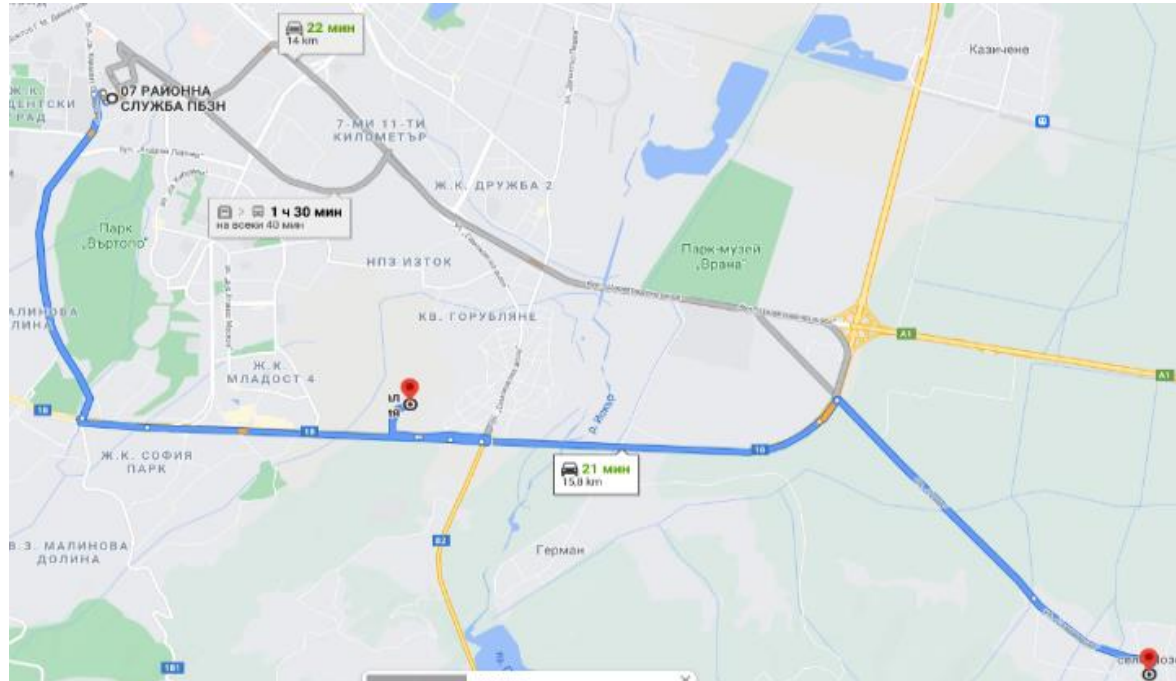
Road obstructions, congestion, parked cars, traffic calming measures, road works, and poorly illuminated or maintained surfaces.

INFLUENCE OF REPAIR ON THE TRAVEL TIME OF THE FRSV

In view of the present analysis, possible FRSV routes passing through the reconstructed section are proposed in Table

Characteristics of possible FRSV routes						
	Origin	Destination	Distance	Route parts		
				Urban	SRR-6 lane	SRR-new
1	07 RSFSCP	Lozen	15.8 km	4.2+4.2 km	2.2 km	5.2 km
2	07 RSFSCP	Gorublyane	9.3 km	5.5 km	2.2 km	1.6 km
3	04 RSFSCP	OMB, Sam. Shose	10.2 km	2.1 km	6.5 km	1.6 km
4	04 RSFSCP	Vrana	16.6 km	4.2 km	6.4 km	6 km

INFLUENCE OF REPAIR ON THE TRAVEL TIME OF THE FRSV



View of possible FRSV routes

INFLUENCE OF REPAIR ON THE TRAVEL TIME OF THE FRSV

With regards to the movement of specialized vehicles, the repair of the road section improves the road conditions, which leads to an increase in the mean travel speed of emergency vehicles, and thus to a general reduction of travel time:

- Increasing the number of lanes in one direction – increases the capacity of the section on the one hand and allows the release of lane for FRSV along the entire route ($\Delta t_k \approx 0$).
- Improvement of the road surface – allows for the overall increase of the speed for all vehicles on the road, and with regard to FRSV traffic with the maximum allowed and higher than the maximum allowed, but safe speed (v_k and v_e).
- Elimination of crossings at one level – provides an opportunity for safe and higher speed traffic on the road section in question.
- Road junctions – reducing the time to turn on and off the city highway, which leads to a reduction in travel time.

INFLUENCE OF REPAIR ON THE TRAVEL TIME OF THE FRSV

The obtained results from the calculations with mean travel speed for the travel time along the considered routes are shown in Table. A maximum ring road speed of 90 km/h was used in the calculations due to the presence of speed limiters mounted on some of the FRSV.

	Travel time per routes.		
route	pre-repair	post-repair	percentage
1	18 min	15 min	17%
2	10 min	9 min	10%
3	9 min	8 min	11%
4	17 min	13 min	24%

CONCLUSION

In this paper, the aim is to determine the impact of the reconstruction of a road section on the travel time of specialized vehicles with a special traffic regime. Four possible routes are considered, starting from the fire stations and ending to the presumed places of the incidents.

From the obtained results it can be seen that the performed reconstruction has a significant impact on reducing travel times along the considered routes. The obtained differences in travel times (and in percentages) are different due to the different relative share of the length of the considered section in the length of the total route.

It should be noted that the section under repair is a natural continuation of a section of the ring road reconstructed in previous years.

REFERENCES

1. N. Georgiev and V. Velyova, “Towards the influence of traffic and infrastructure characteristics on traffic safety”, *Mechanics. Transport. Communications* **16**(3/3), 1664 (2018), (In Bulgarian).
2. T. Berov, “Implementing the Google Maps API to improve vehicle routing problem: distance/travel time matrix”, *XVII International Scientific-Expert Conference on Railways (Railcon'16)*, October 13–14, Niš, Serbia, pp. 77–80 (2016).
3. T. Berov and P. Stoyanova, “Approach for simulation the employment and dispatching of ambulance vehicles in emergency medical services system (EMS) based on MS EXCEL (VBA)”, *Mechanics. Transport. Communications* **16**(3 /1), 1604 (2018), (In Bulgarian).
4. A. Elalouf, “Efficient routing of emergency vehicles under uncertain urban traffic conditions”, [*Journal of Service Science and Management* **5**\(3\)](#), pp. 241–248 (2012).
5. Z. Trendafilov, “A simulation model approach to analysis of the adaptive management of traffic lights”, *Mechanics. Transport. Communications* **16**(3/1), 1601 (2018), (In Bulgarian).
6. I. Pereira and G. Ren, “Travel time estimation for emergency services”, Available at: <https://www.diva-portal.org/smash/get/diva2:1330809/FULLTEXT01.pdf>, Accessed on: 27.06.2021.
7. J. Wang, M. Yun, W. Ma and Y. Xiaoguang, “Travel time estimation model for emergency vehicles under preemption control”, [*Procedia – Social and Behavioural Sciences* **96**](#), pp. 2147–2158 (2013).
8. S. Maerivoet and B. De Moor, “Transportation planning and traffic flow models”, Katholieke Universiteit Leuven, (2005).
9. Naredba № 8121z-1006 ot 24 august 2015 za reda za osashtestvyavane na pozharogasitelnata i spasitelnata deynost ot organite za pozharna bezopasnost i zashtita na naselenieto na ministerstvoto na vatreshnite raboti, Available at: <https://www.mvr.bg> , Accessed on 27.06.2021.
10. Generic Risk Assessment 1.1: Emergency Response and Arrival at the Scene, Availableat:https://assets.publishing.service.gov.uk/government/uploads/system/uploads/attachment_data/file/876525/gra-1-1_archived.pdf, Accessed on 27.06.2021.

Reabilitare drum sătesc, refacere apărare mal și decolmatare pârâu

Alexandru Eduard¹, Rotariu Stefan-Nicolae², Tonco Adrian³ Ancuta Rotaru⁴

¹ Masterand, Specializarea Inginerie Geotehnică, Facultatea de Construcții și Instalații, eduard.alexandru@student.tuiasi.ro

² Masterand, Specializarea Inginerie Geotehnică, Facultatea de Construcții și Instalații, stefan-nicolae.rotariu@student.tuiasi.ro

³ Masterand, Specializarea Inginerie Geotehnică, Facultatea de Construcții și Instalații, adrian-theodor.tonco@student.tuiasi.ro

⁴ Cadru didactic, , Facultatea de Construcții și Instalații, ancuta.rotaru@academic.tuiasi.ro

Rezumat

În localitatea Cotumba din comuna Agăș, județul Bacău, pe strada Mănăstirii, drum ce face legătura între sat și mănăstirea Cotumba, a avut loc o alunecare de teren ce a afectat un sector de drum pe o lungime de aproximativ 200m. Cercetarea geotehnică a terenului a constat în 2 sondaje geotehnice și un foraj geotehnic realizate pentru a pune în evidență natura terenului și factorii ce au dus la instabilitatea versantului. Pe zona investigată, drumul se află în profil mixt, cu rambleu pe partea dreaptă și debleu pe partea stângă (sens de mers spre Cotumba). Rambleul se termină în albia unui pârâu care în timpul perioadelor cu precipitații abundente provoacă eroziuni semnificative la baza taluzului, acesta fiind unul dintre principalii factori ce a condus la declanșarea alunecării. Pentru eliminarea cauzelor ce au favorizat instabilitatea versantului și pentru asigurarea condițiilor normale de exploatare a drumului, s-a propus consolidarea taluzului în bază cu o structură de sprijin din gabioane, amenajarea albiei cu anrocamente și dispunerea unor sisteme de drenaj iar pentru zona drumului, amenajarea unei structuri de tip fundație adâncită de parapet (FAP) dar și realizarea unor sisteme de colectare și descărcare a apelor pluviale.

Cuvinte cheie: alunecare de teren, taluz, elemente de sprijin (gabioane), eroziune, tasare, foraj geotehnic

1. INTRODUCERE

Alunecările de teren reprezintă deplasări ale rocilor care formează versanții unor munți, dealuri, lucrări de hidroameliorații sau alte rambleuri construite de oameni. Alunecările de teren nu produc pierderi și distrugerii la fel de mari ca alte dezastre, ele sunt însă periculoase putând conduce la distrugerea unor construcții prin deplasarea stratului de roci sau prin acoperire.

Taluzurile și versanții sunt masivele de roci, tari sau moi, naturale sau antropice, limitate prin suprafețe înclinate în raport cu orizontala.

Există o multitudine de factori ce controlează stabilitatea masivelor de pământ sau roci: geologic, hidrogeologic, hidrologic, structural, petrografic, geomecanic și geotehnic etc.

1.1. Clasificarea alunecărilor de teren

De-a lungul timpului au fost realizate mai multe clasificări, procesele de alunecare fiind foarte variate, în funcție de cauzele ce le determină, de structură, dimensiune, condiții de formare etc.

Câteva criterii majore de clasificare a alunecărilor de teren iau în calcul: adâncimea la care se situează zona de rupere în raport cu suprafața terenului; viteza de deplasare a maselor de roci; direcția de evoluție a procesului de alunecare; vârsta alunecărilor; distanța de deplasare etc.

1.2. Cauzele producerii alunecărilor de teren

Rareori producerea unor alunecări de teren poate fi atribuită unui singur factor.

Factorul geologic joacă, poate, cel mai important rol în formarea și declanșarea pierderii stabilității terenului, deși nu reprezintă o cauză directă a acestor fenomene. Alunecările apar în corelare cu structura geologică a structurii studiate.

Caracteristicile unui masiv pot favoriza dezvoltarea unor alunecări datorită unor condiții ca de exemplu: omoginitatea și alcătuirea structurală, șistozitatea, sistemele principale de fisuri, o succesiune de straturi permeabile și impermeabile ce permit pătrunderea apei în adâncul masivului.

Factorul hidrogeologic. Prezența apei subterane și deplasarea ei prin masiv influențează condițiile de stabilitate ale acestuia. Un masiv în condiții de umiditate naturală prezintă o stabilitate mai bună decât un masiv în care se găsește apă subterană.

Alți doi factori importanți care sunt luați în calcul sunt vibrațiile și cutremurele de pământ, acești doi factori modificând starea de eforturi din teren implicit și condițiile de stabilitate, prin creșterea aproape instantanee a forțelor de alunecare.

Însumarea agenților declanșatori enumerați mai sus dar și a altor factori precum modificarea unor proprietăți fizico-mecanice, acțiunea îngheț-dezghet, alterarea, săpăturile, relieful conlucrează la formarea și declanșarea alunecărilor de teren.

2. STUDIU DE CAZ - REABILITARE DRUM SĂTESC, REFACERE APĂRARE MAL ȘI DECOLMATARE PÂRÂU – COM. AGĂȘ, JUDEȚUL BACĂU

2.1 Date generale despre amplasament.

Amplasamentul studiat se află în județul Bacău, în comuna Agăș, satul Cotumba. Accesul pe sectorul de drum se face pe DN 12A până în comuna Agăș, apoi pe DC136 până pe Str. Mănăstirii. Drumul face legătura între satul Cotumba și Mănăstirea Cotumba.

Din punct de vedere geologic, zona se găsește amplasată pe unitatea majoră a zonei de fliș a Carpaților Orientali, subunitatea flișului extern (Pânza de Tarcău). Stratigrafic, depozitele din aria flișului extern aparțin intervalului Cretacic inferior – Pliocen. Corpul Pânzei de Tarcău este alcătuit din depozite cretacee, paleogene și miocene. Rocile care imprimă nota caracteristică sunt marnele și calcarele argiloase (marnocalcarele) vinete-albicioase, cu Chondrites și străbătute de diaclaze fine de calcit.

Depozitele acestei formațiuni reprezintă un fliș predominant calcaros, sedimentogenetic datorându-se curenților de turbiditate. În partea de vest, depozitele în facies arenitic, sincrone, au fost denumite drept Formațiunea de Horgazu.

Din punct de vedere geomorfologic zona amplasamentului se încadrează în grupa nordică a Carpaților Orientali. Regimul climato-meteorologic este caracterizat prin temperaturi medii anuale de 4-6°C și cantități medii de precipitații de 700-800 mm, regim ce corespunde unei clime continentale de dealuri și păduri cu altitudine de 200-800 m. Temperatura minimă a aerului coboară până la cca. -30°C în lunile de iarnă și atinge valori maxime de cca. +35°C în cele de vară.

Din punct de vedere tehnic, raionarea climatică a teritoriului național, încadrează amplasamentul în următoarele zone:

- Presiunea de referință a vântului, mediate pe 10 minute $q_{ref} = 0.60 \text{ kPa}$, conform NP 082-04.
- Valoarea caracteristică a încărcării din zăpadă pe sol $s_{0,k} = 2.00 \text{ kN/m}^2$, conform CR 1-1-3-2005.

Adâncimea maximă de îngheț se consideră la **-1.00m**, de la cota terenului natural sau amenajat, conform STAS 6054-77.

Conform reglementării tehnice din indicativul P100-1/2006, zonarea valorii de vârf pentru amplasamentul studiat, accelerația terenului pentru proiectare pentru evenimente seismice având intervalul mediu de recurență IMR = 100 ani, are următoarele valori:

Acelerația terenului pentru proiectare $a_g = 0.25g$ iar perioada de control (colț) T_c a spectrului de răspuns are valoarea de **0.70s**.

În urma precipitațiilor din ultimii ani, pe partea dreaptă a drumului, pe sensul de mers de la Mănăstire spre Cotumba, pe o lungime de aproximativ 200m, s-a dezvoltat o amplă alunecare a versantului, cu extindere spre corpul drumului. Pe zona investigată, drumul se află în profil mixt, cu rambleu pe partea dreaptă și debleu pe partea stângă (sens de mers spre Cotumba). Rambleul se termină în albia unui pârâu, acesta din urmă provocând fenomene de eroziune a taluzului.

2.2 Stratificația terenului

Sondaj realizat în corpul drumului – Zona 1

Strat 1 – 0.00m – 0.22m – Sistem rutier alcătuit din 10cm mixtură asfaltică și 12cm piatră spartă cu intercalații de pământ.

Strat 2 – 0.22m – 2.00m – Argilă nisipoasă, cafeniu-maronie, cu intercalații de pietriș și bolovăniș, cu plasticitate mare, plastic consistentă, saturată.

Nivelul hidrostatic nu a fost interceptat ca acvifer subteran. Au fost identificate infiltrații de apă provenite din zona de versant.

Sondaj realizat la baza gabioanelor la -3.00m/CD

Strat 1 – 0.00m – 0.40m – Pietriș și bolovăniș cu intercalații de pământ.

Strat 2 – 0.40m – 3.00m – Argilă nisipoasă, maronie, cu intercalații de pietriș și bolovăniș, cu plasticitate mare, plastic moale spre consistentă, saturată

Nivelul hidrostatic nu a fost interceptat ca acvifer subteran. Au fost identificate infiltrații de apă provenite din zona de versant.

Foraj realizat în corpul drumului – Zona 2

Strat 1 – 0.00m – 0.75m – Umplutura din pietriș cu nisip și bolovăniș.

Strat 2 – 0.75m – 3.30m – Argilă nisipoasă, cafeniu-maronie, cu intercalații de pietriș și bolovăniș, cu plasticitate mare, plastic consistentă.

Strat 3 – 3.30m – 6.60m – Argilă prăfoasă, cenușiu-cafenie, intercalată cu pietriș și argilă cenușie, plasticitate mare, plastic consistentă.

Strat 4 – 6.60m – 10.00m – Argilă nisipoasă-prăfoasă, cenușie, cu aspect marnos, cu rar pietriș și fragmente de rocă, cu plasticitate mare, tare.

2.3 Împărțirea pe zone a drumului sătesc

În cadrul etapei de cartare geomorfologică de detaliu, s-a procedat la analizarea amplasamentului la nivel de microrelief, în vederea identificării acelor particularități, care împreună cu investigațiile geotehnice de detaliu să ofere informații despre cauzele care au produs degradările și să se poată stabili soluțiile de punere în siguranță a sectorului de drum.

Având în vedere cele constatate la fața locului s-a luat decizia de a împărți amplasamentul în 3 zone principale. (Fig. 1)

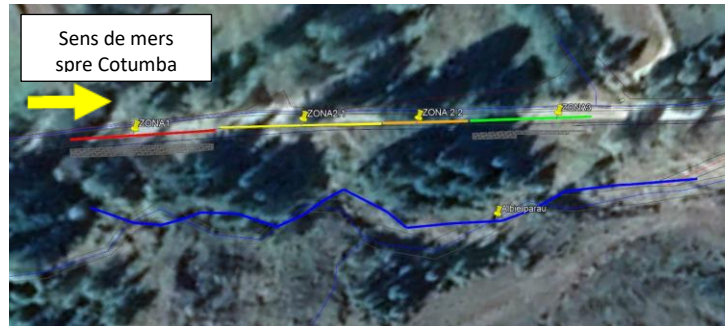


Fig. 1 - Plan de amplasare în zonă

ZONA 1. L = aprox. 40m

Pe acest sector au fost puse în evidență forme de cedare structurală a sistemului rutier și elementelor de sprijin ale acestuia (gabioane), cedare a taluzului de rambleu până în zona albiei.

Diferența de nivel în profil transversal pe zona 1, între albie și drum este de aprox. 13.50m. Structura din gabioane este amplasată cu fundația în zona mediană a taluzului de rambleu. Taluzul de rambleu este afectat de forme de eroziune și cedare de tip regresiv pe fondul acțiunii apei din zona albiei, eroziune directă pe taluz, pe fondul slabei vegetalizări și de tip curgere noroioasă datorită scurgerii necontrolate a apelor de pe versantul din amonte – zona de debleu. (Fig.2)

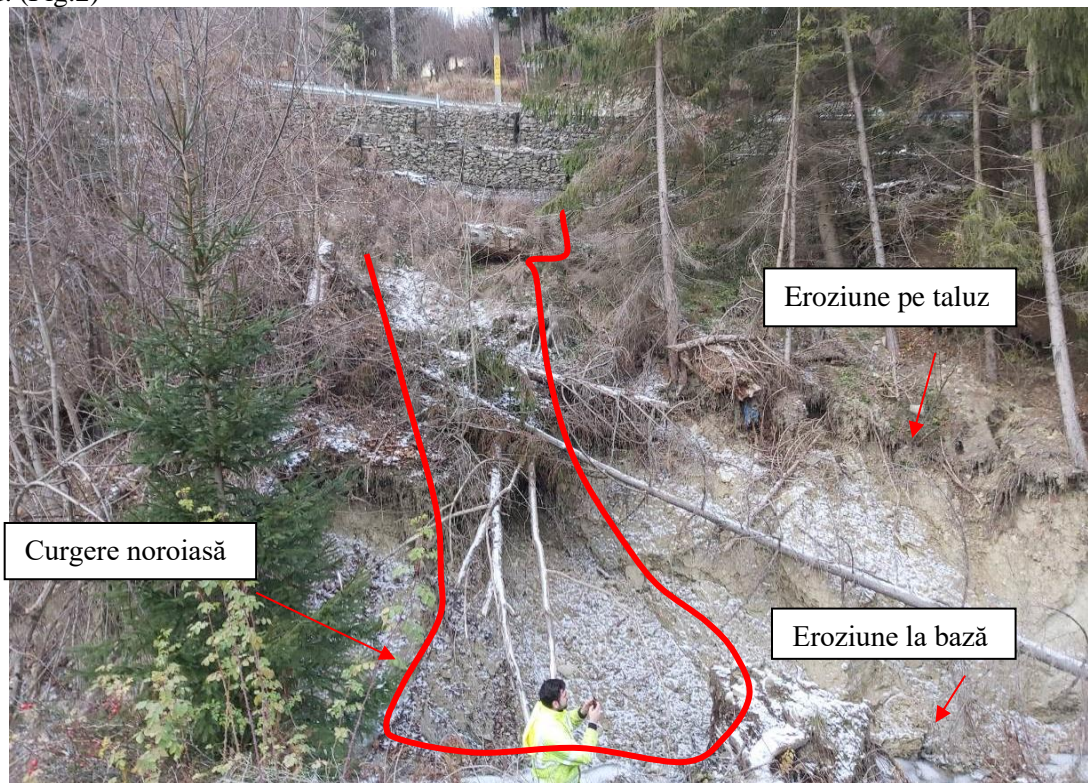


Fig. 2- Zona 1

Natura terenului specifică zonelor subcarpatice și carpatice, de tip argilos – marnos, degradată, cu potențial mare de umflare și de structurare în prezența apei, în special a ciclurilor umezire – uscare și descoperită la zi – acțiune climatică, accentuează degradările identificate.

Structura din gabioane nu are fundație corespunzătoare, aceasta prezentând un risc ridicat de cedare în totalitate și risc ridicat de afectare în totalitate sector de drum. (Fig. 3)

Apele curg necontrolat și înmoaie terenul pe sub structura din gabioane existentă. În zona de debleu, șanțul din beton prezintă multiple fisuri și crăpături iar apa colectată se infiltrează prin aceste fisuri în terasamentul drumului.

Pe zona de debleu, a fost identificat un taluz cu multiple ravene. Apa provenită de pe taluz nu este colectată în totalitate de șanțul din beton. (Fig. 4)



Fig.3-Structura din gabioane



Fig.4-Zona de debleu

ZONA 2. L=aprox. 65m

Zona 2.1. L= aprox. 40m

În corpul drumului au fost dispuși arbori cu rol de consolidare temporară (Fig. 5). Pe zona de aval sunt evidențiate aceleași particularități prezentate pe zona 1.

Corpul drumului este afectat de forme de cedare, circulația se desfășoară cu dificultate. (Fig. 6)

Stratificația preponderent argiloasă și saturată din fundația drumului conduce la apariția tasărilor.

În această zona a fost identificată o ravenă cu o treaptă principală de rupere creată în corpul drumului.



Fig. 5 – Arbori dispuși in corpul drumului



Fig. 6 – Corpul drumului

Zona 2.2. L= aprox. 25m

Prezintă aceleași particularități ca zona 2.1. cu avantajul că există pe taluzul de rambleu o vegetație arboricolă mai densă care nu a fost afectată de alunecare, iar drumul se prezintă în condiții acceptabile, fără a fi identificate forme de cedare. (Fig. 7)



Fig. 7 – Zonă neafectată

ZONA 3. L= aprox. 35m

La nivelul drumului au fost observate forme de tasare accentuată. Sectorul de drum este consolidat cu gabioane, cu fundația în zona mediană a taluzului. Au fost evidențiate forme de tasare accentuată la nivelul gabioanelor. Zona de aval prezintă aceleași particularități ca la zona 1. (Fig. 8)

Taluzul de rambleu prezintă forme de eroziune care pun în pericol gabioanele existente din acea zonă.



Fig. 8 – Tasare la nivelul gabioanelor

ZONA DE DEBLEU – AMONTE DE DRUM

Pe zona de debleu au fost identificate mai multe zone de ravenare – descărcare ape de versanți. Aceste zone nu sunt amenajate și transportă material detritic în zona drumului iar șanțurile existente, longitudinale drumului sunt degradate, crăpate. Apa care provine de pe versant descarcă necontrolat în zona șanțurilor, pe majoritatea zonelor aceasta se infiltrează pe sub șanțul existent și migrează către zona de aval ajungând în zona fundațiilor gabioanelor.

Zona de amonte are un aspect frământat și pe alocuri prezintă ușoare forme de eroziune. (Fig. 9)



Fig. 9 – Zona de debleu al drumului

3. CONCLUZII ȘI DEZVOLTĂRI ULTERIOARE

3.1 Recomandări propuse la nivelul studiului geotehnic cu privire la asigurarea stabilității drumului, colectare și evacuare ape și amenajare teren adiacent - ianuarie 2021

Zona 1 + Zona 2 + Zona 3

Etapa 1. – Lucrări de consolidare și amenajare

Consolidarea taluzului de rambleu din bază, ce face legătura cu albia pârâului, cu o structură de sprijin mixtă (fundăție din beton și elevație din gabioane), cu fundăție directă dispusă la adâncimea de aprox. 1.50m față de cota talvegului amenajat. Adâncimea de încastrare și dimensiunile vor rezulta la proiectul de specialitate – dimensionare structură de sprijin.

Amenajarea albiei cu anrocamente, pe o lățime de minim 6m de la fața zidului de sprijin.

Zidul de sprijin din gabioane (elevația) va avea înălțimea de aprox. 5m de la cota talvegului amenajat.

În amonte de zidul de sprijin se va proceda la o terasare a taluzului prin îndepărtare vegetație și crearea unor berme de legătură cu drumul.

Realizarea unei structuri din pământ armat cu geogriile, pentru a face legătura cu terasamentul drumului.

Amenajarea taluzului se va realiza în strânsă legătură cu etapa 2, în sensul de a asigura lățimea minimă a străzii. În cazul în care vor rezulta umpluturi, în special în zona drumului pentru a asigura lățimea proiectată, acestea se vor realiza armate cu geogriile biaxiale.

Etapa 2 – Lucrări în zona drumului

Pentru asigurarea lățimii străzii și a stabilității pe termen lung, se va dispune pe zona de rambleu o structură de sprijin, cu fundăție directă, la adâncimea de min. 2.50m față de cota drumului. Structura va fi de tip fundăție adâncită de parapet (FAP). Lățimea tălpii va fi de min. 1.50m sub stradă.

În spatele structurii de sprijin se va dispune un sistem de drenaj.

La partea superioară a structurii de sprijin se va dispune un parapet de protecție.

Monitorizare geotehnică, conform SR EN 1997 -1 și P130-1999.

Disponerea unui sistem de drenaj pe zona de amonte a drumului, la adâncimea de min. 2.50m față de axul drumului, cu scopul de a prelua apele ce vin de pe versanți și se infiltrează în terenul de fundare.

Refacerea șanțului sub forma unor structuri ranforsate pentru a susține taluzul de debleu.

Amenajarea zonelor de descărcare de pe zona de amonte cu structuri disipative și canale de curgere betonate.

Suplimentar, pe zona 2:

Îndepărtare în totalitate a arborilor dispuși în corpul drumului cu rol de consolidare temporară și refacerea drumului cu umpluturi organizate, armate cu geogrilă biaxială.

3.2 Soluții adoptate la nivelul proiectului tehnic cu privire la asigurarea stabilității drumului, colectare și evacuare ape și amenajare teren adiacent - decembrie 2021

Zid de sprijin din beton armat fundat direct

Pentru asigurarea stabilității zonei, în locul fostelor sprijiniri existente (gabioane), s-a proiectat un zid de sprijin din beton armat, pe aproximativ aceeași lungime. Pentru reducerea presiunii hidrostactice asupra structurii de sprijin, în spatele zidului se va realiza un sistem de drenaj vertical cu filtru învelit în material geotextil.

Pentru o mai bună discretizare a liniei terenului și pentru o mai bună eficientizare, zidurile au fost concepute pe tronsoane cu o lungime de 5.0m (28 tronsoane). Lungimea totală a zidului este de 140m. Lățimea tălpii fundației este de 1.60m. Elevația are o lățime de 40cm la coronament. Talpa este orizontală cu o grosime de 40/55 cm. Talpa fundației este așezată pe un strat de beton de egalizare în grosime de 10cm.

În terenul din spatele zidului se execută un dren orizontal din pietriș, cu lungimea de 0.30m și înălțimea de 0.93m.

Filtrul este realizat din pietriș sort 7-31mm, învelit în geotextil. Acesta va fi de tip geocompozit drenaj realizat din polipropilenă. Pentru evacuarea apelor colectate de dren, zidul este prevăzut cu barbacane din PVC cu diametrul de 110mm, ce descarcă apa colectată în rigola din fața zidului.

Zid de sprijin din gabioane fundat direct

Pentru asigurarea zonei afectate de alunecări pe zona albiei minore a cursului de apă de pe amplasament, se va executa un zid de sprijin din gabioane ce sprijină pe o fundație din beton simplu și care are ca scop sprijinirea taluzului drumului și a unei structuri din pământ armat cu geogrilă.

Zidul de sprijin va fi alcătuit din 35 tronsoane, cu aceeași secțiune transversală, cu înălțimea elevației de 5.00m și lungimea de 4.0m (35 tronsoane). Lățimea tălpii fundației este de 5.00m cu înălțime variabilă (1.50-1.0). Sub fundația zidului din gabioane se va dispune un strat de piatră brută împănată, 150-300mm, cu înălțimi variabile între 0.15cm-0.65cm. Peste fundația zidului, înaintea de realizarea cutiilor se va realiza un pinten din beton, cu dimensiunea 30x20 cm².

În fața zidului din gabioane, în albie, se va dispune o saltea din anrocamente cu lățimea de 3.0m și înălțimea de 50cm peste care se va turna un strat de beton de 10cm. Umplerea gabioanelor se va face cu piatră brută cu dimensiuni între 120-250mm zidită, uscată, bine împănată.

Structura din pământ (material local) armat cu geogrilă

Se va executa între cele 2 ziduri de sprijin (beton – zid de sprijin din gabioane). Înainte de execuția propriu-zisă a acestora, se vor elimina de pe amplasament gabioanele existentă.

Realizarea structurii implică:

Săpătura în teren existent. Acestea vor fi sprijinite cu dulapi și spraițuri, acolo unde este nevoie.

Realizarea umpluturii de pământ armat cu geogrilă: Se începe de la bază, pe un teren deja nivelat și compactat, cu un strat de geogrilă, după care se așază un strat de pământ în așa fel încât, după compactare, grosimea acestuia să fie de 0.25m, se așază un al doilea strat de balast compactat în grosime de 0.25m după care se întoarce geogrilă inferioară peste cele două straturi compactate. Tipul de geogrilă trebuie să aibă cel puțin următoarele caracteristici: material din polietilenă de înaltă densitate, greutate minim 850g/m² și rezistența la întindere minim 150 kN/m.

"Creații universitare 2021" Al XIV-lea Simpozion Național
Iași, România, 29 mai 2021

Ca material de umplutură se va folosi pământ local. Vor fi compactate la umiditatea optimă de compactare determinată în laborator prin încercarea Proctor.

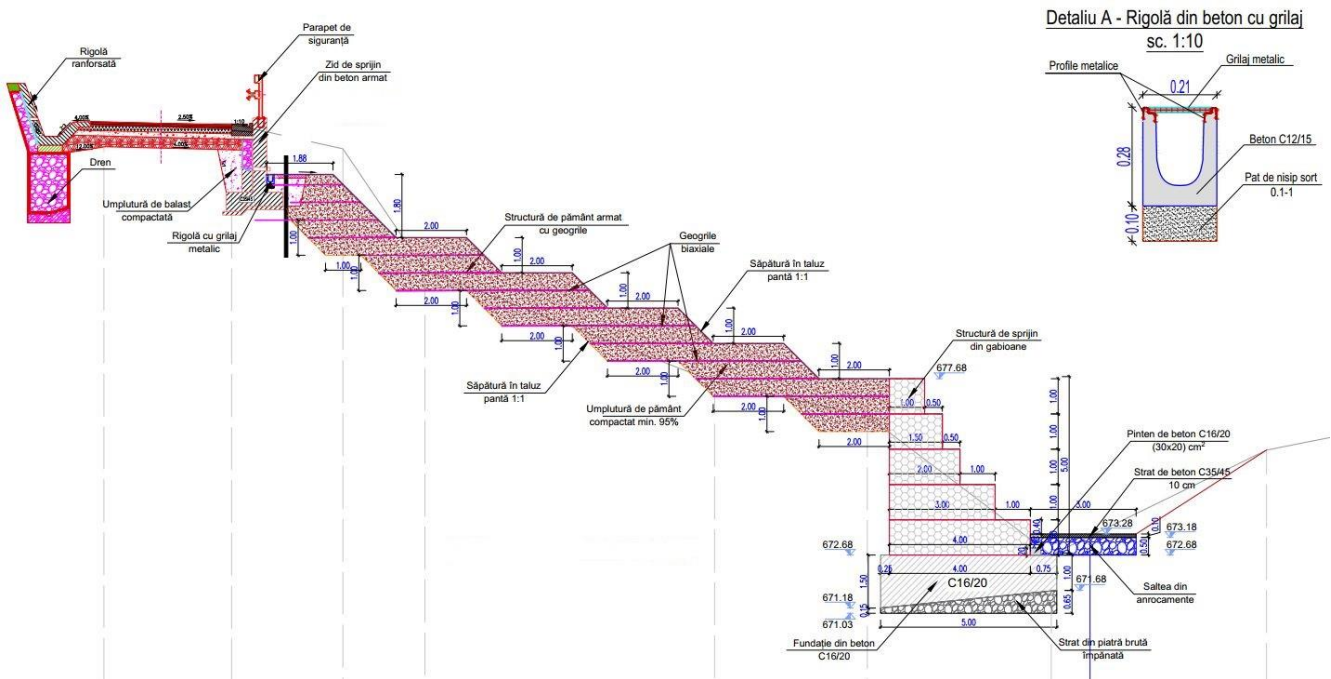


Fig. 10 – Profil transversal cu lucrările proiectate

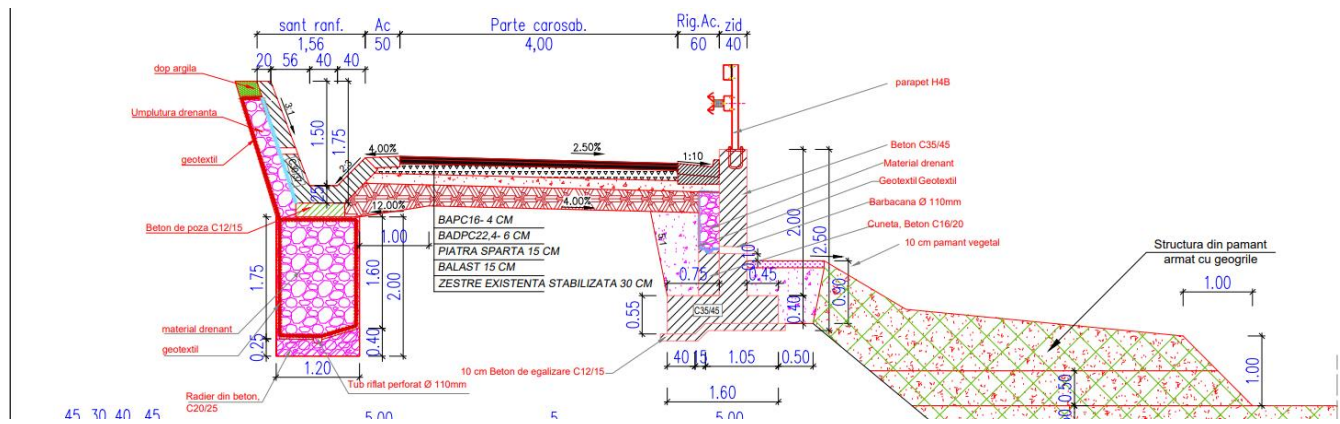


Fig. 11 – Profil transversal cu lucrările proiectate - drum

3.2 Fotografii din timpul execuției – ianuarie 2022



Bibliografie

- (1) Onimus A.N., Else S.O., Other A.N., Document Preparation for Beginners and Advanced Users. Journal of Civil Engineering. and Architecture, 24, 3, 15-24 (2009).
- (2) Irina Lungu, Anghel Stanciu, Mircea Aniculăesi, Iancu-Bogdan Teodoru, GEOTEHNICĂ – Lucrări de laborator, Editura Politehniun, 2013
- (3) Kurino H., Kobori T., Semi-Active Structural Response Control by Optimizing the Force-Deformation Loop of Variable Damper. Proceedings of the 2nd World Conf. On Struct. Control. Kyoto, Japan, 1999. Vol. 1, 407–416.
- (4) Onimus A.N., Else S.O., Other A.N., Development and Experimental Study of Semiactive Fluid Damping Devices for Seismic Protection of Structures. Technical Report NCEER-95-011, National Centre for Earthquake Engineering, Buffalo, New York, 1995.
- (5) P100–1/2013 “Normativ pentru proiectarea antiseismică a construcțiilor de locuințe social-culturale, agrozootehnice și industriale”
- (6) P. Răileanu, V. Mușat, E. Țibichi – ALUNECĂRI DE TEREN – STUDIU ȘI COMBATERE, Editura Venus, 2001.
- (7) ***GP 093 -206 - Ghid privind proiectarea structurilor de pământ armat cu materiale geosintetice și metalice;
- (8) NP 074/2014 – Normativ privind documentatiile geotehnice pentru constructii.
- (9) STAS 6054 - “Adâncimi maxime de îngheț. Zonarea teritoriului României”.
- (10) SR EN 1997 -1 și P130-1999 – ” Proiectarea geotehnică și Normativ privind comportarea în timp a construcțiilor”

U-Wert Notice

Contents

Software presentation	3
Home page	4
Horizontal toolbar	4
Vertical toolbar	4
Values recording	5
Without studs or rafters	5
With studs or rafters	6
Result	7
thermal conductivity U	7
Environmental impact.....	7
Moisture.....	7
Heat.....	8
Diagrams	8
Hints.....	8

Software presentation

This software is German software, it mainly calculates the value of the thermal conductivity of a wall. This calculation considers many given as, the type of materials used, their thicknesses and the order in which these materials are arranged in the wall.

Once all these data have been entered, it is possible to visualize the temperature evolution in the wall according to the external and internal temperatures. We can also see the moisture transmitted in the wall and what this induces as the presence or not of mould in long term.

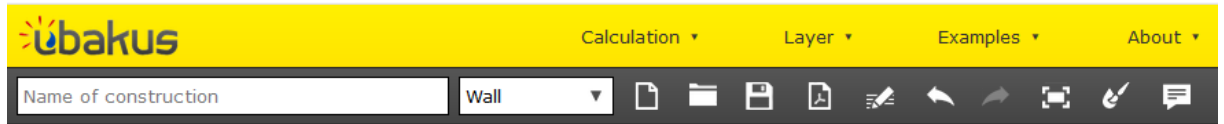
The software also makes us aware of the energy impact of using materials. Indeed, the software shows us the energy used for the construction of our wall by telling us the mass of CO₂ by m².

Finally, the platform offers us ways to improve the energy performance, the resistance to moisture and the environmental impact of our wall by indicating us, for example, materials to use rather than others.

Home page

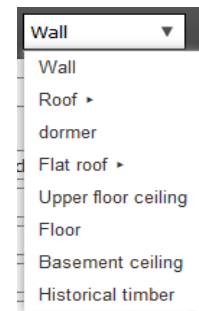
<https://www.ubakus.com> (you can create an account or use the demo version)

Horizontal toolbar



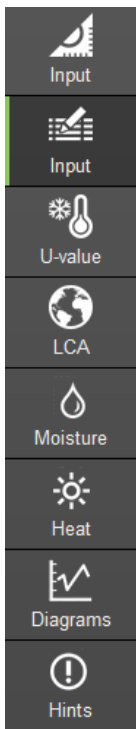
First, you can name your project in the tab « Name of construction ».

Then you can indicate what type of project it is (wall, roof, floor ...)



Also, this bar gives you easy access to the tools to save the project and open a new one. Note that there is an example file (open a new project) with many projects.

Vertical toolbar



This area provides easy access to the software's various menus.

First you will need to enter the different data from your project into the second "Input" tab. Then the other 6 tabs show the results ranked according to their uses; thermal conductivity and thermal characteristics of the project, the ecological impact of the use of materials, the evolution of moisture in materials.

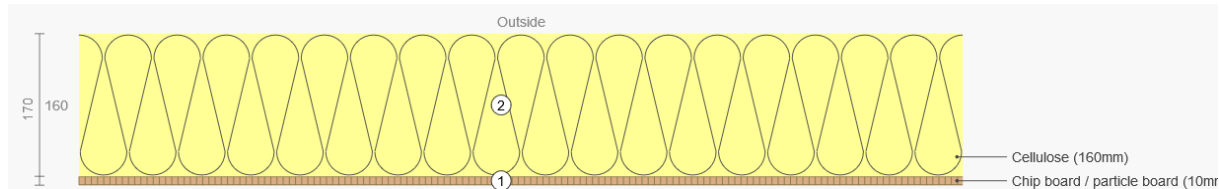


Erasmus+



Values recording

Without studs or rafters



The input is intuitive. As can be seen below; The interface juxtaposes the different possible layers by beginning the inside.

Inside:	Reduced air circulation	20	°C	50	% Humidity	Rsi...
From inside to outside:		reverse	Thickness	Width	Distance	λ
:: 1	Chip board / particle board	10	mm			0,14
:: 2	Cellulose	160	mm			0,04
:: 3			mm			
:: 4			mm			
Outside:	Direct contact to outside air	-5	°C	80	% Humidity	Rse...

The wall is entered by selecting the material used or using it. At the time of selection, a window to recall the characteristics of the material appears.

Concrete

λ = 2 W/(mK) Thermal conductivity

ε = 0,97 Emissivity of long-wave radiation

μ = 80 / 130 Water vapor diffusion resistance factor

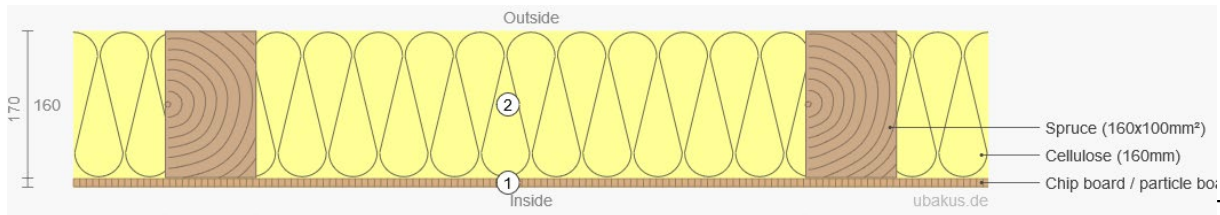
ρ = 2400 kg/m³ Raw density

c = 950 J/(kg·K) Heat capacity

Then the user must enter the thickness of the material.

To finish the user must indicate the different information relating to the indoor and outdoor environment. Like temperature and humidity

With studs or rafters



The input is

always done using the interface presented above.

Reached the level of a layer like layer 2:

- Enter the main material normally.
- Add the frame by clicking on “Place studs or rafters in this layer”

	From inside to outside:	reverse	Thickness	Width	Distance	λ	μ	
1	Chip board / particle board		10 mm			0,14	15/50	
2	Cellulose		160 mm			0,0	1/3	
3								
4								
Outside	Direct contact to outside air		-5 °C	80				

insert internal layer:
 insert external layer:
 Place studs or rafters in this layer
 Duplicate layer

- Enter the corresponding material (the thickness will be generated automatically depending on the thickness put for the main material)
- Grasp the width of the frame and its spacer

	From inside to outside:	reverse	Thickness	Width	Distance
1	Chip board / particle board		10 mm		
2	Cellulose		160 mm		
	Spruce		160 mm	100 mm	600 mm
3					

Result

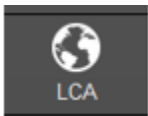
thermal conductivity U



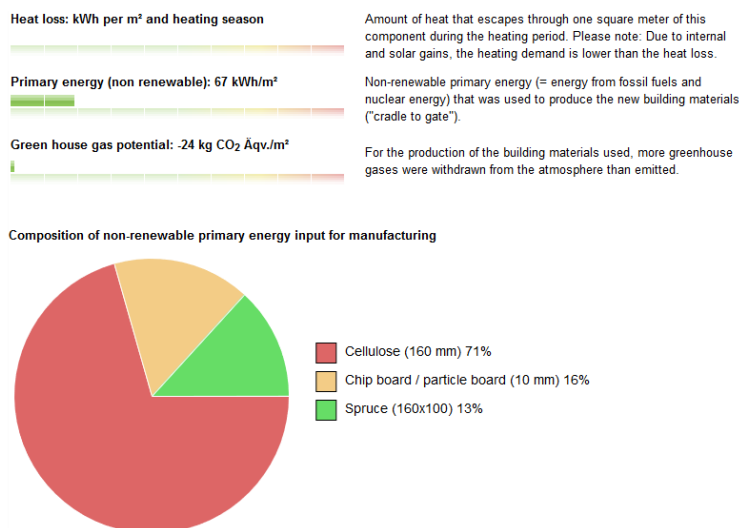
A table is proposed to us to understand the different calculations carried out within each layer. Depending on our overall U value, U-Wert provides a comparison between our value and those of the various German standards available.

#	Material	λ [W/mK]	R [m²K/W]	Temp. [°C] min max	sd-value [m]	Condensate [kg/m²] [%]	Weight [kg/m²]	Heat capacity [J/(kg*K)]
Thermal contact resistance			0,130 (0,250)	18,6 20,0				
1	1 cm Chip board / particle board	0,140	0,071	18,2 18,6	0,15	-	6,5	1800
2	16 cm Cellulose	0,040	4,000	-4,8 18,2	0,48	-	8,0	2100
Thermal contact resistance			0,040	-5,0 -4,8				
17 cm Whole component			4,241		0,63	-	14,5	

Environmental impact

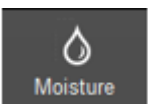


Here the U-Wert page allows us to estimate on different points, such as: primary energy, global warming also possible to visualize a diagram, and a set of complementary regarding the environmental impact



have an Heat losses, potential. It is composition the form of a information of materials.

Moisture



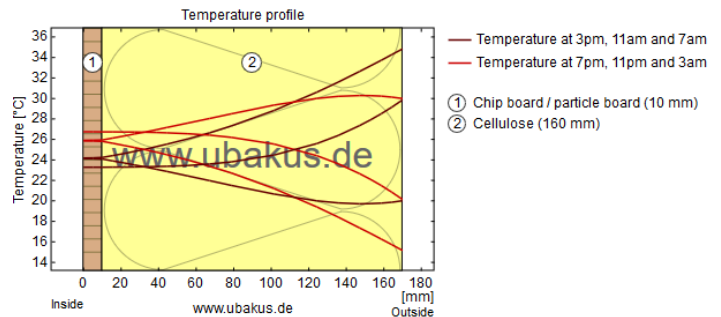
This page allows you to diagnose humidity within the walls. Here the calculation tool allows to know If our walls are sensitive to condensation or not.

On the graph below, we can visualize the humidity in each point of our wall according to its position. In addition, we can see some advice to protect our wall against the mould.

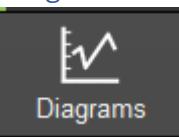
Heat



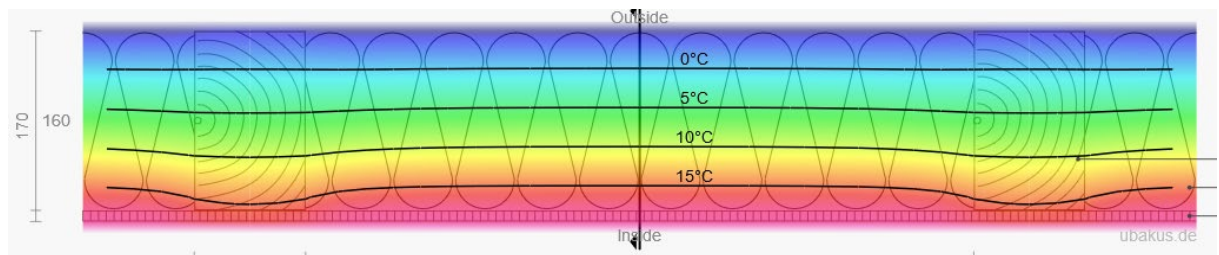
In this tab, U-Wert allows you to know the different temperatures within each layer according to the different hours of the day. The evolution of temperature whether indoors or outdoors. And finally, a set of information relating to the link between the walls and the absorption of solar energy.



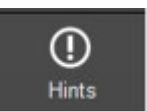
Diagrams



This part is a recap of all information that we can have on the software. We can see humidity and temperature evolution. It allows us to easily see this both evolutions.



Hints



This last part displays some remark on our construction. we can find information there whether we respect the standards or if our structure can be improved.

Rear ventilation level

The thickness of the rear ventilation level is 3 cm. Generally, the thickness should be at least 3 cm. If the inclination of the rear ventilation plane is less than 40°, e.g. for (flat) roofs, a larger value must be selected. The same applies if the air inlet and the air outlet are particularly far apart.

The part of your component that is relevant to the calculation ends at the inside of the rear ventilation level. Outlying layers do not need to be entered.

Beams and joists which penetrate the rear ventilation level are only considered up to the inside of the rear ventilation level.

Please note: The U-value calculator basically assumes that a rear ventilation level is adequately permeated by outside air. Whether this is actually the case depends not only on the thickness of the rear ventilation level, but also on their width and length and possible obstacles in the air inlet and outlet and can not be assessed by the U-value calculator.

University of Pretoria, South Africa, December 2017

Some Aspects on Landslide Risk Mitigation

by

Ancuța Rotaru

**“Gheorghe Asachi” Technical University
Iasi, Romania**

LANDSLIDE RISK MITIGATION

CHALLENGE

STRATEGY

LANDSLIDE RISK MITIGATION

CHALLENGE

STRATEGY

LANDSLIDE RISK MITIGATION

CHALLENGE

- A. PROCESSES RESPONSIBLE FOR LANDSLIDES**
- B. DYNAMICS OF A LANDSLIDE SURFACE**

CHALLENGE

A. PROCESSES RESPONSIBLE FOR LANDSLIDES

Processes Responsible for Landslides

The causes of landslides can be divided into

EXTERNAL

a heightening of the slope by river erosion or man-made excavation

the deposition of material along the upper edge of slopes and earthquake shocks

INTERMEDIATE

rapid drawdown

sub-surface erosion

spontaneous liquefaction

INTERNAL

increase of pore-water pressure

decrease of the cohesion of the material adjoining the slope

Some important causes responsible for landslide triggering are:

- **external change of stability conditions;**
- **spontaneous liquefaction;**
- **seepage from artificial and natural sources of water;**
- **the presence of ground water in landslide;**
- **the identification of weak zones of a saturated clay landslide**

I. EXTERNAL CHANGE OF STABILITY CONDITIONS

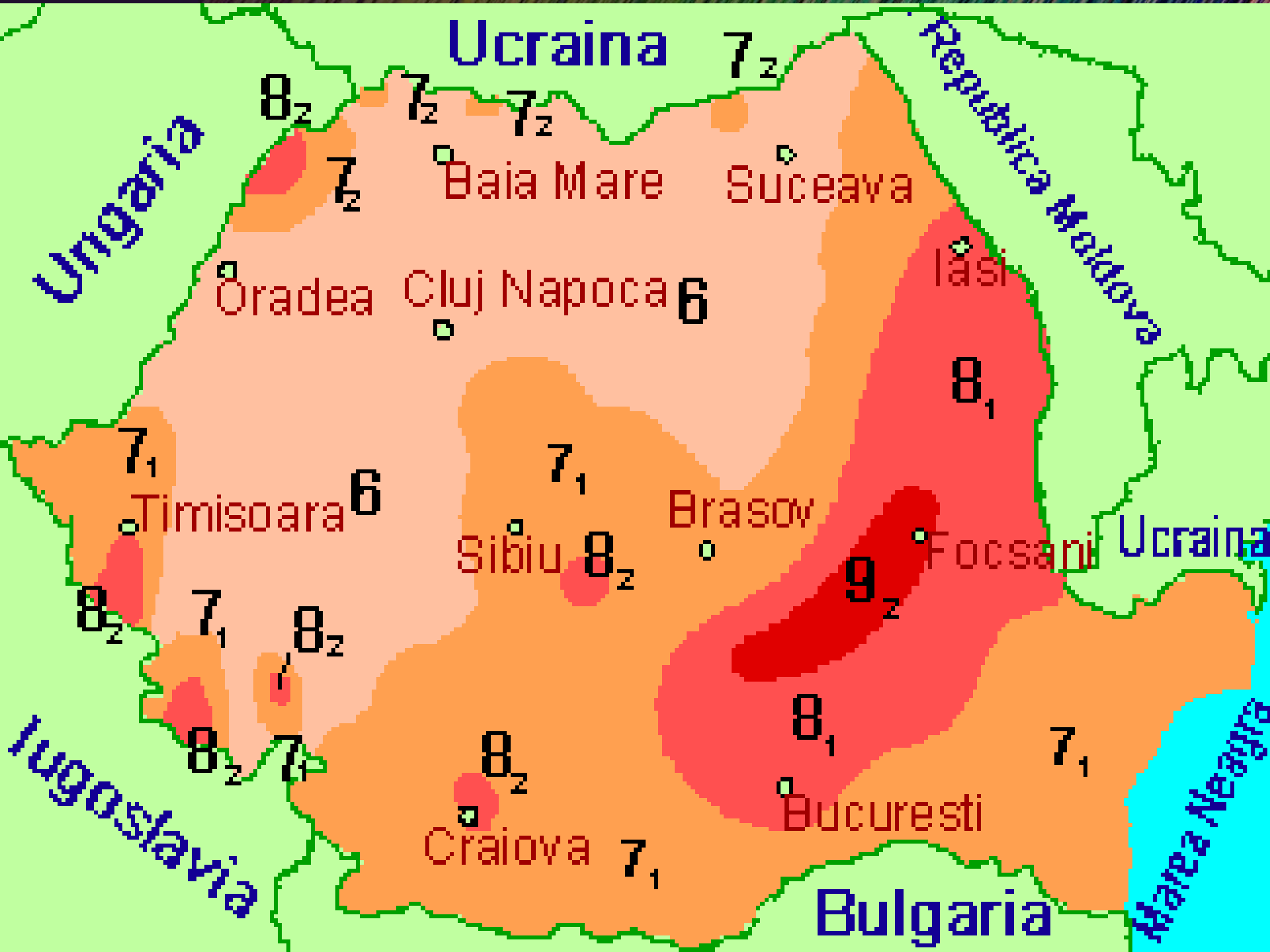
- The undercutting of the foot of a slope
- The deposition of earth or other materials along the upper edge of the slope.

Both operations produce an increase of the shearing stresses in the ground beneath the slope. If and as soon as the average shearing stress on the potential surface of sliding becomes equal to the average shearing resistance, a landslide occurs.

A slope failure on a man-made slope may occur during or at any time after construction. If the slope fails several weeks after construction or later, the slide can be ascribed only to an internal cause which reduced the shearing resistance of the slope material. Delayed slides occur most commonly during heavy rainstorms.

I. EXTERNAL CHANGE OF STABILITY CONDITIONS

- Earthquake shocks increase the shearing stresses along the potential surface of sliding, whereas the shearing resistance remains unchanged.



II. SPONTANEOUS LIQUEFACTION

The arrangement of the grains of fine sand or coarse silt can be so unstable that a slight disturbance of the equilibrium of the grains may cause a rearrangement of the grains, whereby the grains settle into more stable positions, and the porosity of the sediment decreases.

II. SPONTANEOUS LIQUEFACTION

If this process takes place above the water table it has no other effect than a settlement of the ground surface.

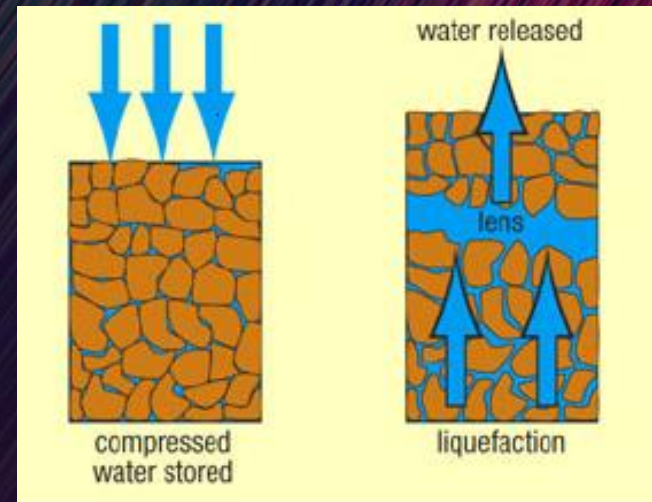
By contrast, if it occurs below the water table its consequences can be catastrophic, because the viscosity of the water, which occupies the voids of the sand, prevents a rapid decrease of the porosity.

The transformation into the liquid state is known as spontaneous liquefaction.

II. SPONTANEOUS LIQUEFACTION

The effect of spontaneous or earthquake liquefaction is simply a sudden change of the material from solid to liquid.

Liquefaction may affect the full depth of the material (usually if fully saturated), or only a thin basal layer.



III. SEEPAGE FROM ARTIFICIAL AND NATURAL SOURCES OF WATER

Seepage from artificial sources of water may compromise the stability of existing slopes, depending on the character of the slope-forming material and on the conditions of stratification.

It may:

- reduce the shearing resistance of the ground;
- eliminate apparent cohesion produced by the surface tension in drained soils;
- eliminate real cohesion by removing cementing materials in solution;
- cause a slope failure by underground erosion due to water veins emerging at the foot of the slope.

III. SEEPAGE FROM ARTIFICIAL AND NATURAL SOURCES OF WATER

Seepage from artificial sources of water may compromise the stability of existing slopes, depending on the character of the slope-forming material and on the conditions of stratification.

It may:

- reduce the shearing resistance of the ground;
- eliminate apparent cohesion produced by the surface tension in drained soils;
- eliminate real cohesion by removing cementing materials in solution;
- cause a slope failure by retrogressive underground erosion by water veins emerging at the foot of the slope.

III. SEEPAGE FROM ARTIFICIAL AND NATURAL SOURCES OF WATER

The analysis results shows that:

(1) The evaporation has influence on the behaviour of unsaturated soil causing the suction to increase and a volume contraction in the surface layer of soil-structure.

III. SEEPAGE FROM ARTIFICIAL AND NATURAL SOURCES OF WATER

(2) Because the shrinkage or volume contraction of unsaturated soil can induce the fracture or tension crack in the soil surface, the permeability behaviour of surface layer of soil structure will be modified. The depth of crack zone and the change range of S_f can be estimated.

III. SEEPAGE FROM ARTIFICIAL AND NATURAL SOURCES OF WATER

(3) When the evaporation action is considered, the tension crack zone in surface layer of slope will increase the water volume of seepage into slope. The safety factor of slope in the case of considering rain/evaporation activity is less than if only rain condition would be considered. So, it is important to consider the influence of rain/evaporation process for the stability analysis of slope.

IV. THE PRESENCE OF GROUND WATER IN LANDSLIDE

Most of the slope failure disasters in a humid area are caused by heavy rain.

The topography of the surface of underground water does not follow the topography of ground surface.

The topography of ground water surface in moved masses of a landslide is complex and forms a series of vein-streams.

Detecting the veins of the ground water on landslide mass is the first necessary stage for planning drainage network and any other prevention works.

V. THE IDENTIFICATION OF WEAK ZONES OF A SATURATED CLAY LANDSLIDE

Soils such as silt and clay are weaker than rock and commonly have complex (or multiple) planes of weakness. In saturated clays the relative movements bring about mechanical swelling, and consequently, the increase of water and the shear strength of soil is drastically diminished to the residual value, provoking local failure.

This happens in clays which are very near from the base of a loessian stratum and in which there is free water source (Tulucesti, Dobrogea, Romania).

A weak area, right under the loess appeared. This trigger the landslide.

CHALLENGE

B. DYNAMICS OF A LANDSLIDE SURFACE

Classification of landslides after velocity

Landslide velocity	Destructive significance
< 1.6mm/yr	Imperceptible without instruments. Construction possible with precautions.
16mm/yr to 1.6m/yr	Permanent structures undamaged by movement.
1.6m/yr to 13m/mon	Insensitive structures can be maintained.
13m/mon to 1.8m/hr	Some insensitive structures can be temporarily maintained.
1.8m/hr to 3m/min	Escape evacuation possible. Structures and equipments destroyed.
3m/min to 5m/sec	Some lives lost because not all persons are able to escape.
> 5 m/sec	Catastrophe of major violence. Buildings destroyed. Many deaths.

Movements of a landslide

4 stages

**PRE-FAILURE
STAGE**

**SOIL MASS
CONTINUOUS**

**FAILURE
STAGE**

**CONTINUOUS
SHEAR
SURFACE**

**POST-FAILURE
STAGE**

**MOVEMENT
OF THE SOIL**

**REACTIVATION
STAGE**

**ROCK MASS
SLIDES ALONG
SHEAR
SURFACES**

**I.
MOVEMENTS
PRECEEDING A SLIDE**

**shearing resistance
of the ground /
shearing stresses
on the potential surface
of sliding = 1**

**instantaneous
decrease
of the ratio**

**earthquakes and
spontaneous
liquefaction**

**gradual
decrease
of the ratio**

**progressive deformation
of the slice of material
above the potential
surface of sliding**

II. MOVEMENTS DURING THE SLIDE

Shear failures + decrease of the shearing resistance

1. Phase the sliding masses advance at an accelerated rate

2. Phase the accelerated movement changes into a retarded one

3. Phase the movement stops or assumes the character of creep

TYPES OF LANDSLIDE MOVEMENT

Falls: abrupt movements

Topples: the forward rotation of a mass

Slides: displacement along shear surfaces
Rotational and transitional slides

Spread: liquefaction of the softer material

Flows: surfaces of shear are short-lived, closely spaced, and usually not preserved

Complex landslides: involve more than one type of movement mechanism

**III.
MOVEMENTS
AFTER SLIDE**

SLOW CREEP PHASE

**mechanical
mixture
of the slide
material
with water**

**destruction
of the intergranular
bonds at
unaltered
water content
of the material**

**IV.
REACTIVATION
STAGE**

CREEP PHASE

**tectonic activities
through the faults**

**earthquakes and
spontaneous
liquefaction**

increase in rainfall

**high
groundwater levels**

**stress conditions
along the slip surface**

**shear deformations
do occur**

Slopes affected by reactivation of landslides in Eastern Carpathians























STRATEGY

RISK MITIGATION MEASURES

The rational design of a landslide repair cannot begin until the *sensitive factors* of site geology are properly evaluated.

If a slope has started to move, the means for stopping the movement must be adapted to the processes that started the slide.

It is hardly an exaggeration to say that most slides are due to an abnormal increase of the pore-water pressure in the slope-forming material or in a part of its base. In such instances radical drainage is indicated.

If drainage is difficult or if its success is doubtful, the ground movements can be stopped either by reducing the slope angle or by constructing artificial barriers, such as heavy retaining walls or rows of piles across the path of the moving material.

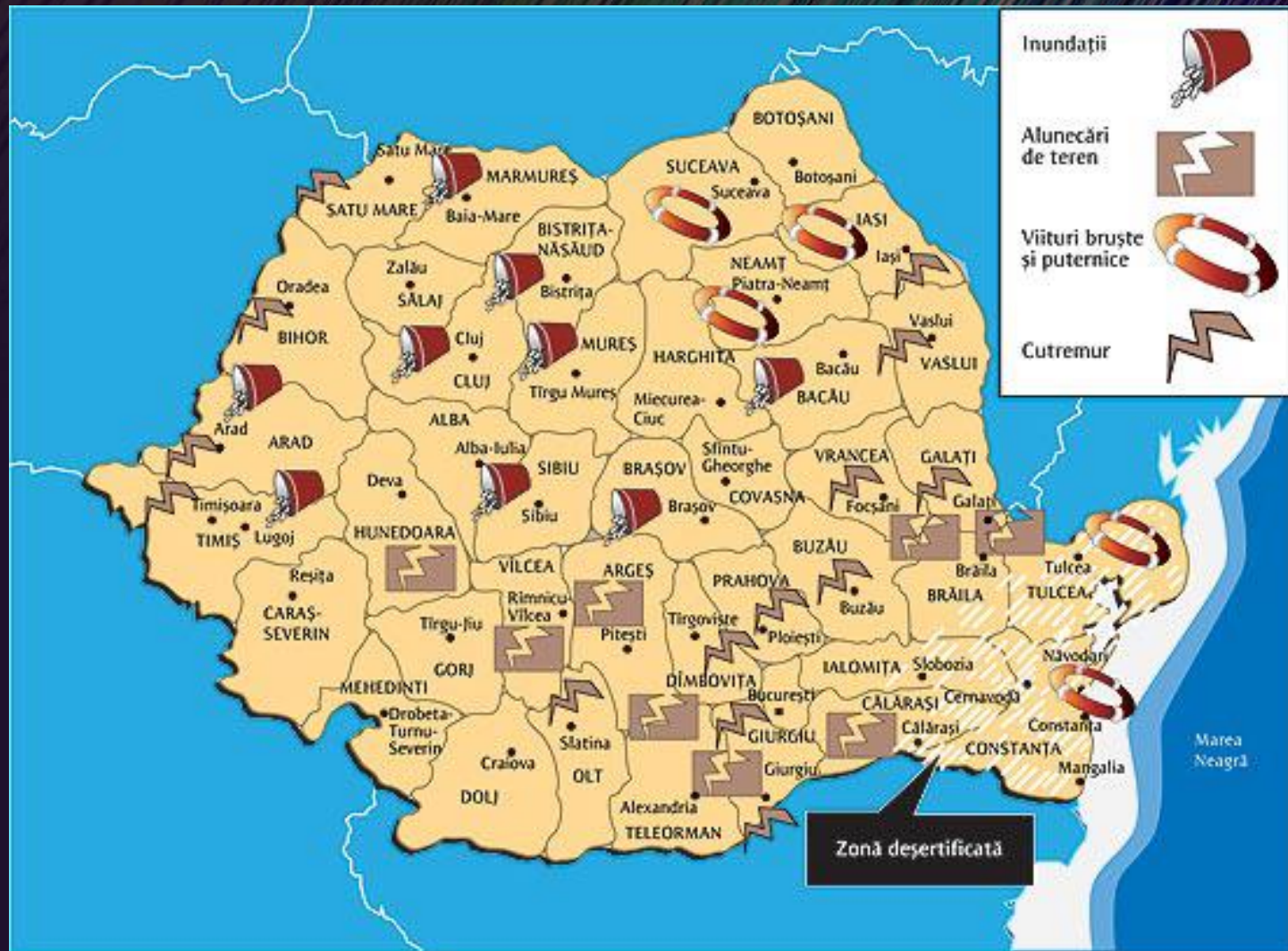
<u>LANDSLIDE TRIGGERS</u>	<u>NATURAL TRIGGERS</u>	<u>HUMAN TRIGGERS</u>
Removal of support	Erosion by streams, waves, glaciers	Excavation at the base of a slope
Removal of vegetation	Forest fires	Timbering
Addition of moisture	Rainfall or snowmelt	Sewage disposal, broken water pipes
Addition of weight	Snowfall, volcanic ash, landslides	Placement of fill
Over-steepening	(term used as "removal of support")	Placing fill
Vibrations	Earthquakes, nearby landslides	Blasting, operation of heavy equipment

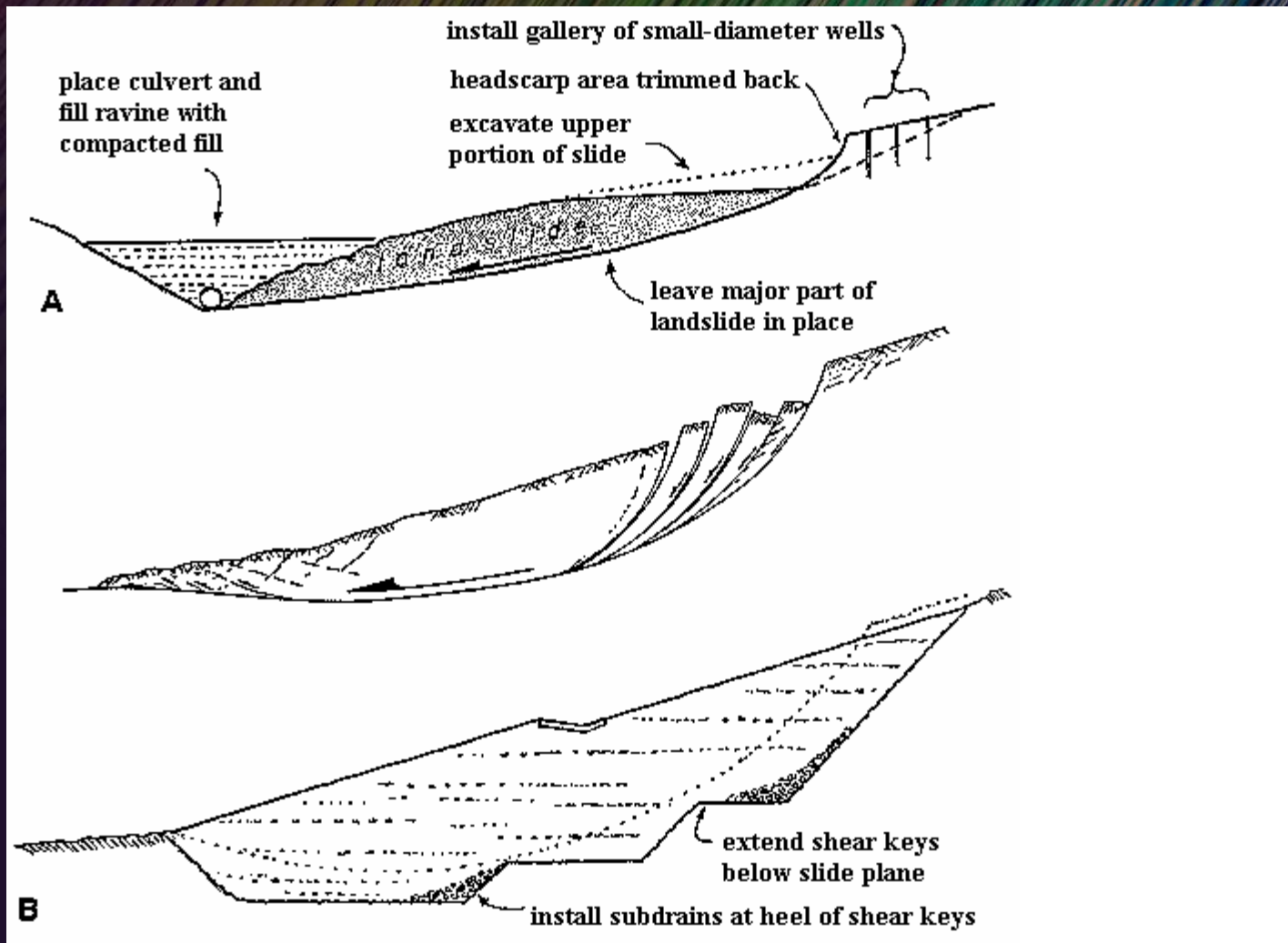
Every landslide or slope failure is the large-scale experiment that enables competent investigators to draw reliable conclusions regarding the shearing resistance of the materials involved in the slide.

Once a slide has occurred on a construction job, the data derived from the failure may permit reliable computation of the factor of safety of proposed slopes on the same job and modification of the design in accordance with the findings.

All too often, sites prone to landsliding have been the scenes of repeated repair attempts within a few years of each other. Experience over the past half-century tends to suggest that many landslide repair attempts are made without benefit or full understanding of the geometry and hydrologic properties of the affected sites. In addition, the blind implementation of a traditional engineered repair scheme such as recompaction, may not serve to adequately mitigate all manner and form of future slope instability.

Romanian Risk Microzonation Map

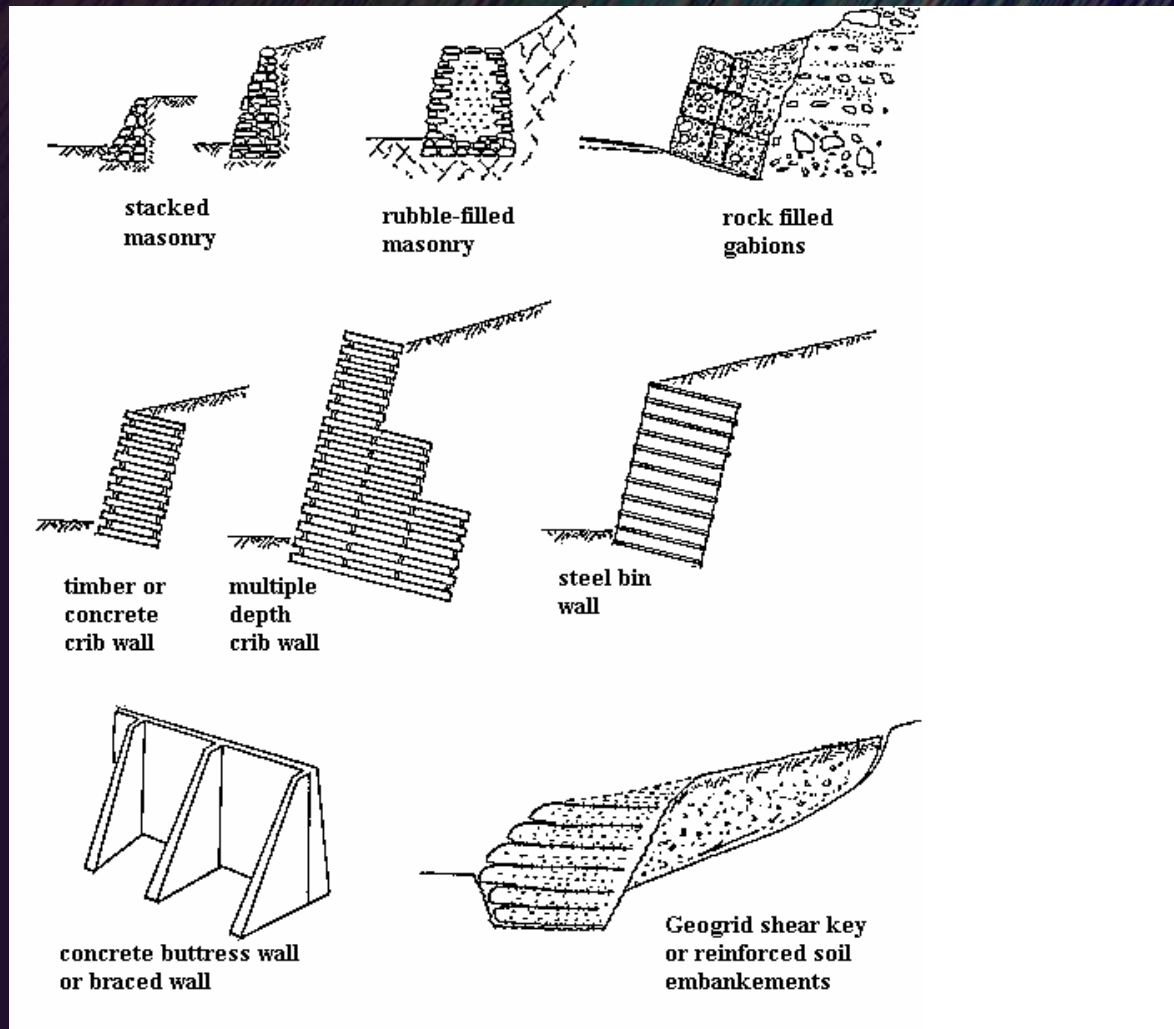




The selection of soil slope stabilization techniques considers the factors that influence the choice and the examination of the landslide.

Vegetation is one of the most economical and effective alternatives for a surface treatment in case of the relatively flat slopes. The aesthetic impression for the public also tends to result in giving a high advantage to the choice of the vegetation as a surface treatment.

The number of alternatives for soil slope stabilization is large; ranging from simple drainage measures, through the use of bio-engineering techniques to the more traditional use of gravity and embedded retaining structures.



CONCLUSIONS

The enormous damages from landslides can be reduced. The primary objective is to reduce long-term losses from these hazards by improving our understanding of the causes of ground failure and suggesting mitigation strategies.

Some Aspects on Landslide Risk Mitigation

by

Ancuța Rotaru

**“Gheorghe Asachi” Technical University
Iasi, Romania**



**THE 3rd DECEMBER 2013
MONTESCAGLIOSO
LANDSLIDE
-ITALY-**

What is a landslide and what causes one?

A landslide is defined as the movement of a mass of rock, debris, or earth down a slope. Landslides are a type of "mass wasting," which denotes any down-slope movement of soil and rock under the direct influence of gravity. The term "landslide" encompasses five modes of slope movement: falls, topples, slides, spreads, and flows. These are further subdivided by the type of geologic material (bedrock, debris, or earth). Debris flows (commonly referred to as mudflows or mudslides) and rock falls are examples of common landslide types.

- Almost every landslide has multiple causes. Slope movement occurs when forces acting down-slope (mainly due to gravity) exceed the strength of the earth materials that compose the slope. Causes include factors that increase the effects of down-slope forces and factors that contribute to low or reduced strength. Landslides can be initiated in slopes already on the verge of movement by rainfall, snowmelt, changes in water level, stream erosion, changes in ground water, earthquakes, volcanic activity, disturbance by human activities, or any combination of these factors. Earthquake shaking and other factors can also induce landslides underwater. These landslides are called submarine landslides. Submarine landslides sometimes cause tsunamis that damage coastal areas.

The village of Montescaglioso (Basilicata region, Southern Italy) is located on the top of a hill at about 350 m a.s.l. along the left bank of the Bradano River.

In this paper the landslide occurred on the 3rd December 2013 involving the south western slope is dealt with. The landslide caused severe damages to private houses, commercial buildings and main infrastructures. Several studies were focused so far on this event (Amanti et al. 2014; Manconi et al. 2014; Raspini et al. 2015; Pellicani et al. 2016; Amanti et al. 2016), which provided a comprehensive description of the phenomenon.

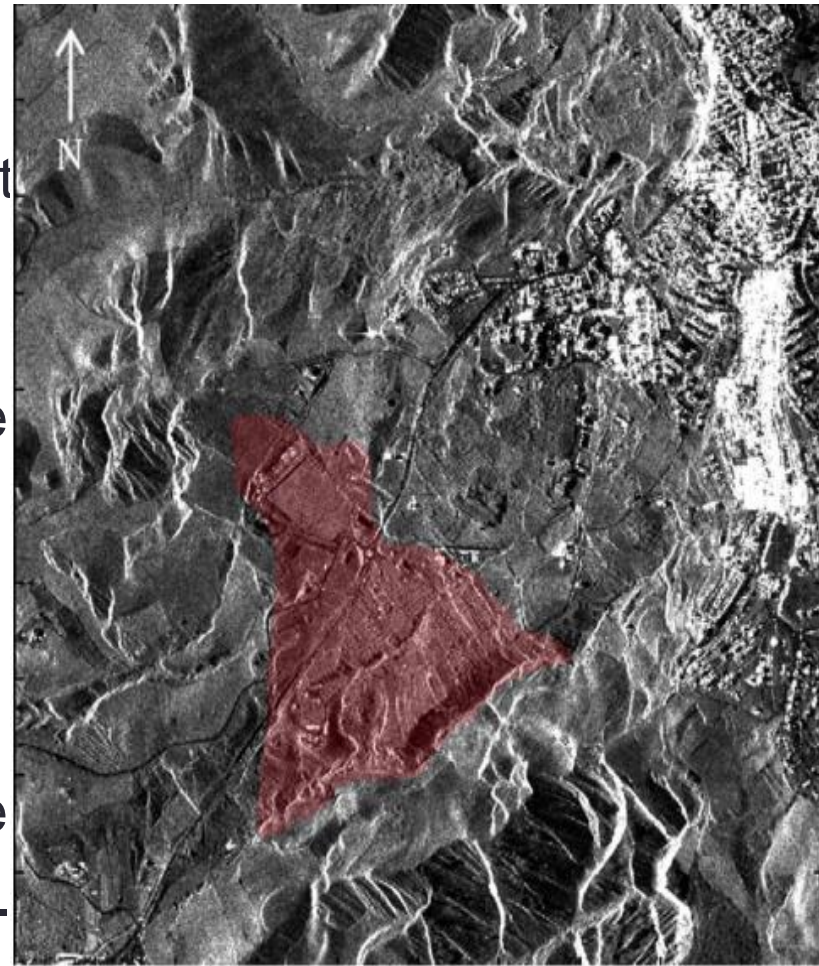


Figure: SAR reflectivity map of post-landslide dataset. The landslide area is highlighted in Red.

On December 3, 2013, a large landslide activated on the SW slope of Montescaglioso (Matera province, Basilicata), affecting an area with evidence of past instability. The landslide involved some 500 m of the main road to the village, and also interested several houses and other buildings.



The landslide occurred on the south-western slope of the Montescaglioso hill, over an area about 500,000 m² wide. A maximum depth of 40 m for the failure surface is presumed, with an estimated volume of about 8 millions of cubic meters.

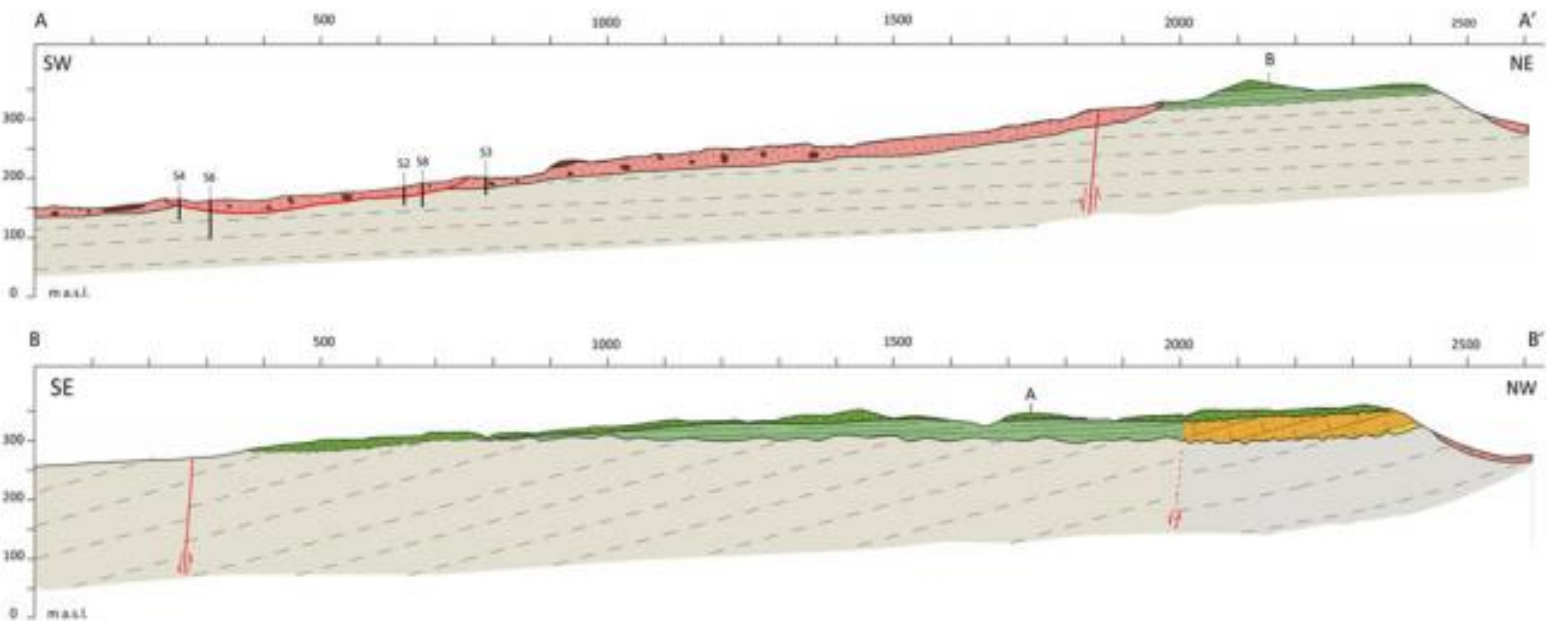
The landslide shows a triangular-shaped area, which is delimited by the main crown, at an elevation of about 200 m a.s.l., the foot, located in Capo Iazzo stream about at 100 m a.s.l., with a total length of 1200 m and a width of 800 m. The intense rainfall, occurred between the 5th and 8th October 2013 and the 30th November and 2nd December 2013, have been regarded as the trigger for the landslide event. More in particular, the rain gauges located at Ginosa (8 km east of Montescaglioso), recorded 246 mm in 68 h for the event of October and 151.60 mm in 56 h,

between 02.00 PM of 30th November 2013 and 10.00 PM of 2nd December. Considering the intensity of the last event (cumulated rainfall of 151.60 mm), a return period of about 20–50 years can be attributed according to Pellicani et al. (2016). Moreover, according to the same Authors, if the annual maximum daily precipitation is accounted for, the measured daily rainfall (125 mm) has a return period ranges from 20 to 100 years, depending on the stations considered.

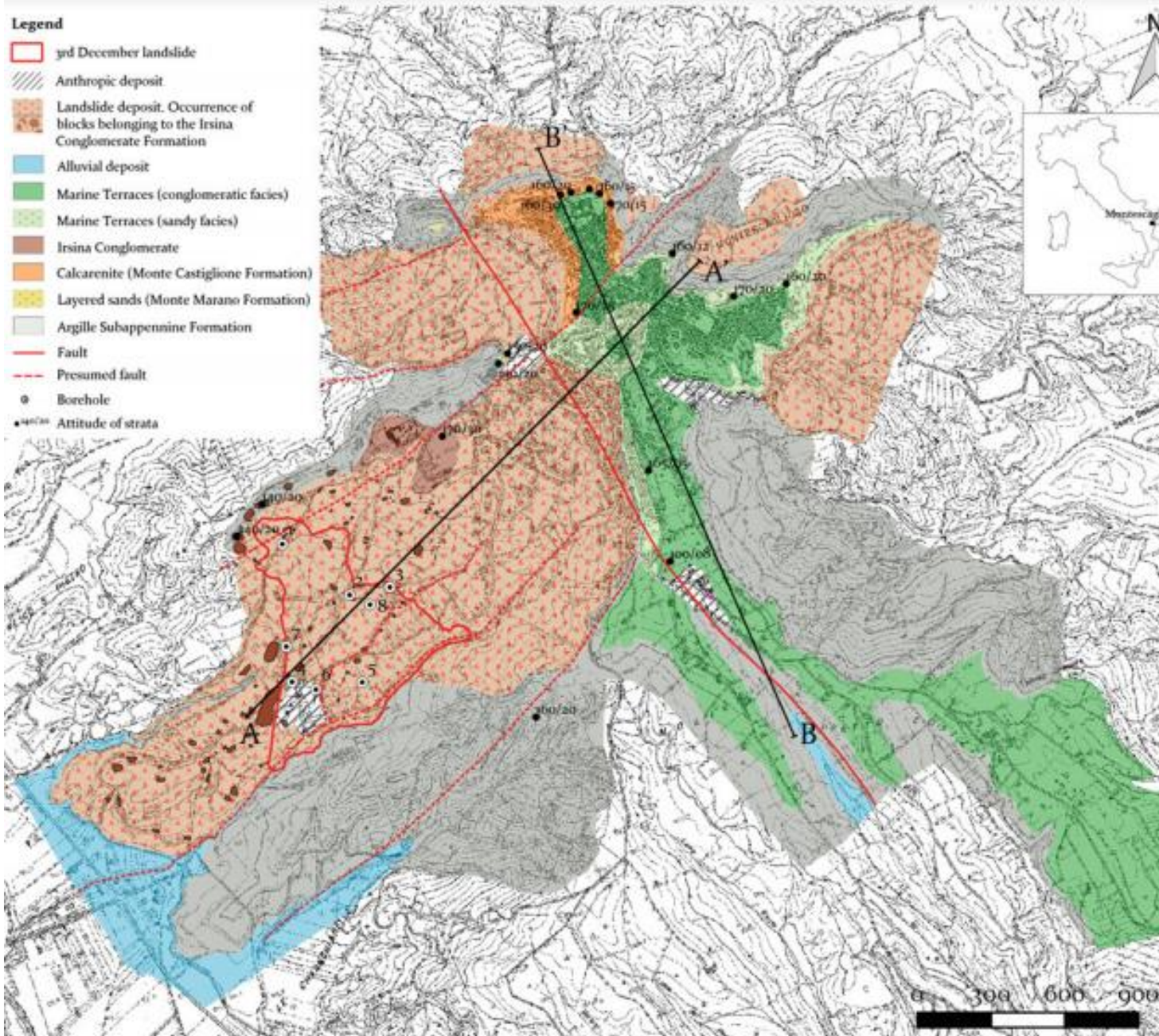


Area involved in the 3rd December Montescaglioso landslide

- The 3rd December landslide had a complex manifestation. The evidences of ground failures were collected at 01.00 PM of the same day, in proximity of the main road (namely Piani Bradano road), for a length of about 500 m. In the following hours, several private houses have been damaged, as proved by displacement up to 6 m of their foundations. However, some damages were documented by local witnesses in private areas the day before the event localized at the toe of the landslide (Pellicani et al. 2016). The last phase of the movement (occurred in the night between the 3rd and 4th December) was typified by a retrogressive style, causing a northward replacement of the landslide area.



Geological cross sections A-A', B-B' of the Montescaglioso hill.



Geological map of the Montescaglioso hill

• Monitoring and geomorphological analysis

- Monitoring the Montescaglioso landslide and surrounding areas, aimed at recognizing likely widenings or reactivations of the main movement, and carrying out further activities and analyses aimed at the comprehension of the phenomenon, and to provide useful indications to the planning and design of stabilization works.
- Methods:
- Topographic and inclinometric monitoring. Landslide inventory maps. Detailed geomorphological mapping. Monitoring of the road at present used as main route to the village. Definition of the geological-technical model of the landslide.

- Results:
- Occurrence of the large landslide on December 3, 2013, pointed out the high proneness to landslides of the Montescaglioso territory, and the negative effects deriving from anthropogenic activities, especially performed through changes in the natural hydrographic network. The on going studies will further clarify and deepen the preliminary results obtained.



- Products:
- Map of surface deformations produced by the landslide. Thematic maps on landslide inventory, and multi-temporal maps of the slopes affected by the 2013 landslide. Weekly bulletin of topographic monitoring. Monthly bulletin of inclinometric monitoring.



639200

640000

4489500

4489500

4489500

4489500

Surface Deformation Map

-  The December 03, 2013, Montescaglioso event
-  Anthropogenic scarp
-  Crack with evidence of strike-slip movement
-  Narrow crack
-  Pressure ridge
-  Scarp
-  Small landslide
-  Tension crack
-  Uphill-facing scarp
-  Water line
-  Pond
-  Trench
-  Highly disturbed area

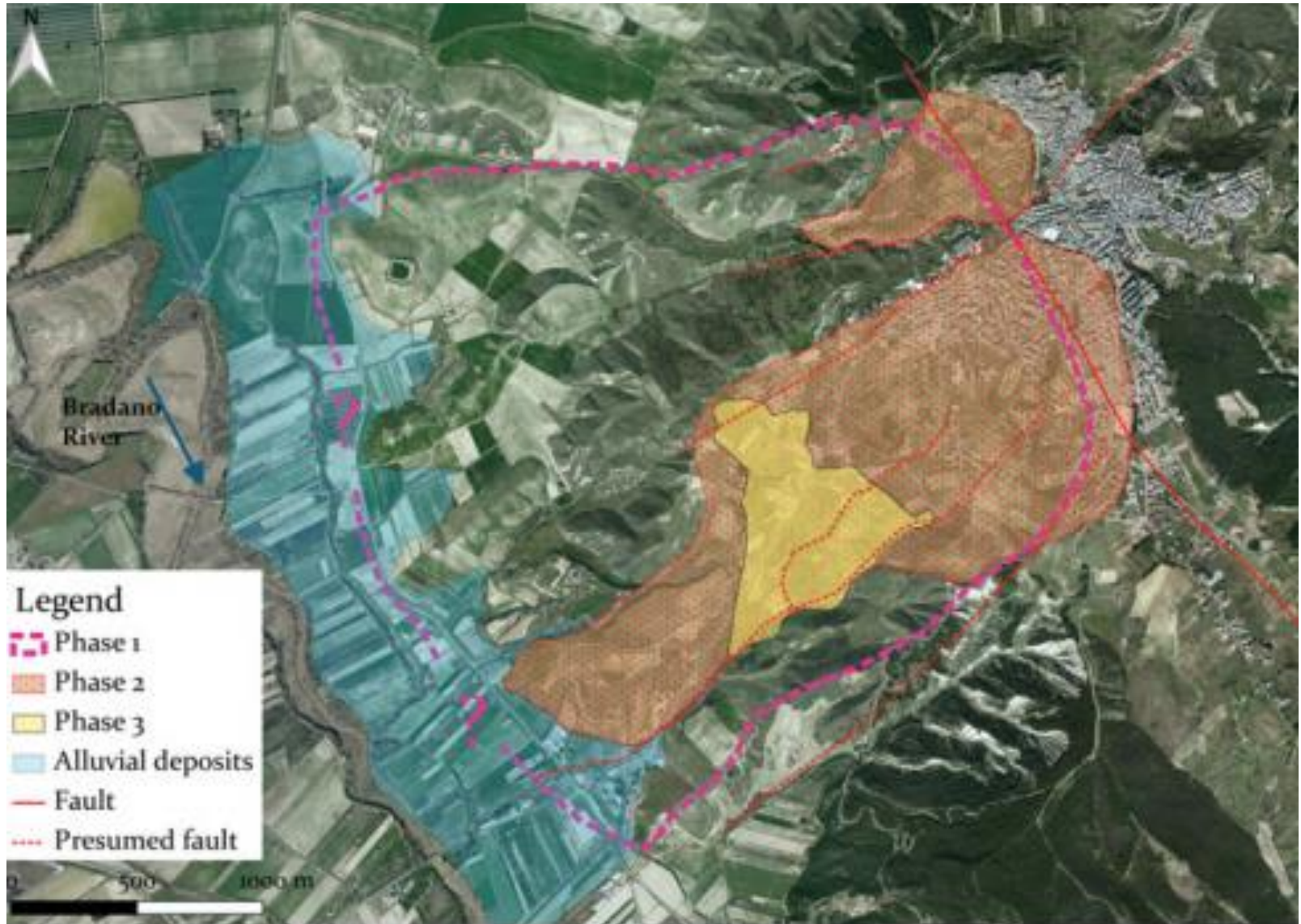


639200

640000

- Conclusions:

- The monitoring activities (still on going) allowed since the first week after the event to control its evolution over a wide area, well beyond the landslide limits. In cooperation with the other experts involved, the first surveys have been carried out, which outcomes are at present in phase of elaboration and analysis.



Schematic evolution of the western slope of Montescaglioso hill





References:

- https://www.researchgate.net/publication/261017685_Brief_communication_Rapid_mapping_of_event_landslides_the_3_December_2013_Montescaglioso_landslide_Italy
- <https://blogs.agu.org/landslideblog/2013/12/05/an-interesting-landslide-at-montescaglioso-in-southern-italy/>
- <file:///Users/macbookproretina/Desktop/nhess-14-1835-2014-supplement.pdf>
- <http://www.irpi.cnr.it/en/project/monitoraggio-e-studi-sulla-frana-di-montescaglioso-mt-del-3-dicembre-2013/>
- https://www.nhazca.it/wp-content/uploads/2020/06/Bozzano_et_al_2017_Montescaglioso.pdf



Thermo-Hydro-Mechano-Chemical Fatigue of Historical Buildings : Myths and Realities

With collaboration and curtesy of : Kevin BECK⁽¹⁾, N. BELAYACHI⁽¹⁾, D.P. DO⁽¹⁾

Prof. Dashnor HOXHA⁽¹⁾

University of Orleans, Polytech Orleans,

Laboratory of Mechanics “Gabriel Lamé”, Centre Val de Loire

8 rue Léonard de Vinci, 45072, Orleans, FRANCE



Outline

- 1 – Motivation
- 2 – Stone decay : an eternal silent fight story
- 3 – Expert analyses and hypothesis
- 4 – Theoretical bases for analyses and state evaluation
- 5 – Experimental and numerical checking :when some myths fall
- 6- Conclusions



Outline

- 1 – Motivation
- 2 – Stone decay : an eternal silent fight story
- 3 – Expert analyses and hypothesis
- 4 – Theoretical bases for analyses and state evaluation
- 5 – Experimental and numerical checking :when some myths fall
- 6- Conclusions

Do you know what is what ?



Do you know what is what ?



IV century – 989 - 1278-1568



“ Hundreds of firemen of the Paris Fire Brigade are doing everything they can to bring the terrible [#NotreDame](#) fire under control. All means are being used, except for water-bombing aircrafts which, if used, could lead to the collapse of the entire structure of the cathedral.
– Sécurité Civile Fr (@SecCivileFrance) [April 15, 2019](#)

“ So horrible to watch the massive fire at Notre Dame Cathedral in Paris. Perhaps flying water tankers could be used to put it out. Must act quickly!
– Donald J. Trump (@realDonaldTrump) [April 15, 2019](#)

1- MOTIVATION

Interaction structure- environment



The stone is internal

... the erosion too ...

Various kinds of degradations ...



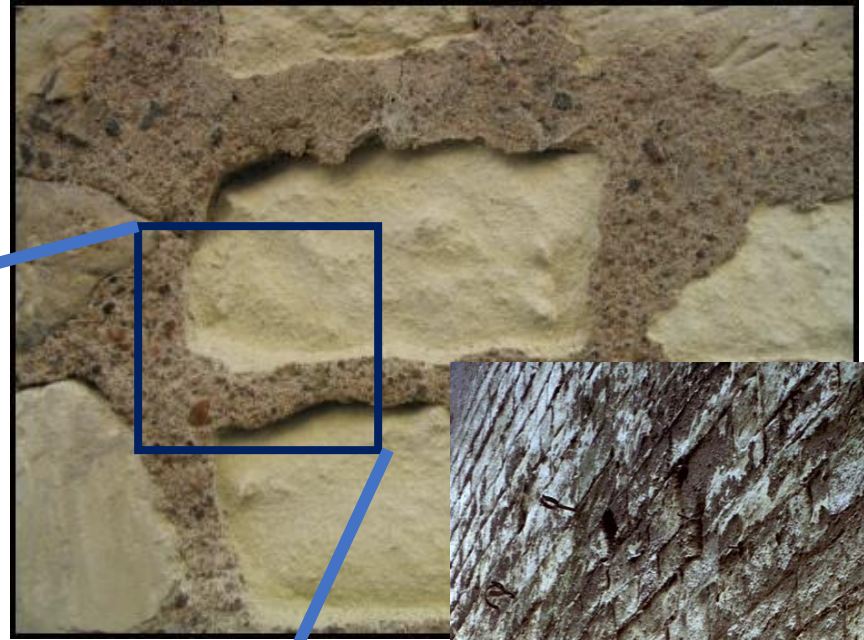
1- MOTIVATION

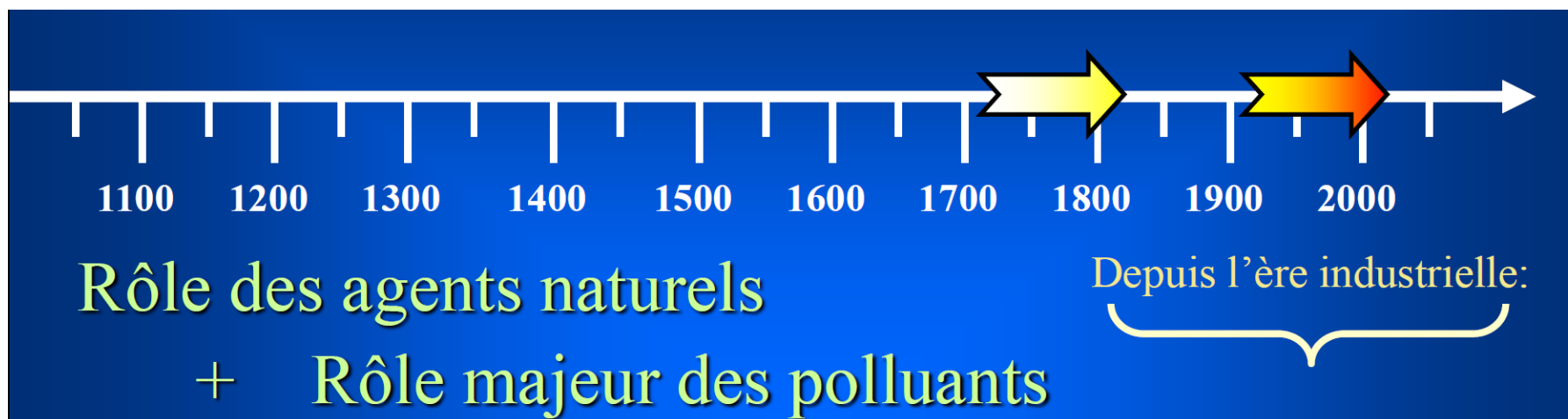
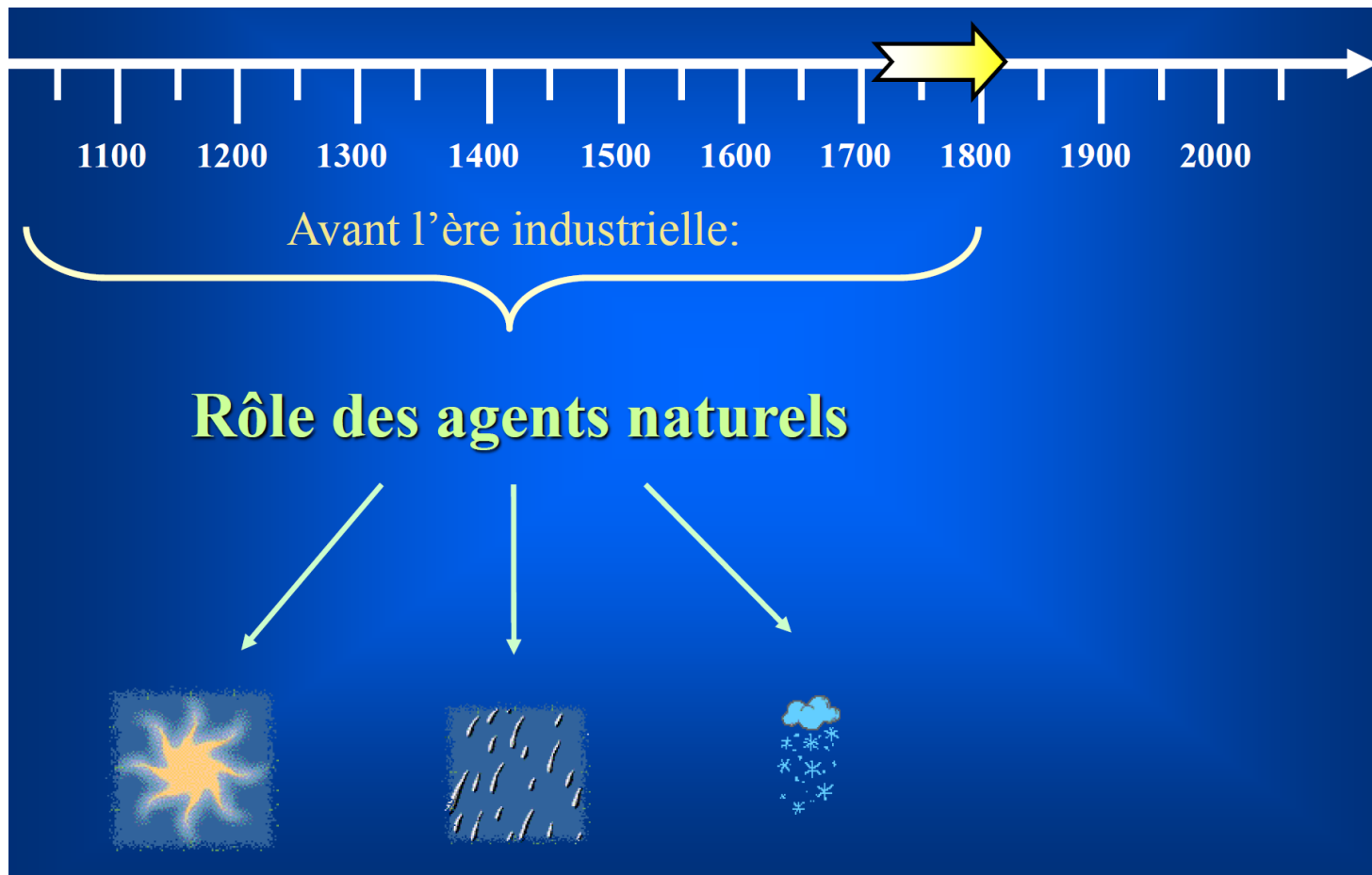
These very good bad ideas !!!!



Stone-Stone compatibility (From K. Beck)

These very good bad ideas !!!!





→ Le nettoyage

- Le gommage ®

projection d'une fine poudre (ϕ 30 à 100 μ m) sous faible pression (avec ou sans eau)



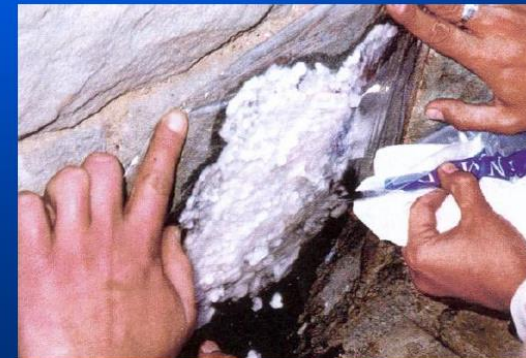
- Le nettoyage laser

vaporisation des salissures en surface par l'impact d'un faisceau laser à impulsions



- Les cataplasmes (procédé tollis ®)

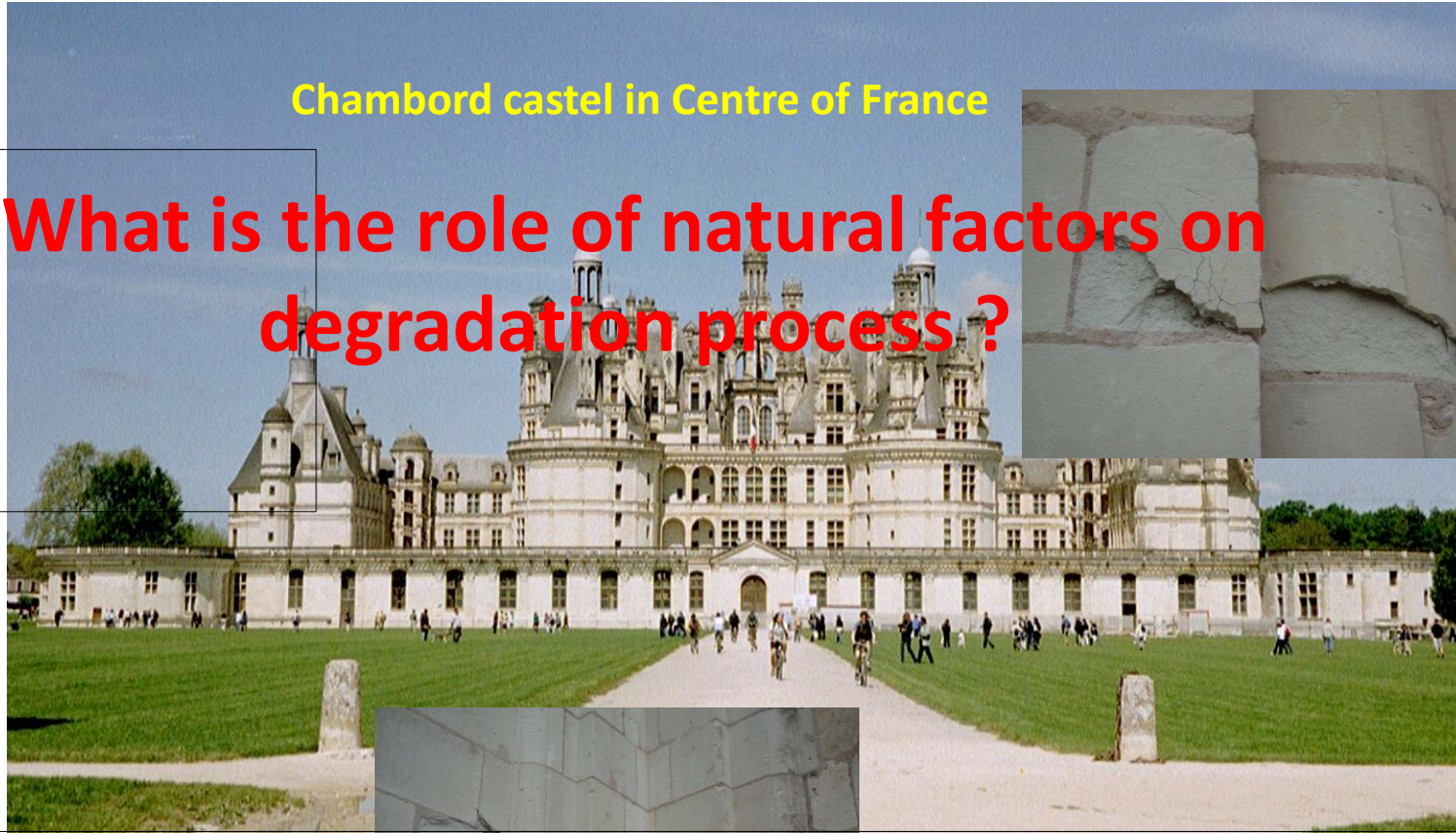
application d'un cataplasme de laine de roche dissolvant les salissures et dessalinisant la pierre



1- MOTIVATION

Chambord castel in Centre of France

What is the role of natural factors on degradation process?



- No known urban pollution sources from anthropological activity
- However various degradation ...

Credits : <http://www.crmd>





Outline

1 – Motivation

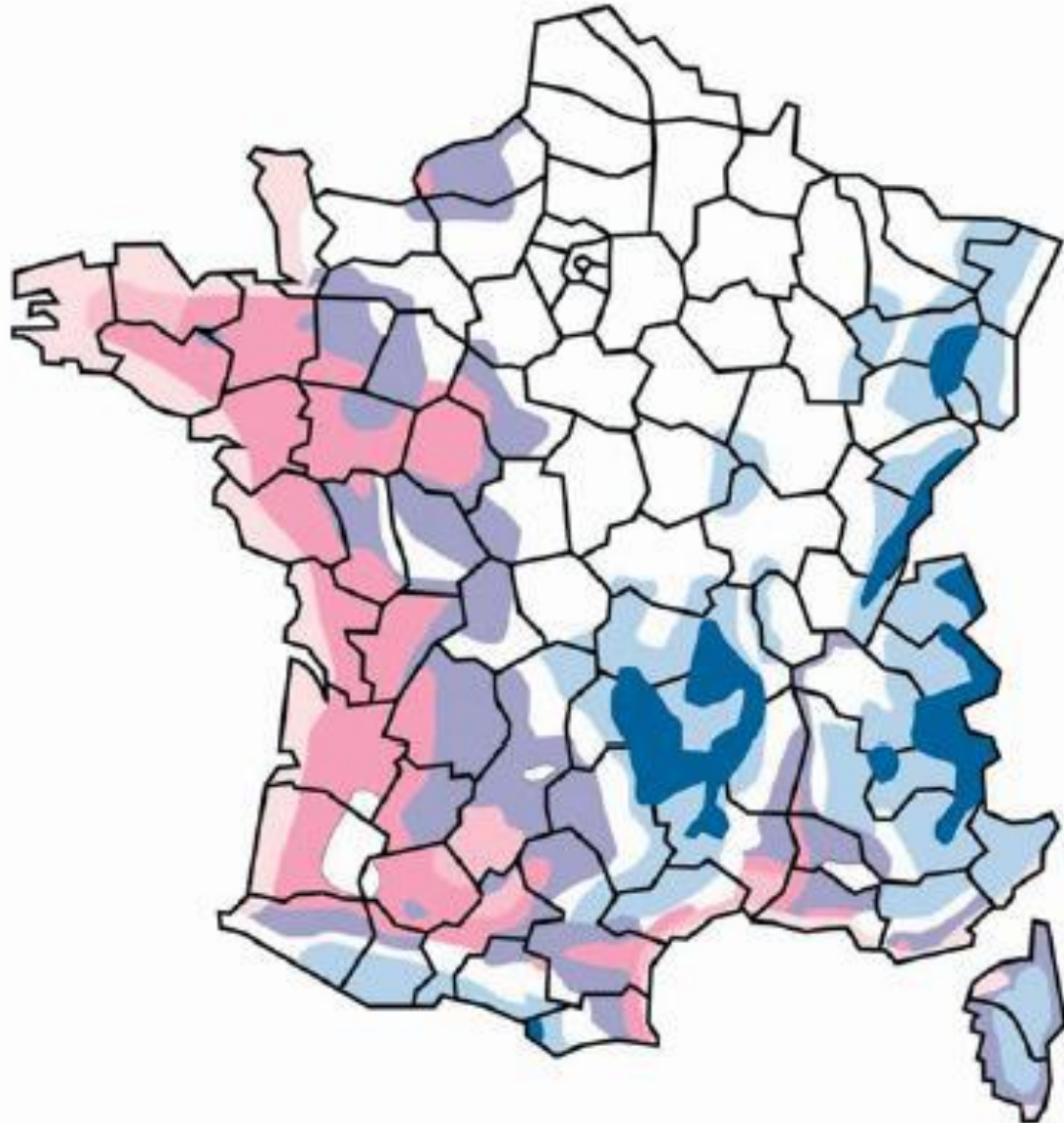
2 – Stone decay : an eternal silent fight story

3 – Expert analyses and hypothesis

4 – Theoretical bases for analyses and state evaluation

5 – Experimental and numerical checking :when some myths fall

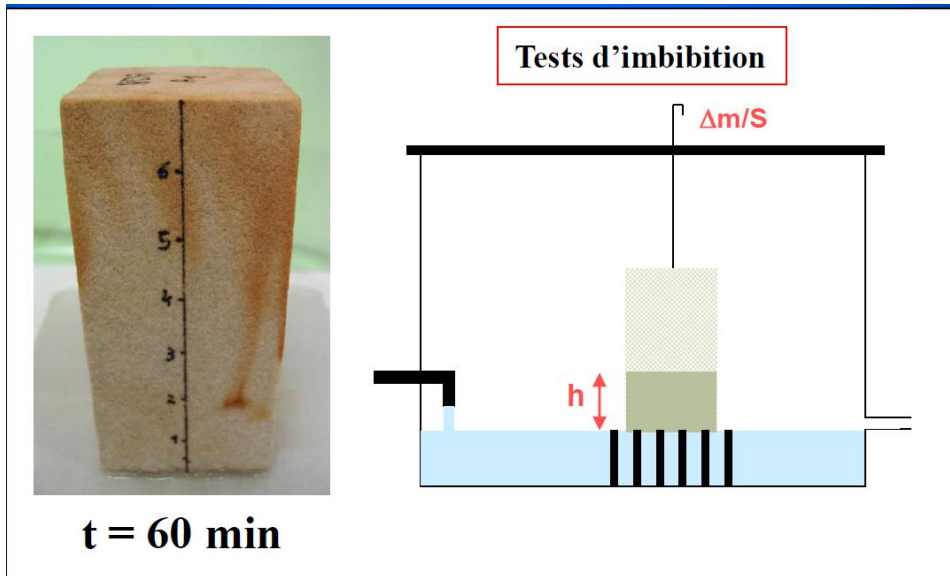
6- Conclusions



freezing

- gel modéré
- gel modéré à gel sévère suivant l'altitude
- gel sévère
- gel très faible
- gel très faible à gel faible suivant l'altitude
- gel faible
- gel faible à gel modéré suivant l'altitude



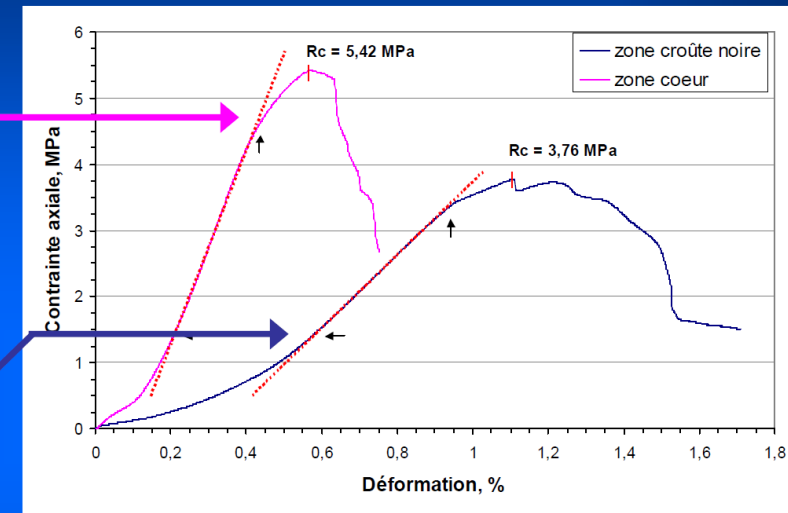
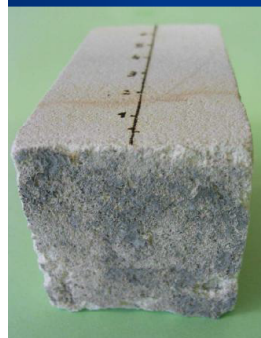


L'altération : étude de cas

Approche macroscopique :

Cas du Tuffeau blanc

Résistance mécanique



Zone de coeur



Zone de surface

état sec



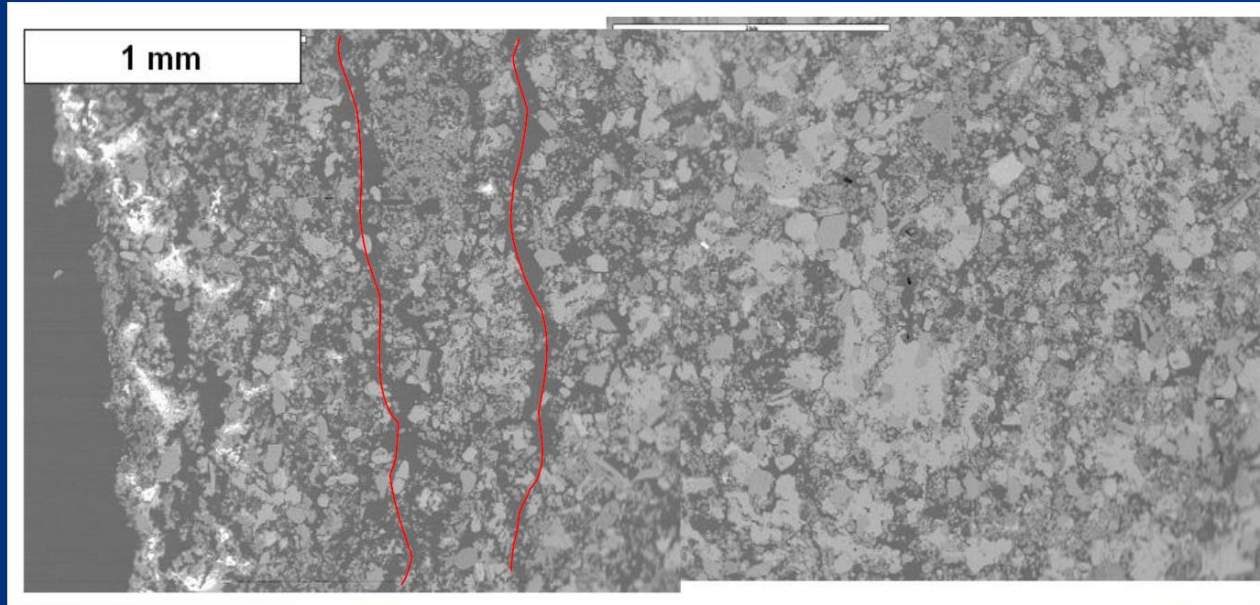
La zone de surface est fragilisée

L'altération : étude de cas

Approche microscopique :

Cas du Tuffeau blanc

Milieu poreux



**Nombreuses microfissures
sous-jacente à la croûte noire**

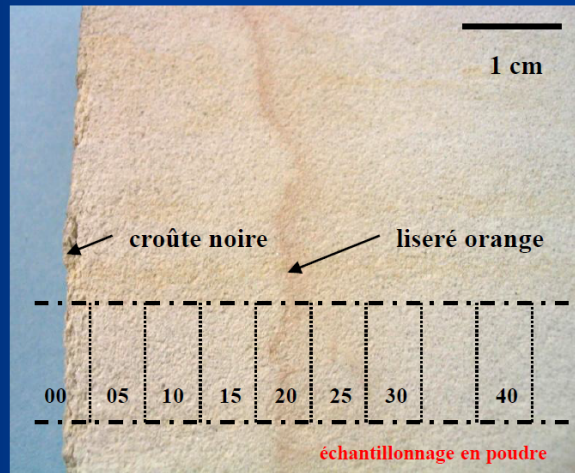
L'altération : étude de cas

Approche microscopique :

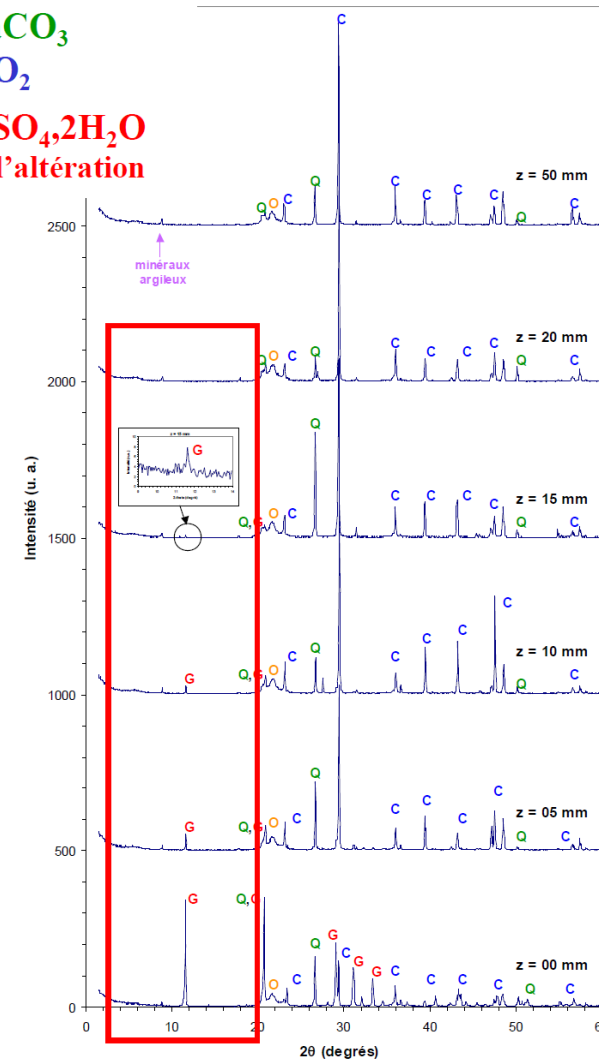
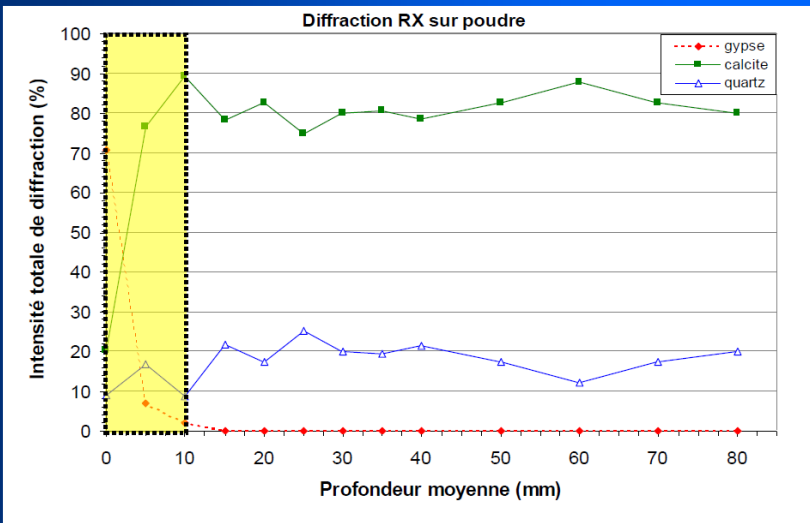
Cas du Tuffeau blanc

Minéralogie

DRX sur poudre



Calcite : CaCO_3
 Quartz : SiO_2
 Gypse : $\text{CaSO}_4 \cdot 2\text{H}_2\text{O}$
 = produit de l'altération



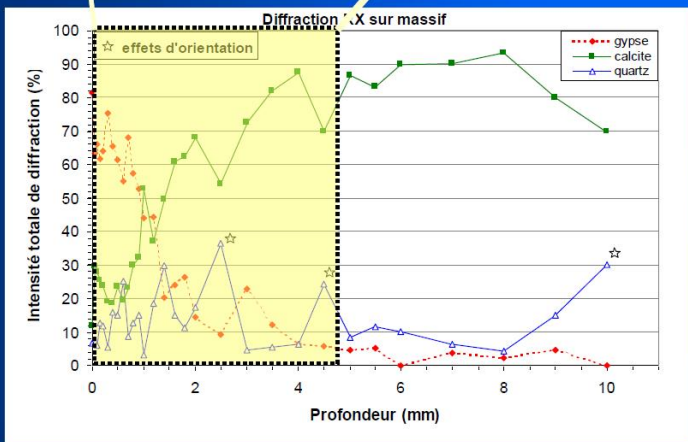
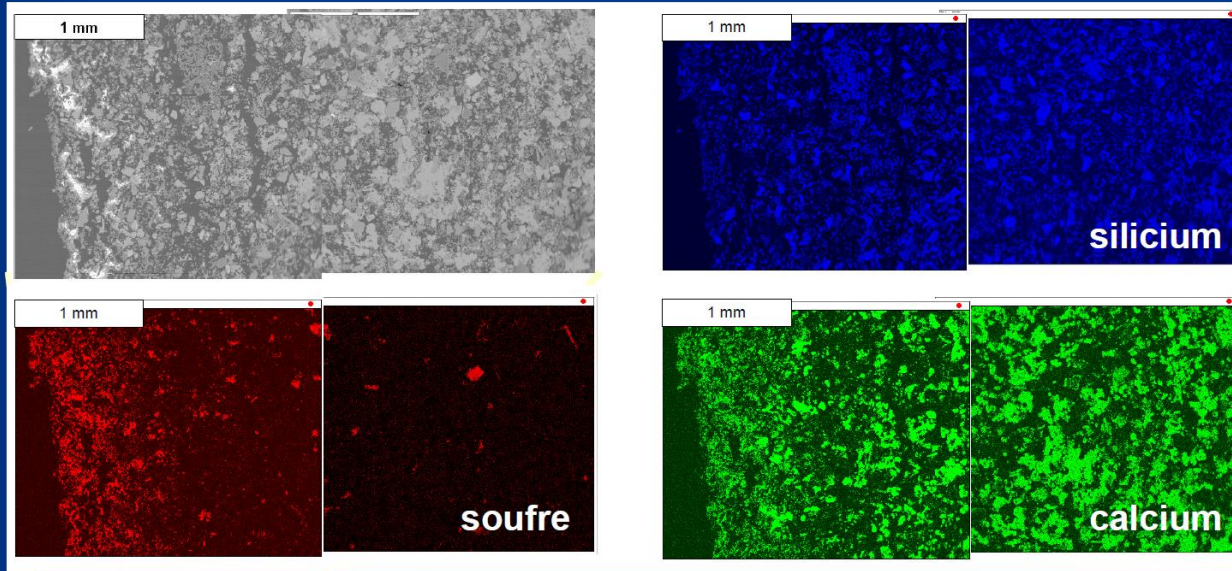
L'altération : étude de cas

Approche microscopique :

Cas du Tuffeau blanc

Minéralogie

DRX sur poudre et sur massif, ATG, ICP, MEB, ...



Calcite : CaCO_3

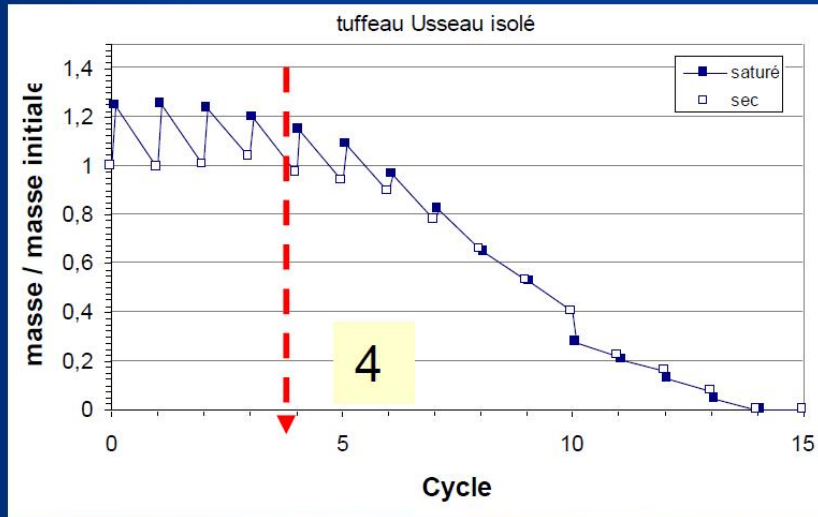
Quartz : SiO_2

**Gypse : $\text{CaSO}_4 \cdot 2\text{H}_2\text{O}$
= produit de l'altération**

D'autres agents d'altération

Les sels : cas du Na_2SO_4

Na_2SO_4
14%



Protocole d'altération:
cycles : imbibition avec de l'eau salée
↔ séchage à 105°C

(Norme EN12370)



cycle n°0



cycle n°3



cycle n°6



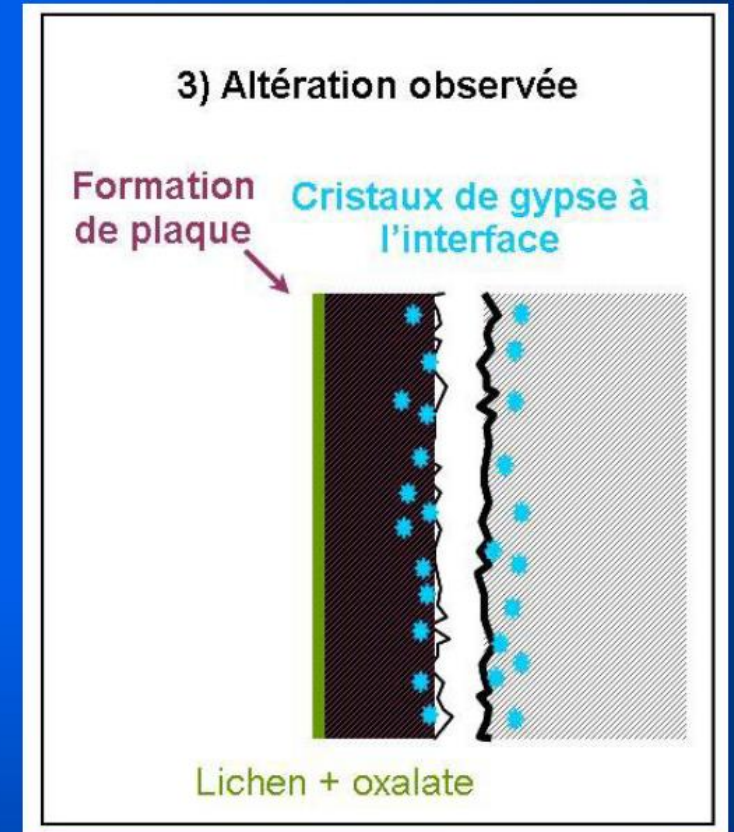
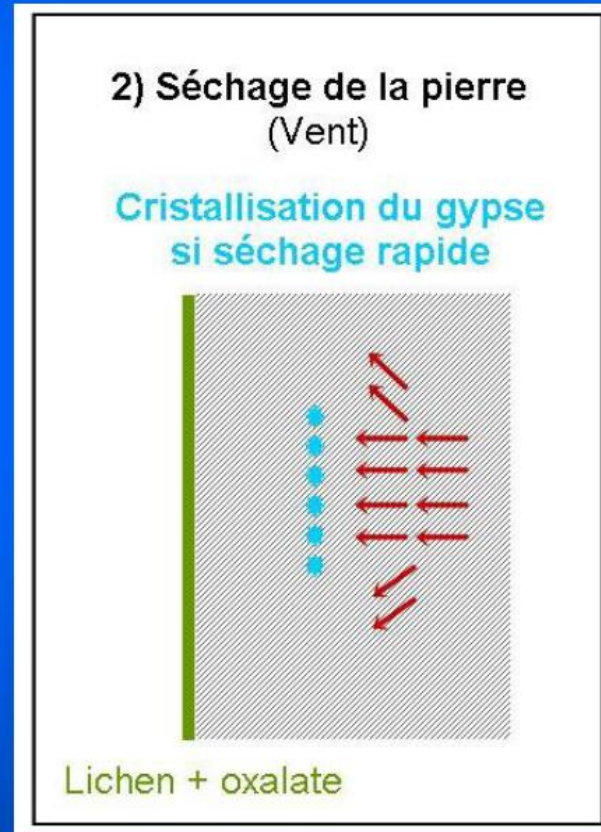
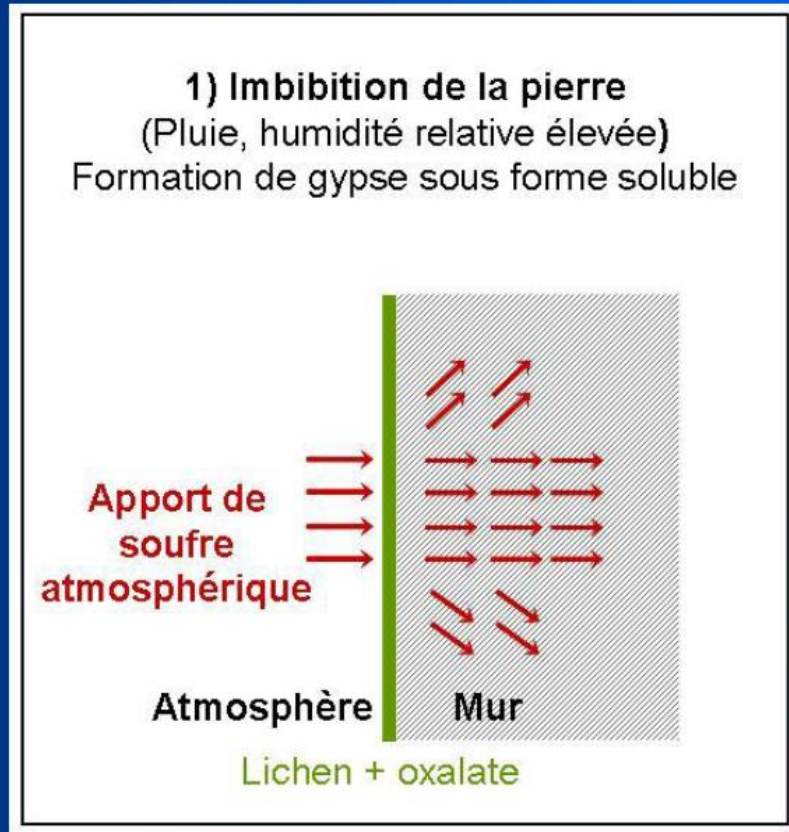
cycle n°9



cycle n°12

Hypothèses émises

- Le gypse : facteur déclenchant de l'altération en plaques



Following K. Beck



Outline

- 1 – Motivation
- 2 – Stone decay : an eternal silent fight story
- 3 – Expert analyses and hypothesis
- 4 – Theoretical bases for analyses and state evaluation
- 5 – Experimental and numerical checking :when some myths fall
- 6- Conclusions

POROMECHANICS THM-C FRAMEWORK

- Multiphase flow

$$\frac{M_j}{\rho_j} = \lambda_j (-\nabla P_j + \rho_j \underline{F}) \quad j = \begin{cases} w \rightarrow \text{water liquid,} \\ gz \rightarrow \text{gaz} \end{cases}$$

Darcy law for unsaturated media

$$\lambda_j = \frac{k_{in} \cdot k_j^{rel}(S_{lq})}{\mu_j} \quad k_l^{rel}(S_{lq}) = S_{lq}^m$$

$$C_{vp} = \frac{p_{vp}}{p_{gz}} \quad \frac{M_{vp}}{\rho_{vp}} - \frac{M_{as}}{\rho_{as}} = -F \nabla C_{vp}$$

Fick diffusion

+ masse conservation law

Multiphase equilibrium

✓ Kelvin law:

parfait gases (air and water vapor)

$$P_C = \frac{\rho_l \cdot R \cdot T}{M_l^{ol}} \ln(Hr)$$

POROMECHANICS THM-C FRAMEWORK

For non-isothermal conditions

$$\underline{\underline{\sigma'}} = \underline{\underline{\sigma}} + b \pi \underline{\underline{I}} + 3\alpha K \Delta T \underline{\underline{I}}$$

thermics

hydrics

- **Thermal diffusion**

$$\underline{q} = -\lambda_T \nabla(T)$$

Fourier law

$$\sum_i h_i^m \dot{m}_i + \sum_i \text{div}(h_i^m \underline{M}_i) + \text{div}(\underline{q}) + Q' = \Theta$$

Energy conservation

i = liquid, dry air, vapour, dissolved gas

POROMECHANICS THM-C FRAMEWORK

Proposal for a sequential solving schema

Hypothesis :

Weak M->C coupling (but strong C->M coupling)

$$\underline{\underline{d\varepsilon}} = \underline{\underline{d\varepsilon}}^m + \underline{\underline{d\varepsilon}}^h + \underline{\underline{d\varepsilon}}^{th} + \underline{\underline{d\varepsilon}}^{ch} = \underline{\underline{d\varepsilon}}^{THM} + \underline{\underline{d\varepsilon}}^{ch}$$

$$\underline{\underline{d\sigma}} = \underline{\underline{C}} : (\underline{\underline{d\varepsilon}} - \underline{\underline{d\varepsilon}}^p) - b \cdot \underline{\underline{\delta}} dp - 3\alpha_t dT \cdot K \underline{\underline{\delta}}$$



$$\underline{\underline{d\sigma}} = \underline{\underline{C}}(c_i) : (\underline{\underline{d\varepsilon}} - \underline{\underline{d\varepsilon}}^p - \underline{\underline{d\varepsilon}}^{ch}) - b(c_i) \cdot \underline{\underline{\delta}} dp - 3\alpha_t(c_i) dT \cdot K \underline{\underline{\delta}}$$

c_i **Effective concentration**

THM-C analyse on decay of historical buildings

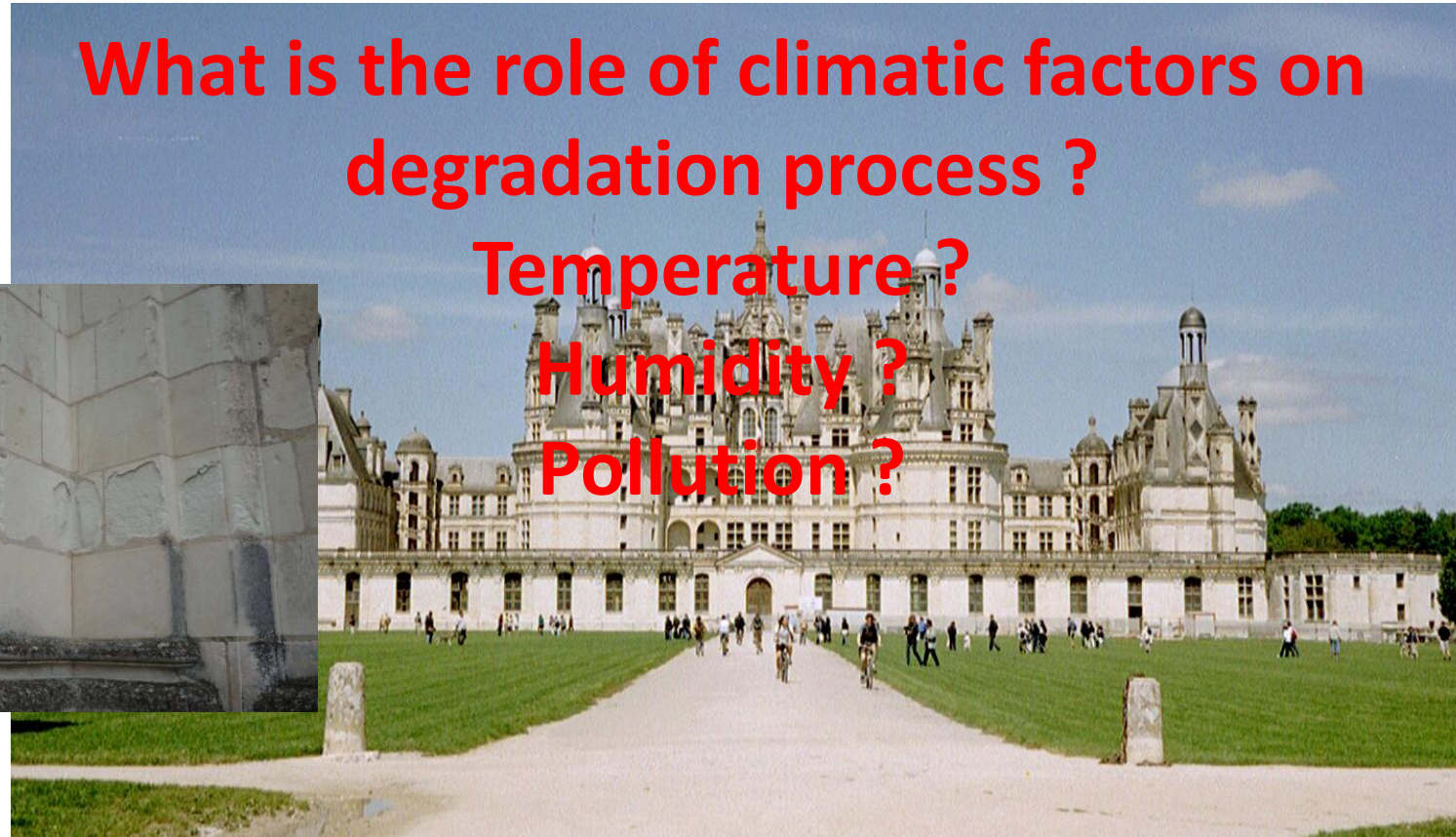
Chambord castel in Centre of France

What is the role of climatic factors on degradation process ?

Temperature ?

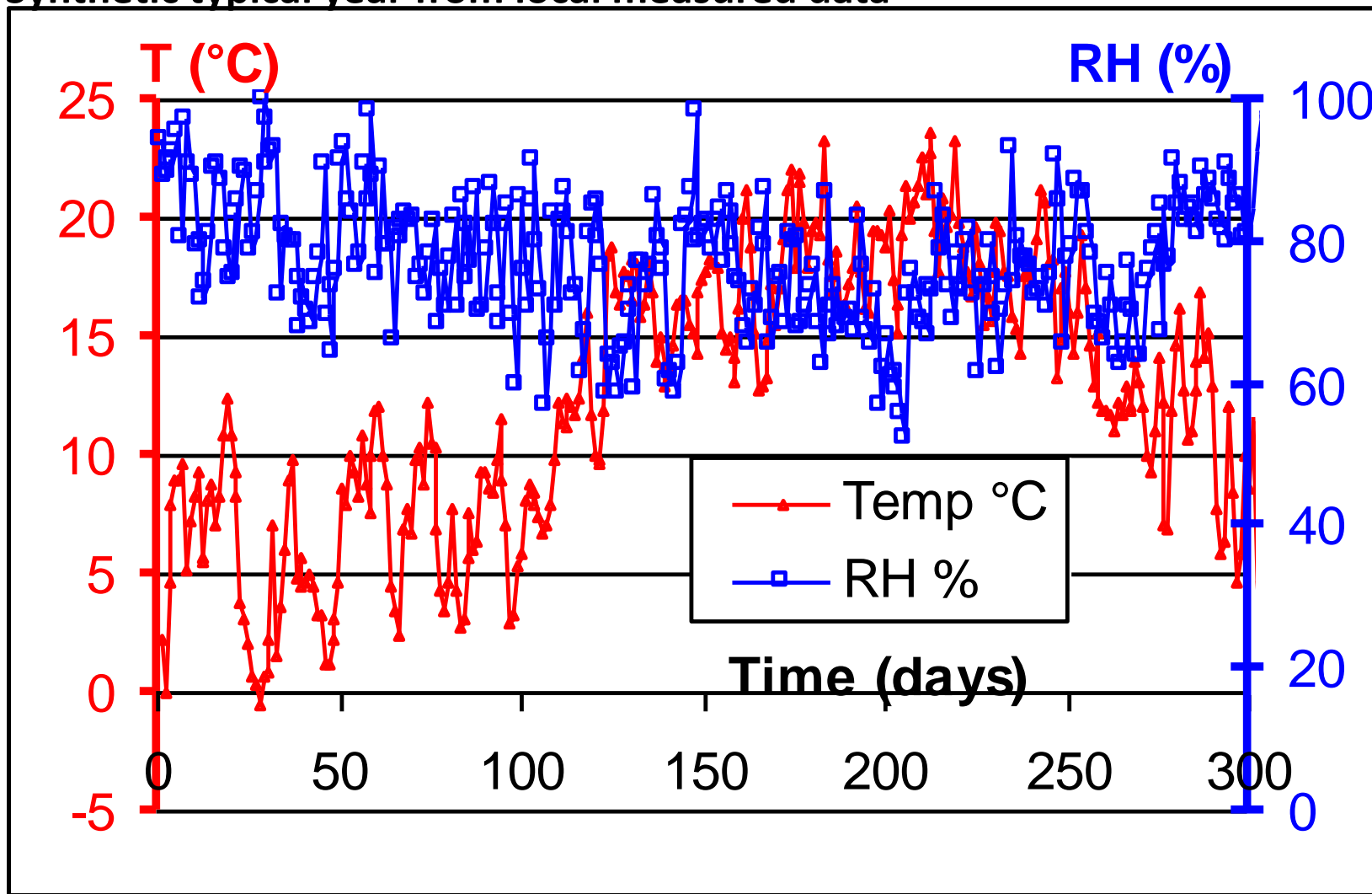
Humidity ?

Pollution ?



THM-C analyse on decay of historical buildings

Synthetic typical year from local measured data



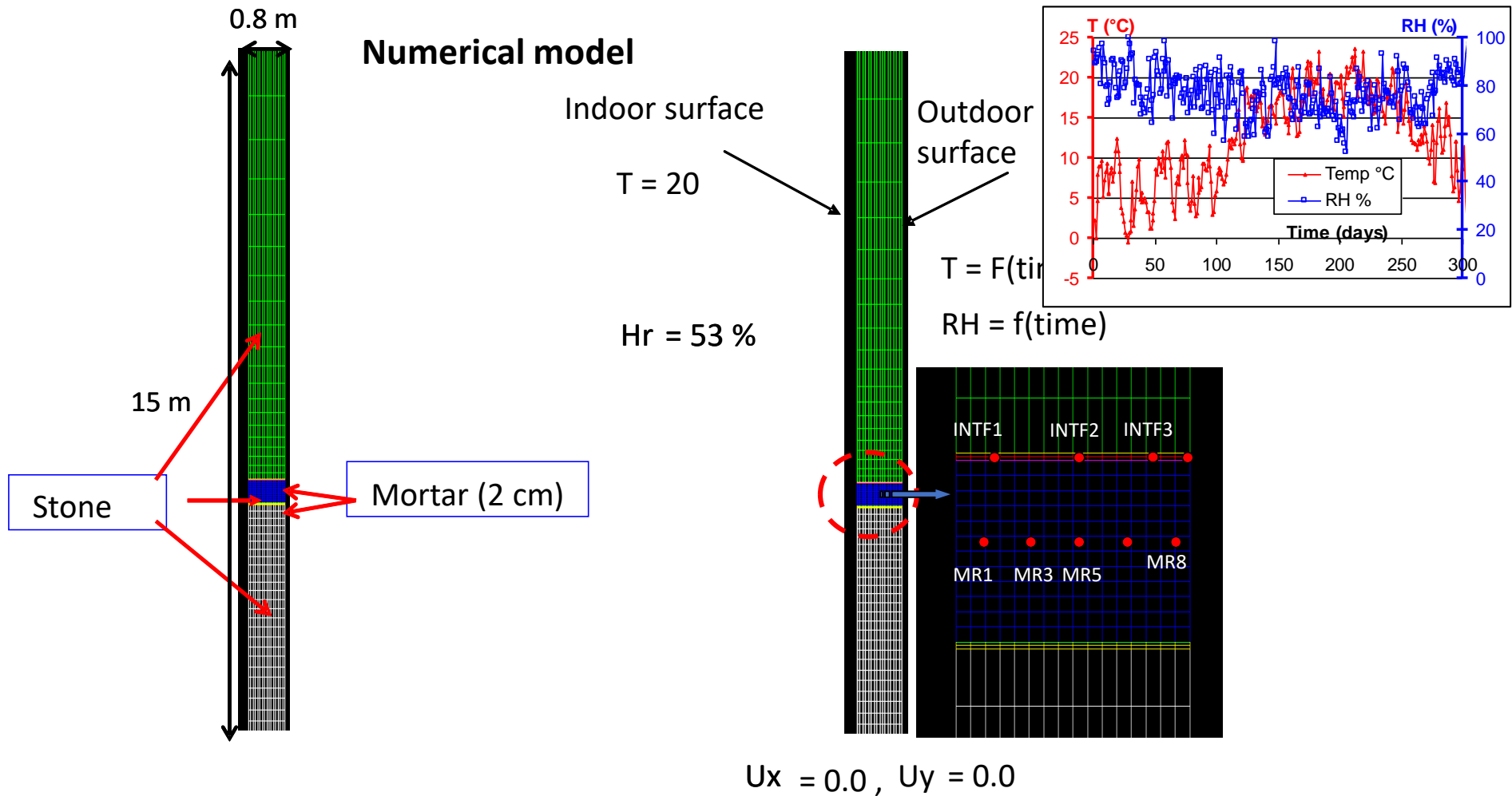
Material parameters (stone and mortar)

- ✓ Most of parameters identified from laboratory tests.
- ✓ Some are calibrated from in situ measurement)

		Stone tuff	Mortar
Mechanics	Young's modulus Poisson coefficient	$E_0=1953 \text{ MPa}$ $\nu_0=0.19$	$E_m=1604 \text{ MPa}$ $\nu_m=0.205$
Hydraulics	Intrinsic permeability Porosity Fick's diffusion coefficient	$k_{\text{int}} = 10^{-13} \text{ m}^2$ $\Phi = 42\%$ $F=2.05 \times 10^{-6} \text{ m}^2/\text{s}$	$k_{\text{int}} = 0.2 \cdot 10^{-13} \text{ m}^2$ $\phi = 50\%$ $F=2.05 \times 10^{-6} \text{ m}^2/\text{s}$
Thermics	Thermal conductivity Specific heat	$\lambda=0.56 \text{ W}\cdot\text{m}^{-1}\cdot\text{K}^{-1}$ $C_p=800 \text{ J}\cdot\text{kg}^{-1}\cdot\text{K}^{-1}$	$\lambda=0.56 \text{ W}\cdot\text{m}^{-1}\cdot\text{K}^{-1}$ $C_p=800 \text{ J}\cdot\text{kg}^{-1}\cdot\text{K}^{-1}$
Coupling THM	Biot's coefficient	$b=0.5$	$b=0.5$
	Retention curve	$n=1.37$ $Pr =0.013 \text{ MPa}$	$n=1.37$ $Pr =0.013 \text{ MPa}$
	Relative permeability	$m=3$ $k_l^{rel}(S_l) = S_l^m$; $k_g^{rel}(S_l) = (1 - S_l^m)$	$m=3$
	Thermal expansion coefficient	$\alpha=6 \times 10^{-6} \text{ K}^{-1}$	$\alpha=12 \times 10^{-6} \text{ K}^{-1}$

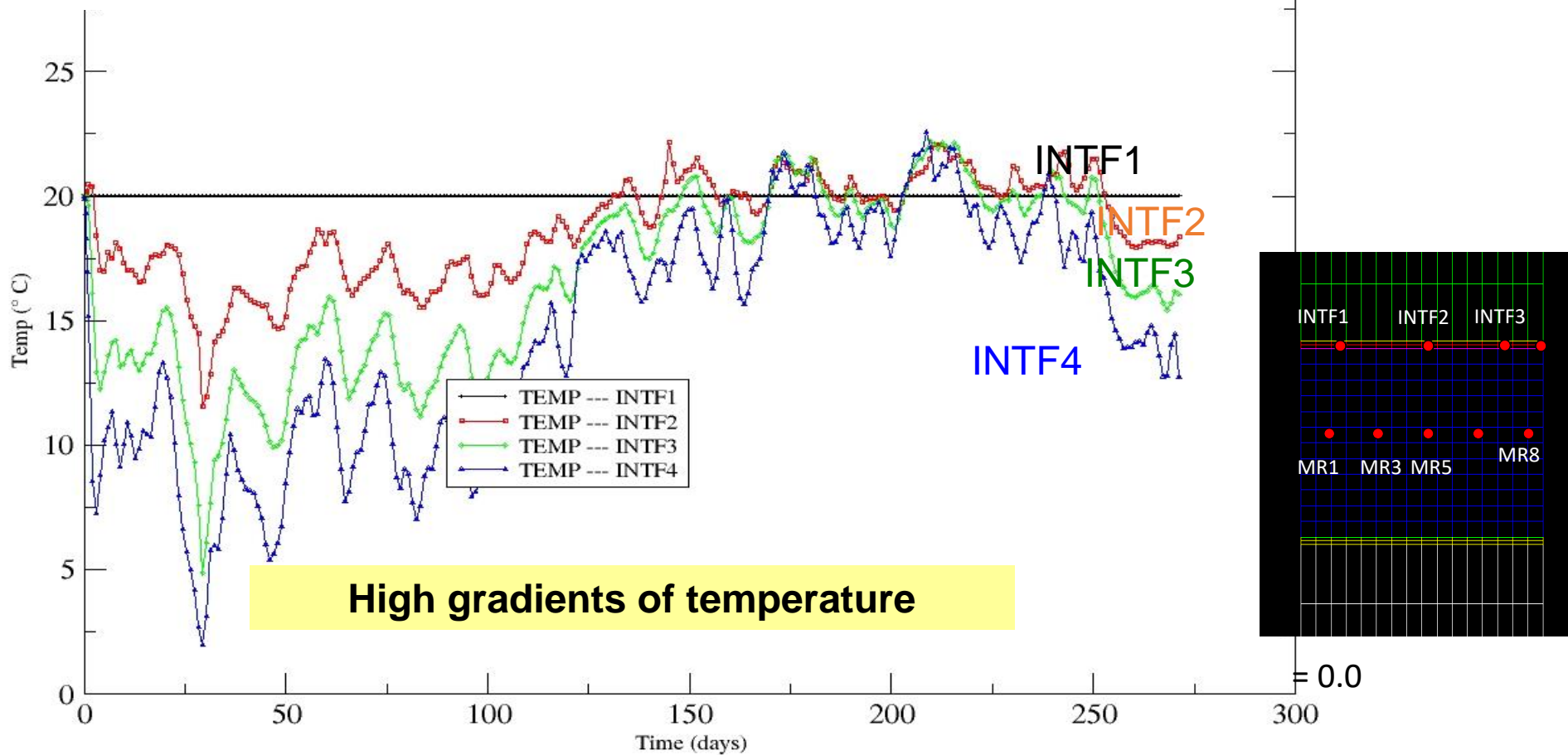


THM-C analyse on decay of historical buildings



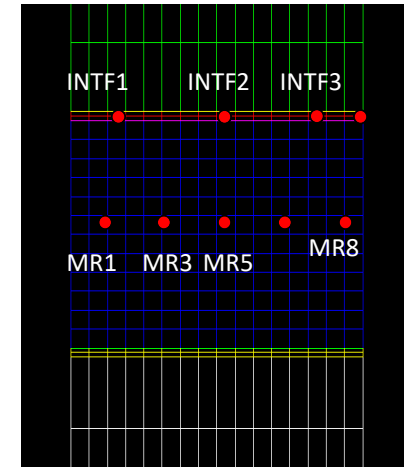
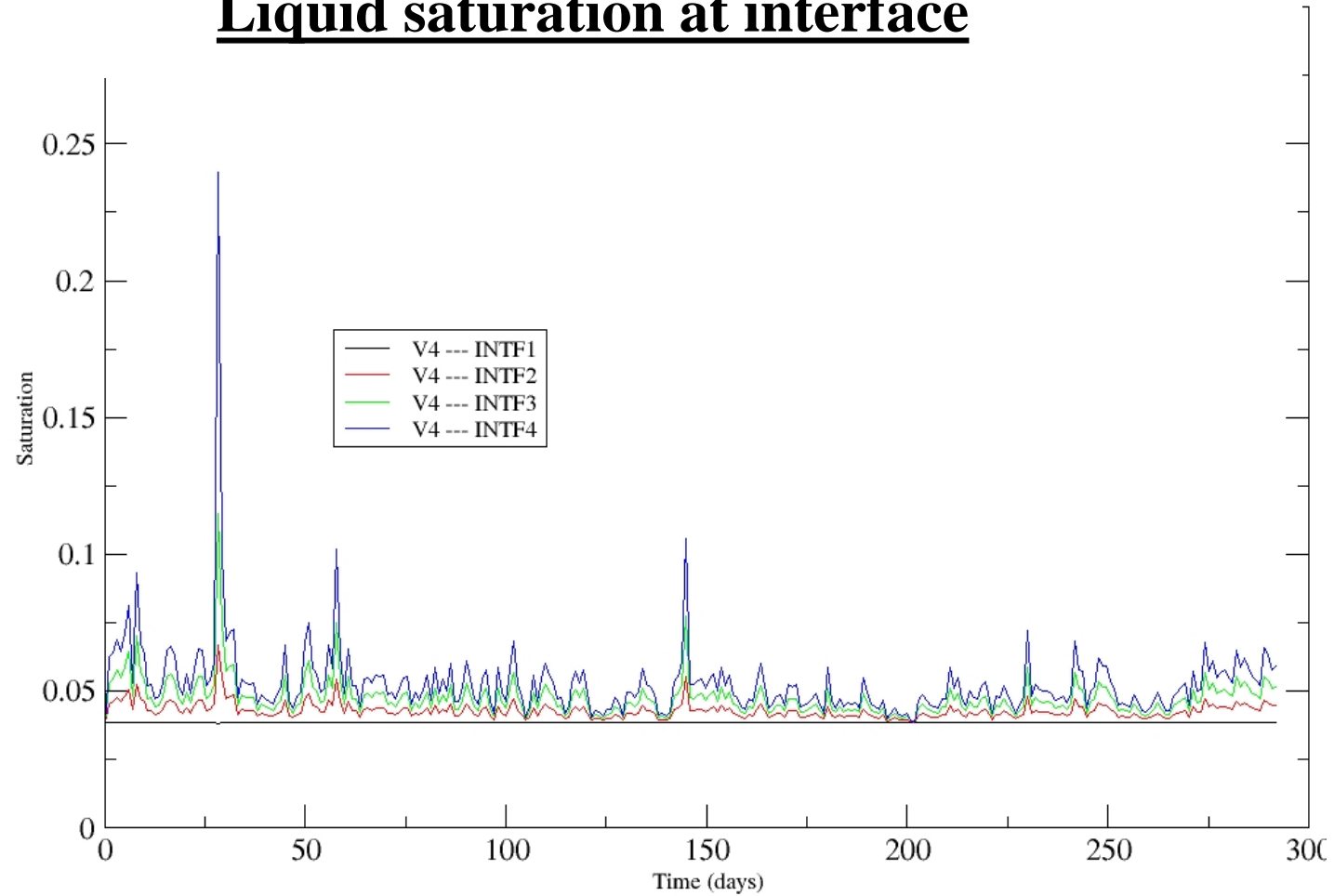
THM-C analyse on decay of historical buildings

Temperature variation in stone-mortar interface



THM-C analyse on decay of historical buildings

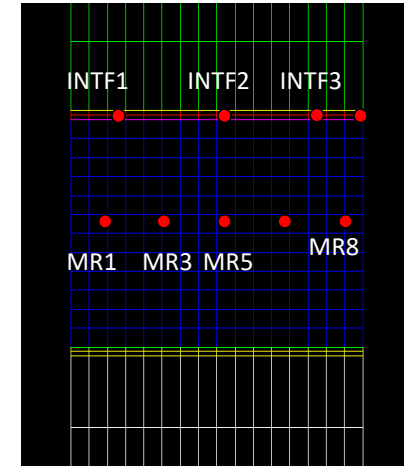
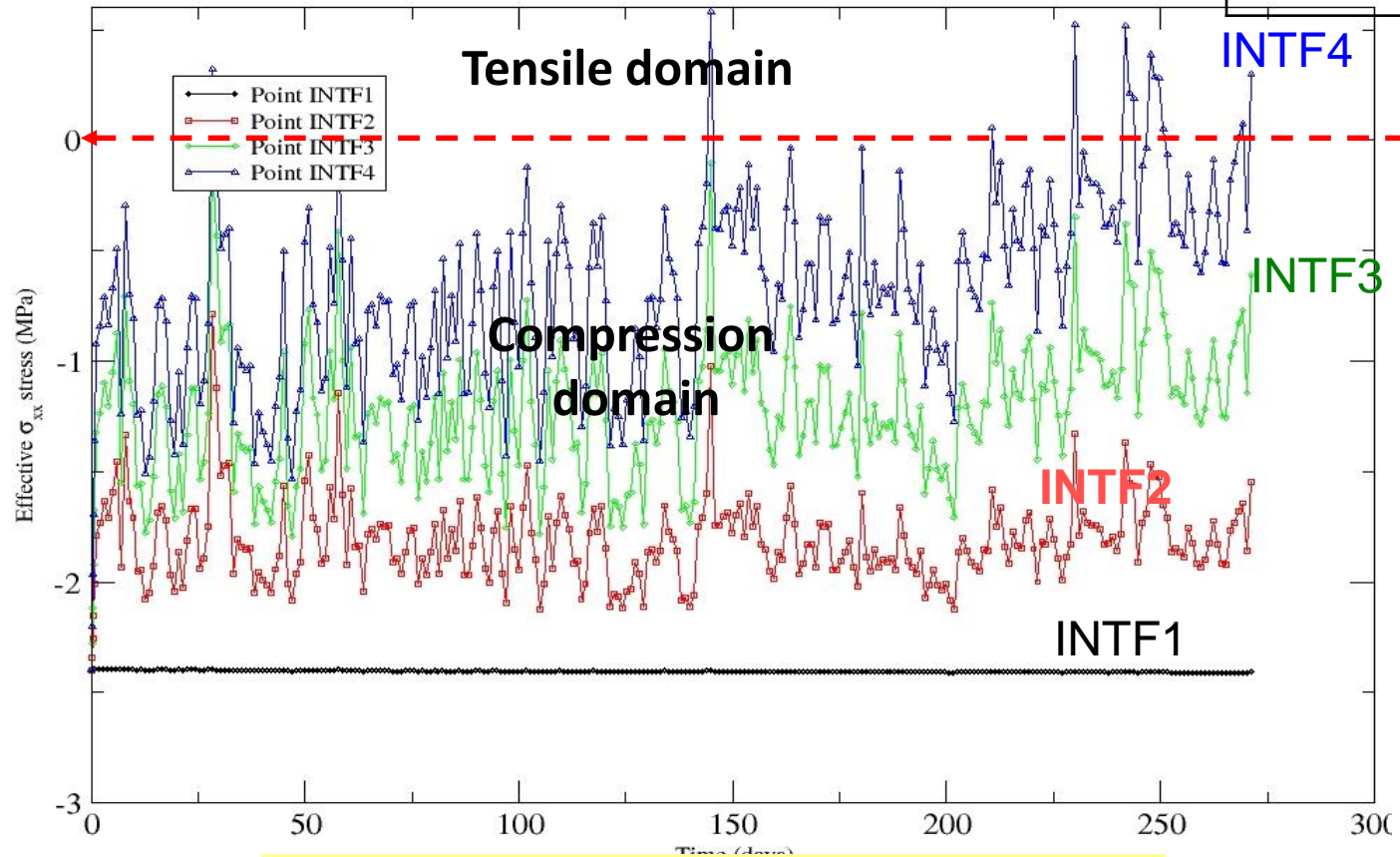
Liquid saturation at interface



THM-C analyse on decay of historical buildings

Effective stress variation in interface

$$\alpha = 12 \times 10^{-6} \text{ K}^{-1}$$

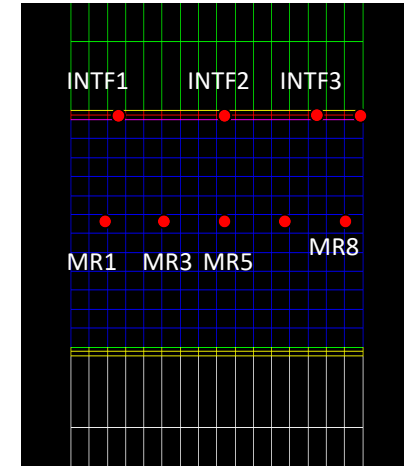
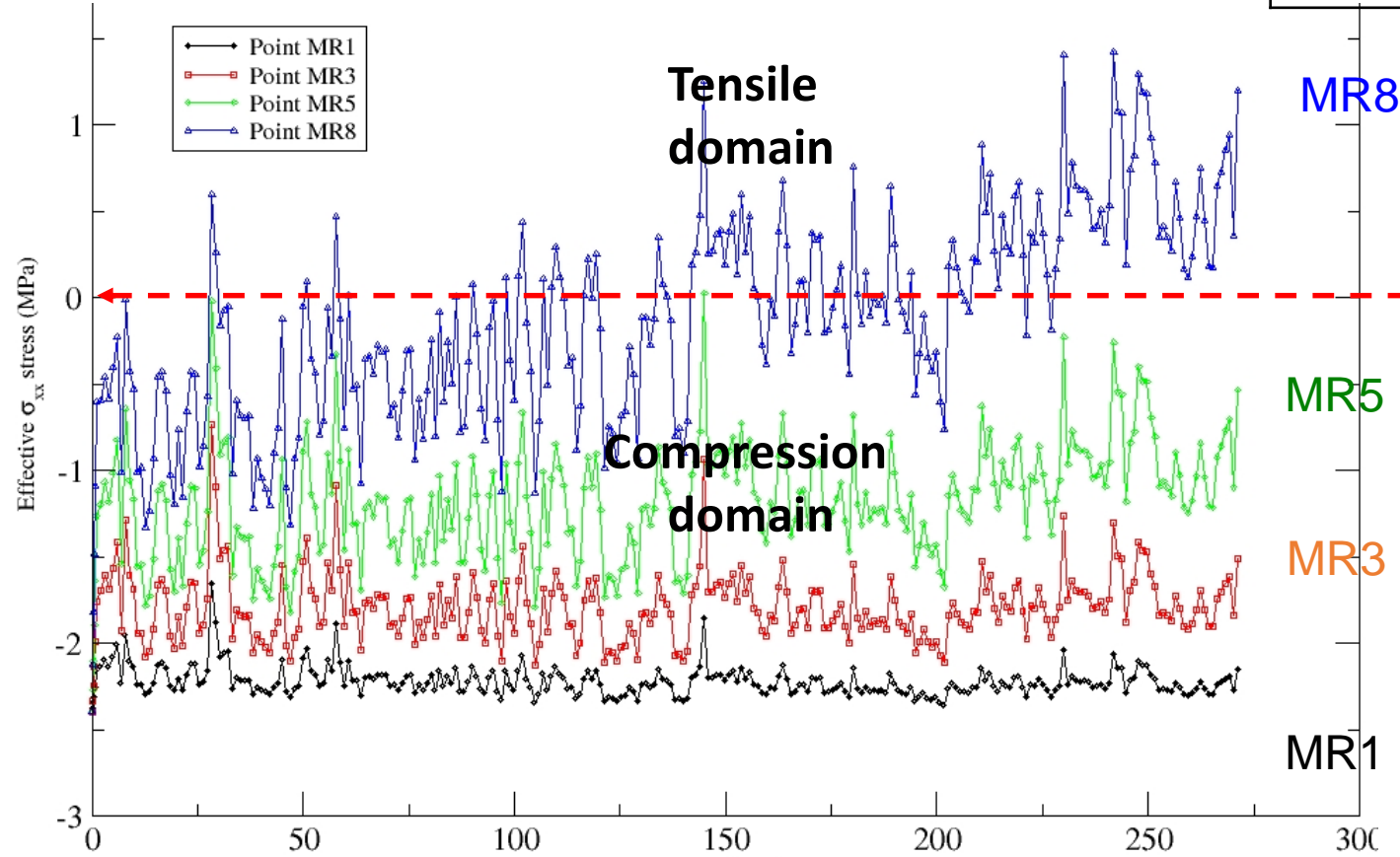


Cyclic variation of stress

3-c THM-C on decay of historical buildings

Effective stress variation in stone

$$\alpha = 12 \times 10^{-6} \text{ K}^{-1}$$



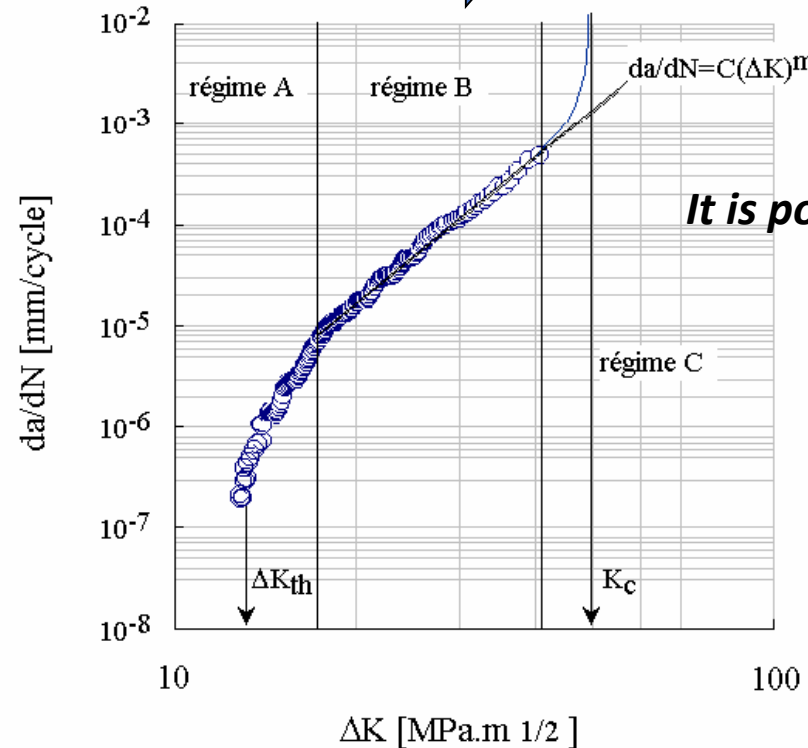
High amplitude of stress variation in outdoor surface of the wall

3-c THM-C on decay of historical buildings

- The stress values are inferior to the limits of strength materials
- However stress variation due to meteorological factors are to be studied carefully



Damage by fatigue ? Subcritical crack growth ?



Paris law of fatigue :

It is possible to make prediction of time to failure

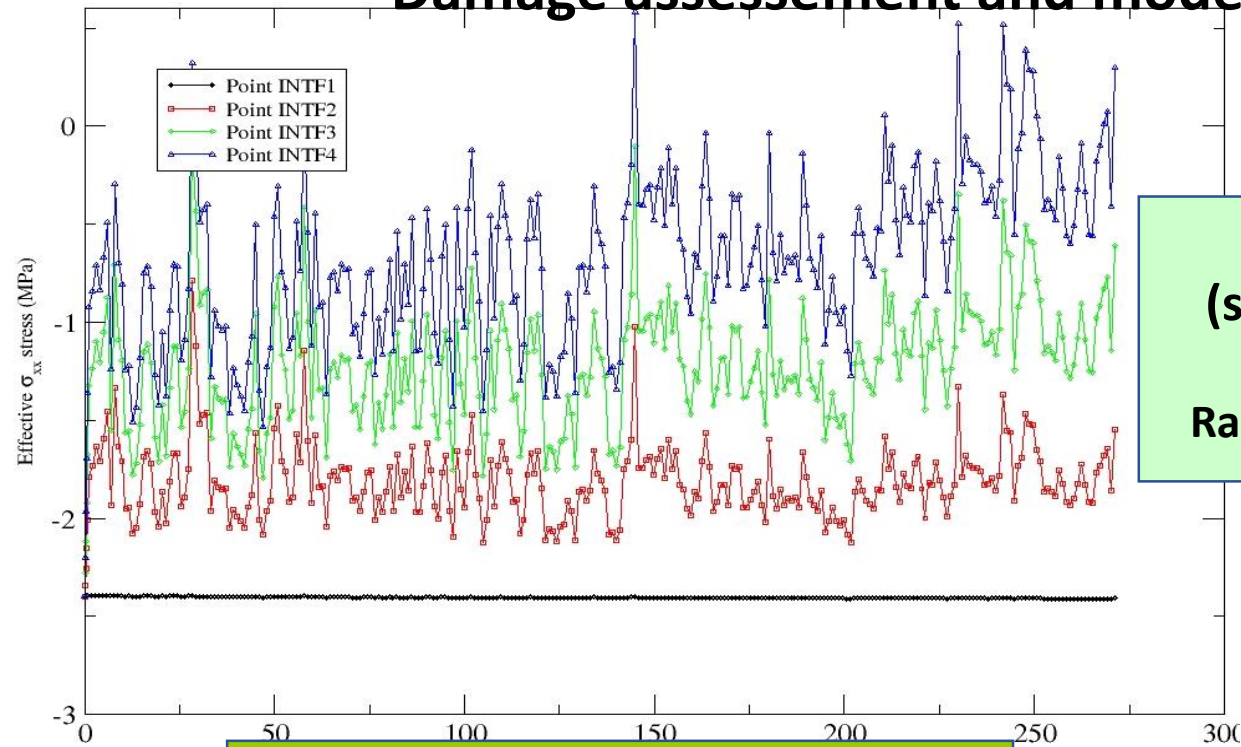
$$K = K_c \Rightarrow S_y \sqrt{\pi a_c} \quad K_c \Rightarrow a_c = \frac{1}{\pi} \left(\frac{K_c}{S_y} \right)^2$$

$$\underbrace{\frac{da}{dN} = C \cdot \Delta K^m}_{\text{Loi de Paris}} \Rightarrow N = \int_{a=a_0}^{a=a_c} \frac{da}{C \cdot (\Delta S_y \sqrt{\pi a})^m}$$

Calcul de la durée de vie par intégration de la loi de Paris entre a_0 et a_c

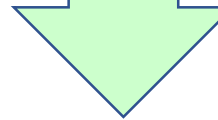
3-c THM-C on decay of historical buildings

Damage assesement and modeling



Cycles assesement
(strains, stress, energy)

Rainflow counting method,
RCC_M



Modeling

Lemaitre model

Restoration Works
previsions

4 –Damage assesement and modeling

Generalized Lemaitre model

$$\begin{cases} \dot{D} = \left[\frac{Y}{S} \right]^s & \text{if } \gamma^p > \gamma_D^p \\ \dot{D} = 0 & \text{otherwise} \end{cases}$$

$$Y = \frac{\sigma_{eq}^2}{2E(1-D)^2} R_\nu$$

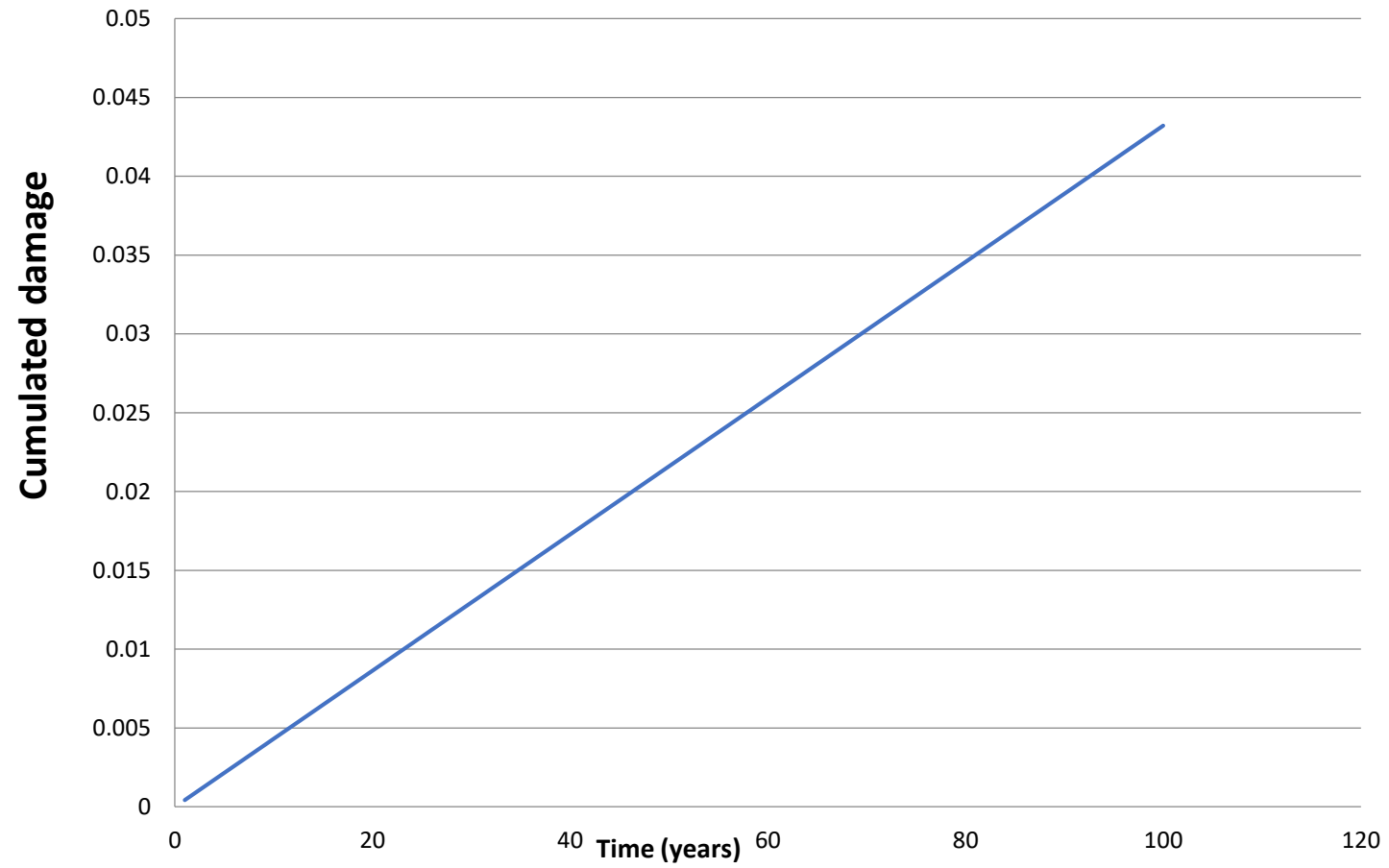
Energy restitution rate

$$R_\nu = \frac{2}{3} (1 + \nu) + 3(1 - 2\nu) \left(\frac{\sigma_H}{\sigma_{eq}} \right)^2$$

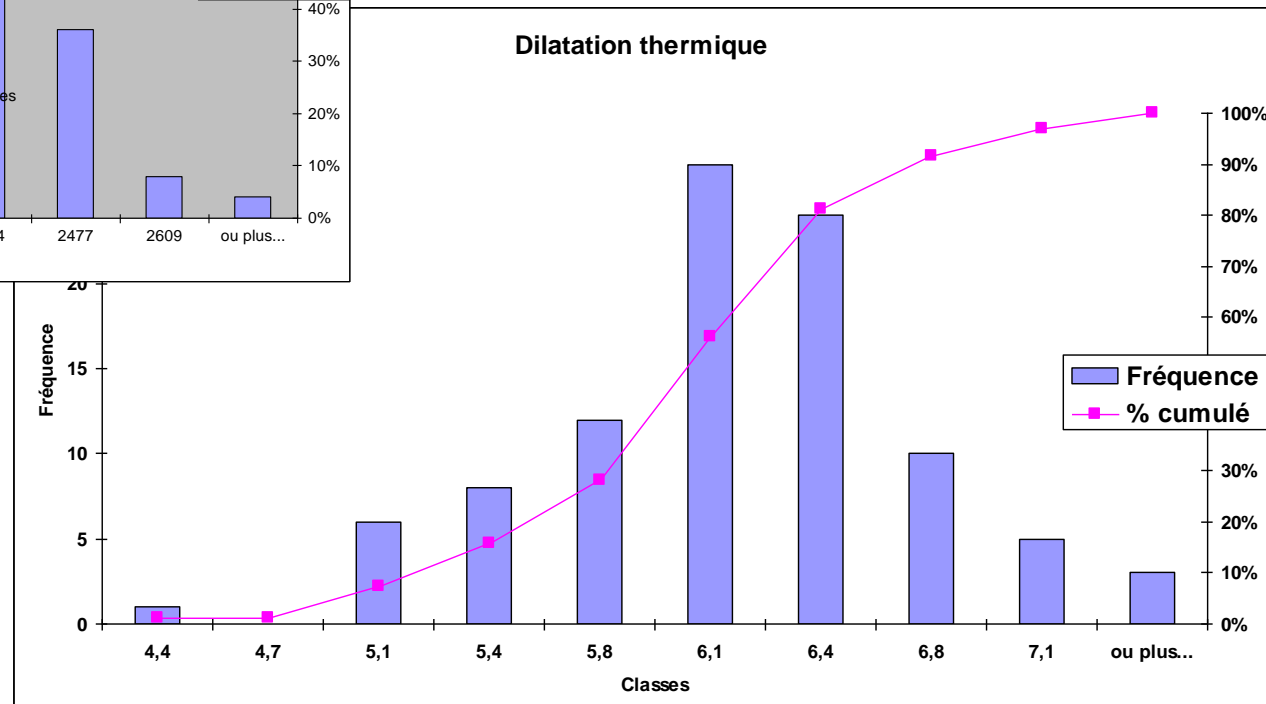
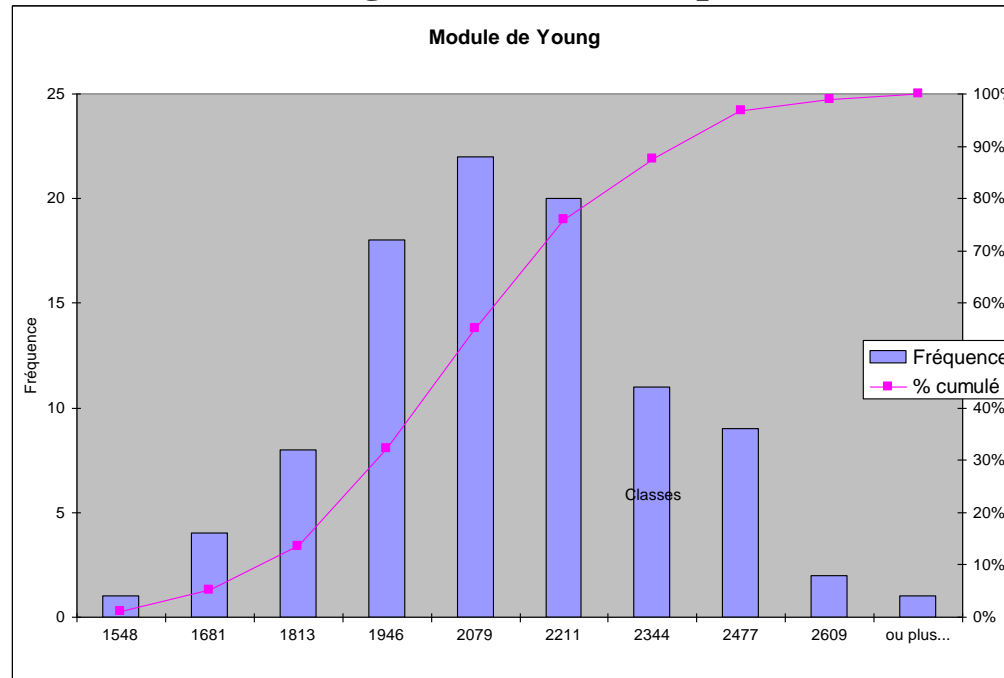
Threaxiality function

S, s, γ_D^p

Model parameters



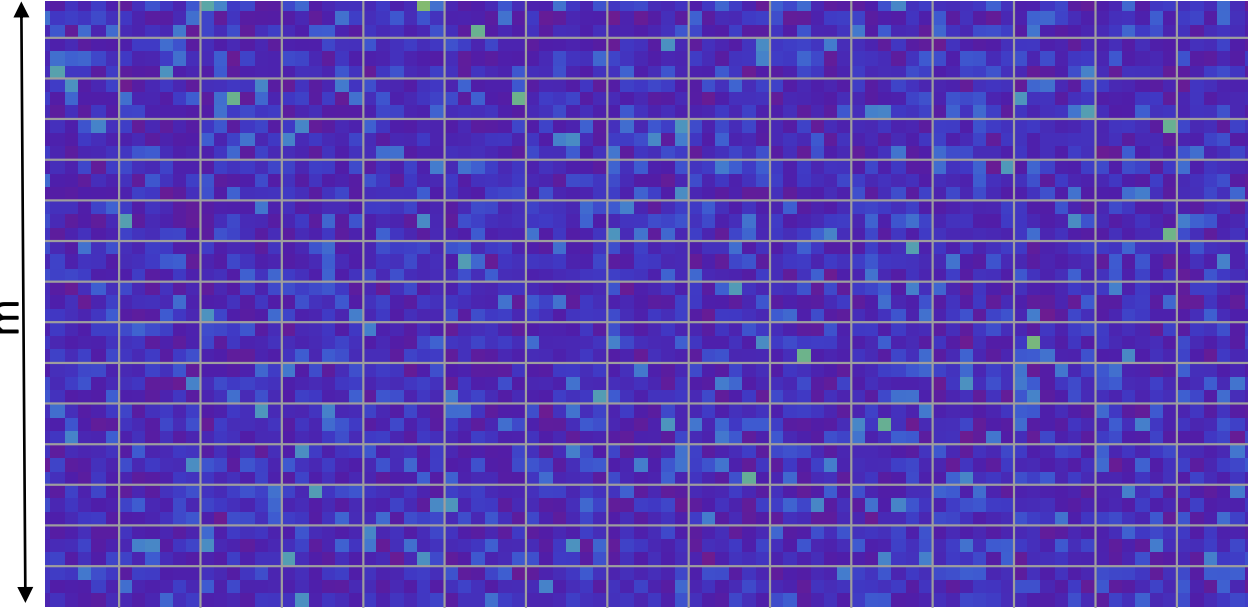
■ **Taking account for the spatial variation of parameters on the wall**



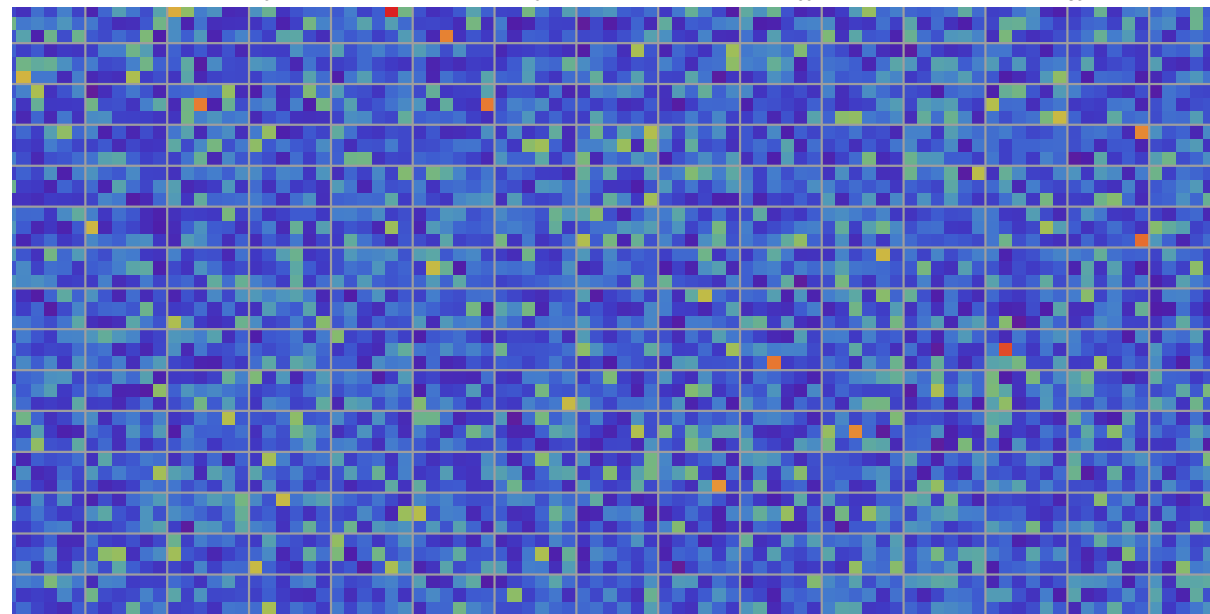
Damage distribution : North Face

15

m



30 years



100 years

THM-C on decay of historical buildings

What about impact of pollution ?

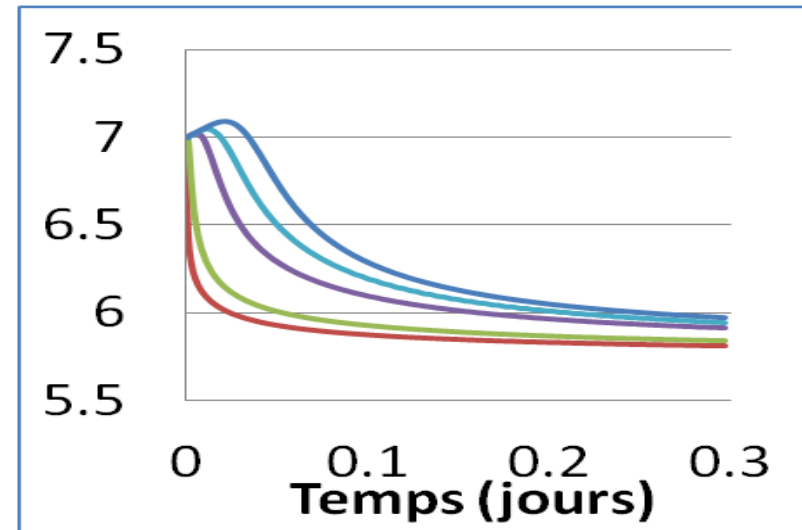
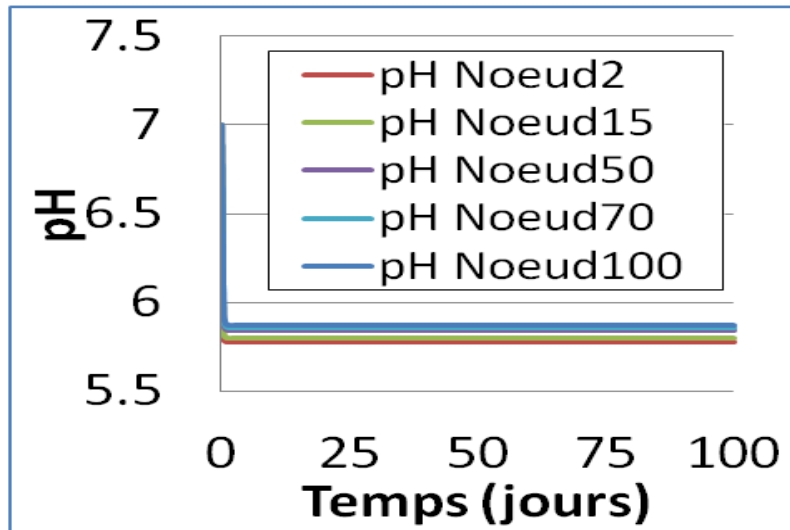
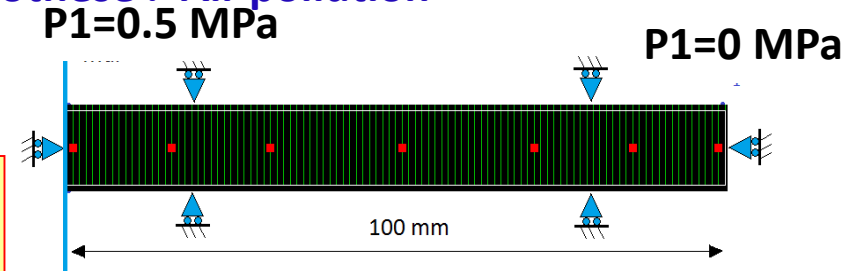
First hypothese : Air pollution

Partial gas pressures [SUR 00]

SO₂ 2.01E-7 atm

CO₂ 3.3E-4 atm

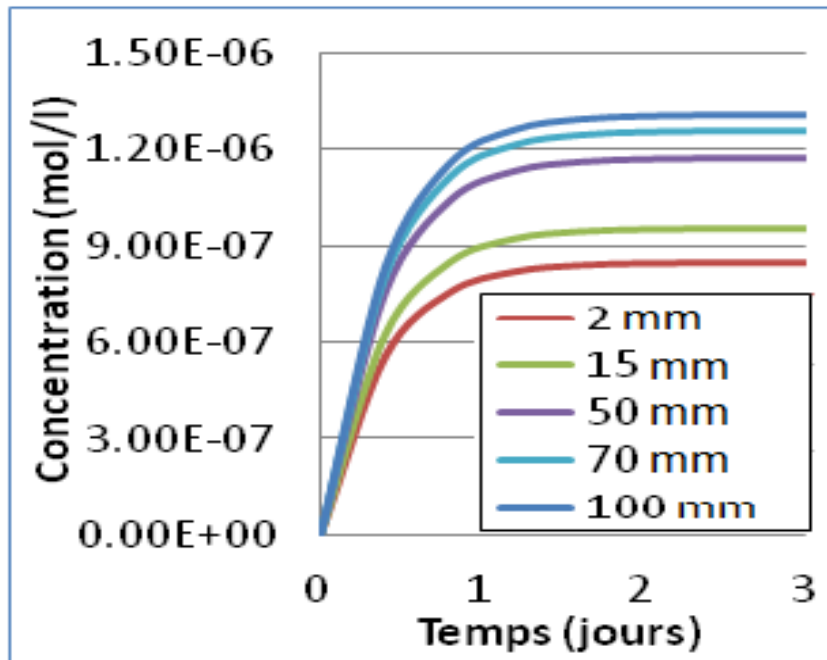
SO₂
CO₂



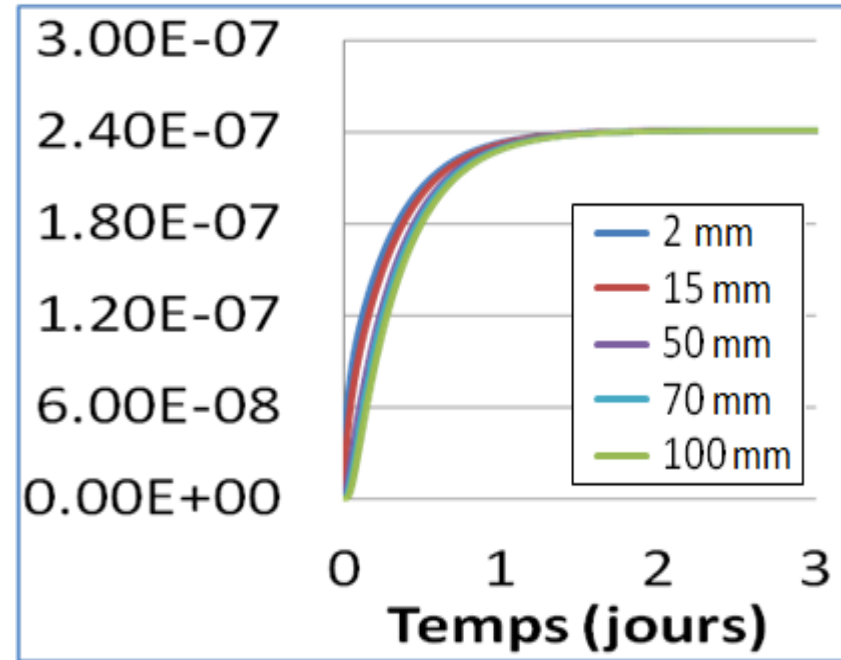
➤ pH decreases with the time

3-c THM-C on decay of historical buildings

Ca²⁺



SO₄²⁻



➤ Increase of Ca²⁺ and SO₄²⁻ concentration

➤ **But not gypse precipitation!!**

3-c THM-C on decay of historical buildings

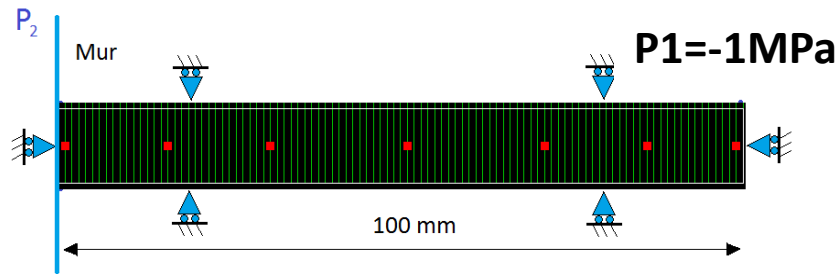
Second hypothese : Acid rain pollution AND air pollution

Partial gas pressure [SUR 00]

SO₂ 2.01E-7 atm CO₂ 3.3E-4 atm

SO₂
CO₂

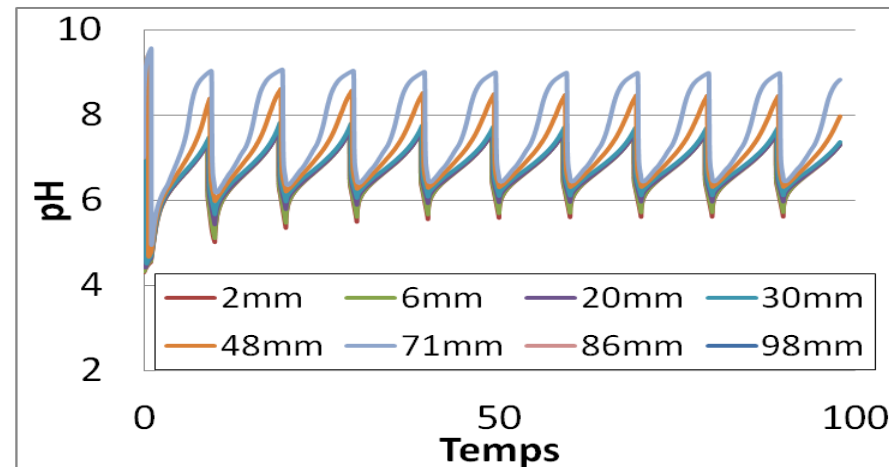
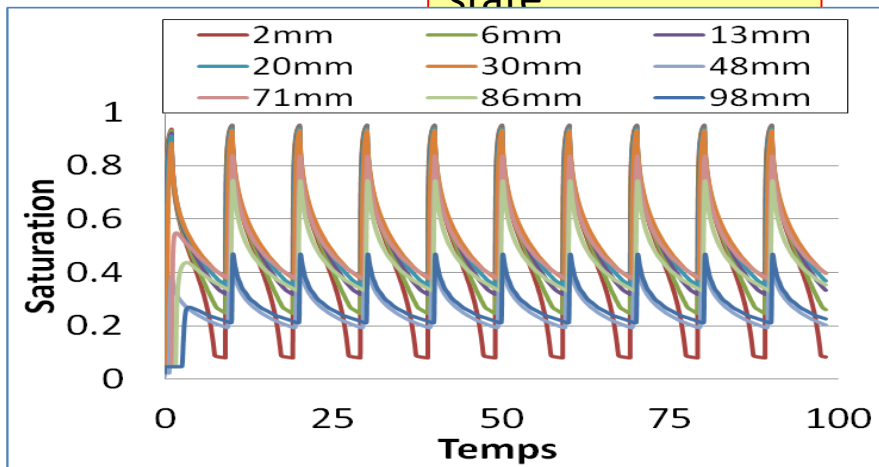
Pluie



Partially saturated state

Acid rain composition [PAR 99]

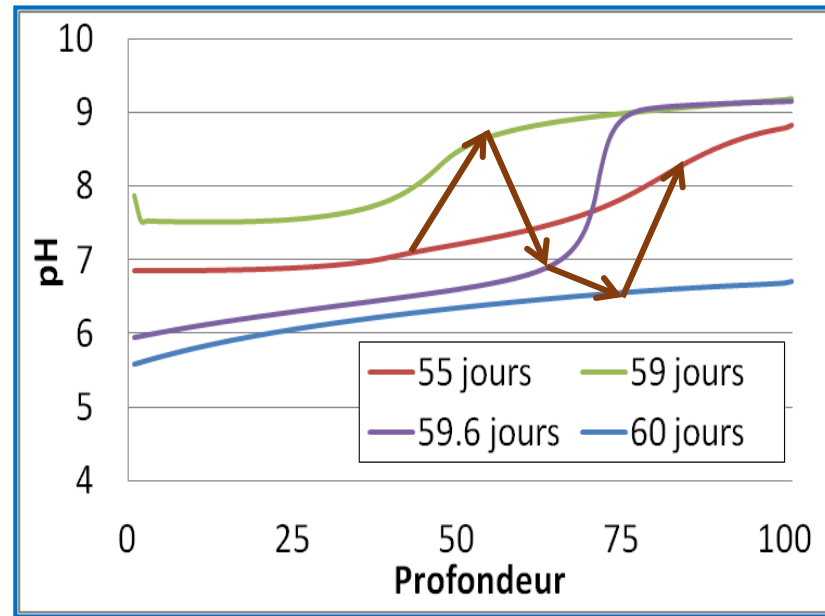
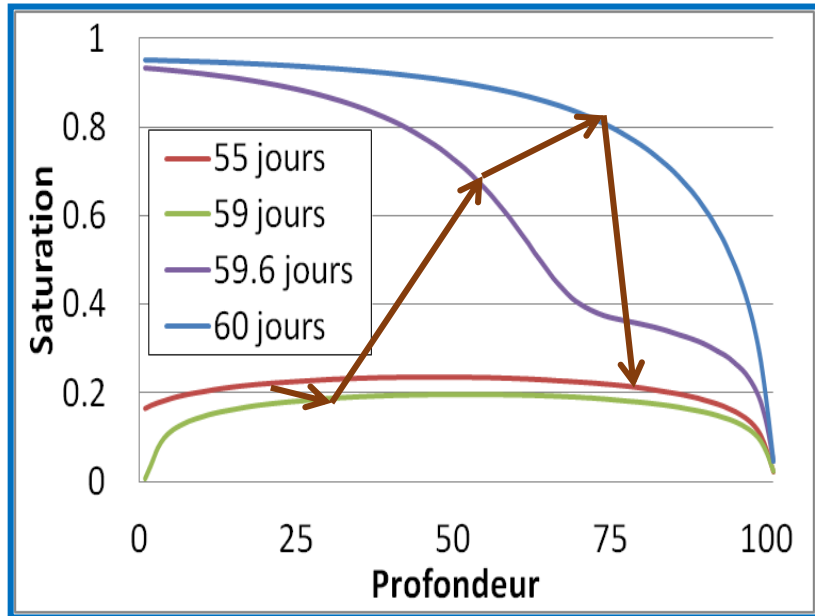
- pH 4.23
- Ca²⁺ 9.6E-6 mol/l
- Na⁺ 6.1E-6 mol/l
- CO₃²⁻ équilibre phase de CO₂
- SO₄²⁻ 4.1E-5 mol/l
- NH₄⁺ 1.5E-5 mol/l
- NO₃⁻ 1.7E-5 mol/l



➤ Variation en cycle pluie-séchage

3-c THM-C on decay of historical buildings

Hydric state variation



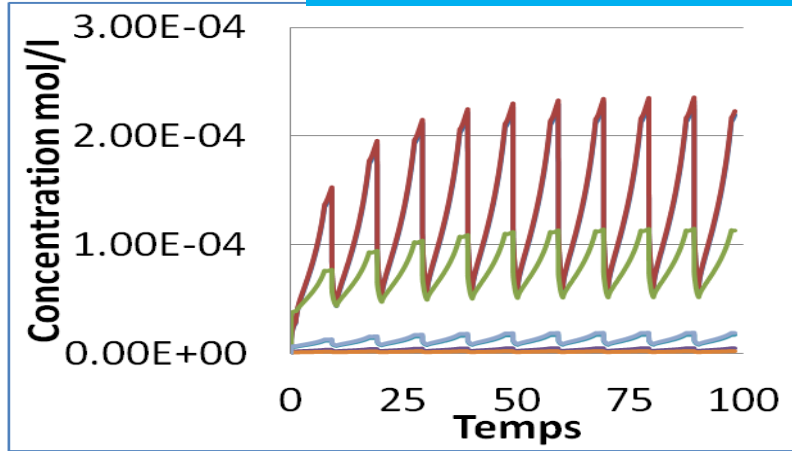
① Middle drying period

③ Middle raining period

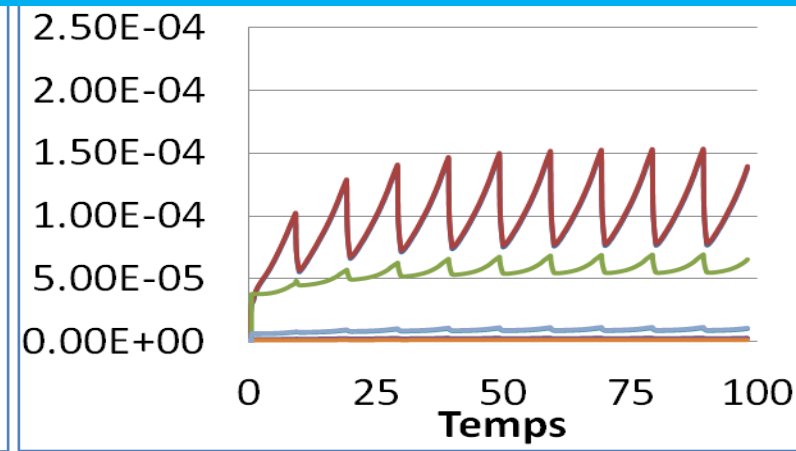
② Just before rain

④ Just after rain

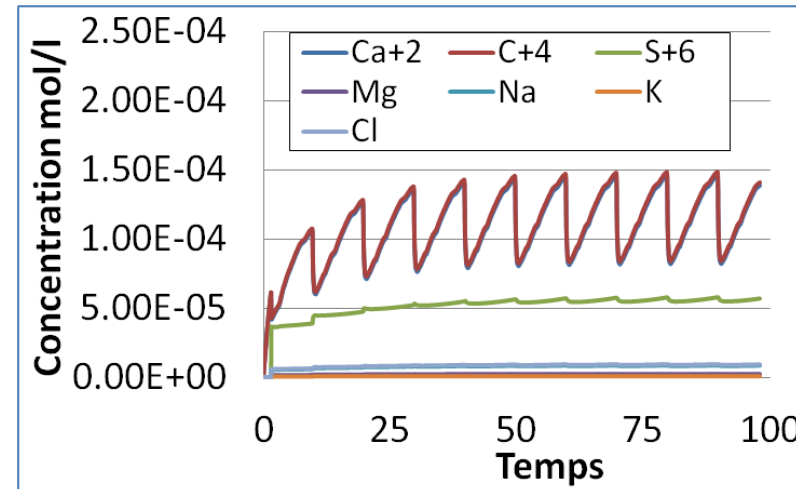
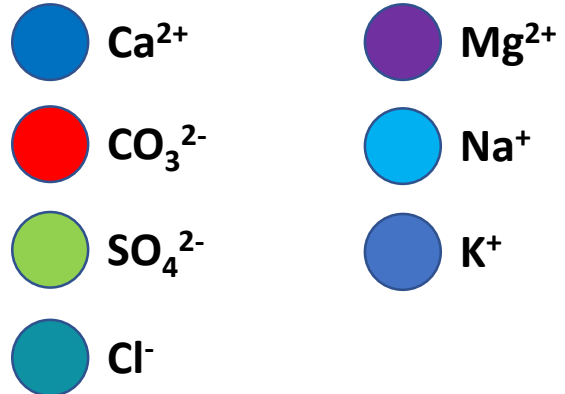
3-c THM-C on decay of historical buildings



At 2 mm from the surface



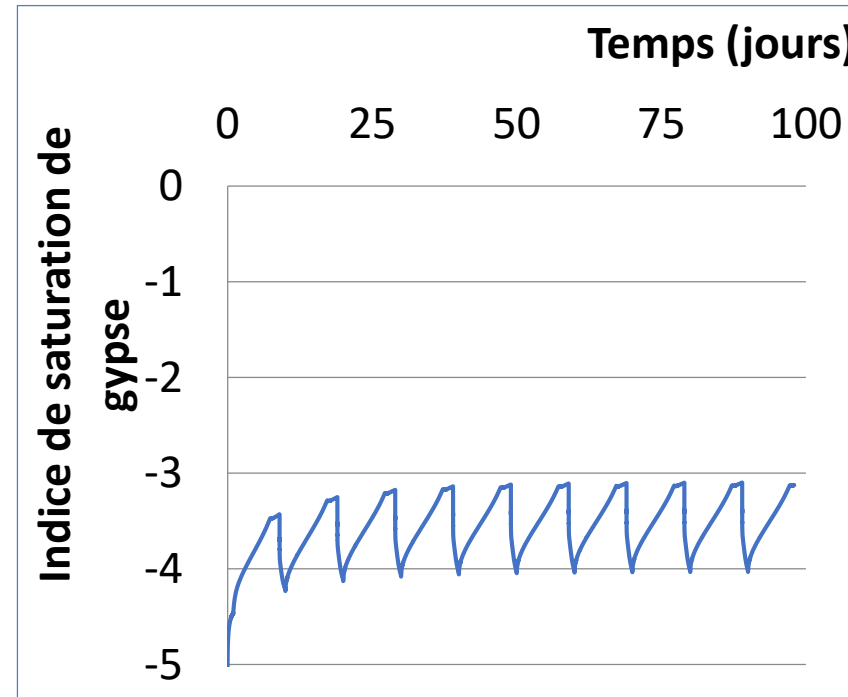
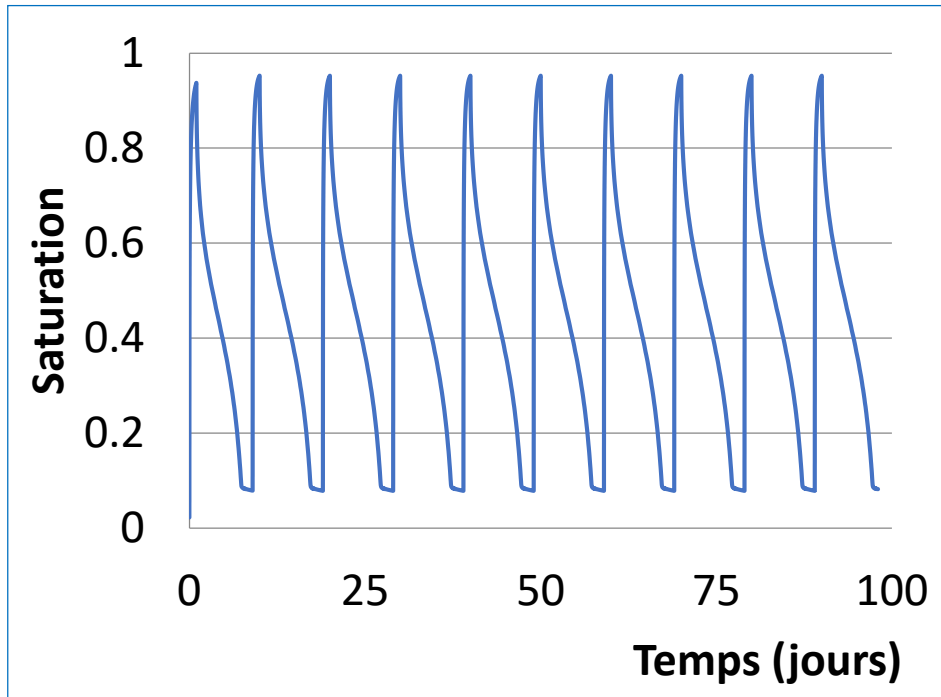
At 48 mm



At 86 mm

3-c THM-C on decay of historical buildings

At 2 mm from the surface



- **Water saturation varies between 0.008 and 0.94**
- **No gypse precipitations !!!**

Conclusions

1- Durability of materials → calling for global approach
- the first step THM-C coupling

2- Poromechanics : strong analytic and *design* tool

3- Necessity of interdisciplinary knowledges

Good enough to respond a great number of engineering questions

Understanding → Taking into account microscopic organisation and phenomenon and multiscale approach

Be careful to very good ideas and to designed guilteurs